

Draw

SPACE
SYSTEMS

CR-119933
GE DOCUMENT NO. 71SD4241

A JOINT HEAT TRANSFER DATA CRITICAL STUDY AND DESIGN GUIDELINE

FINAL REPORT
CONTRACT NAS 8-26490

JUNE 1971

FACILITY FORM 602	<u>71-36346</u>	(ACCESSION NUMBER)	<u>G3</u>	(THRU)
	<u>95</u>	(PAGES)	<u>71SD4241</u>	(CODE)
	<u>CR-119933</u>	(NASA CR OR TMX OR AD NUMBER)	<u>33</u>	(CATEGORY)



GENERAL  ELECTRIC

August 30, 1971

MEMO

TO: Distribution of NAS 8-26490 Final Report

SUBJECT: Errata to Final Report

Gentlemen:

Attached is an errata sheet for the final report of Contract NAS 8-26490, entitled "A Joint Heat Transfer Data Critical Study and Design Guidelines" (GE No. 71SD4241).

In addition to these errata, five pages of the original report have been modified slightly. New sheets have been prepared and are attached following the errata list. The new pages (22/23, 59/60, 61/62, 63/64 and 79/80) should replace those of the original report.


E. Fried
Principal Investigator

/kar

Att.

Errata

Final Report - Contract NAS 8-26490

<u>page</u>	<u>correction</u>
11 ✓	denominator for harmonic mean conductivity should be $(k_1 + k_2)$
15 ✓	in chart, Value of S when $(i_1 + i_2)$ is between $10 \times 10^{-6} \text{m}$ and $30 \times 10^{-6} \text{m}$ should be $(30 \times 10^{-6})^{1/3} / (i_1 + i_2)$
17 Do	ordinate of graph should be $(\bar{h}a/k_s) = N_m$
49 Do	change "decree" to "decrease" in last line of CAUTION statement
54 ✓	in Eq. 3-8, last term should be $2\bar{n}a k_s$, not $Z\bar{n}a k_s$
55 ✓	seventh conversion should be $1 \text{ lb-in}^{-2} = 6.89 \times 10^3 \text{ Newton-m}^{-2}$
76 Do	delete reference to Figure 3-1 in Eq. 3-2 label

GE DOCUMENT NO. 71SD4241

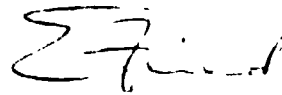
A JOINT HEAT TRANSFER DATA
CRITICAL STUDY AND DESIGN GUIDELINES
FINAL REPORT
PREPARED UNDER CONTRACT
NAS 8-26490

SPACE SYSTEMS ORGANIZATION
GENERAL ELECTRIC COMPANY
VALLEY FORGE SPACE CENTER
POST OFFICE BOX 8555
PHILADELPHIA, PENNSYLVANIA 19101

FOR

GEORGE C. MARSHALL SPACE FLIGHT CENTER
NATIONAL AERONAUTICS AND SPACE ADMINISTRATION
MARSHALL SPACE FLIGHT CENTER, ALABAMA 35812

PREPARED BY:



E. Fried
Principal Investigator

APPROVED BY:



H. D. Thompson, Manager
Vehicle & Structures Eng.

JUNE 7, 1971

TABLES

2-I	Bolted Joint Investigations
2-II	Averaged Values of Joint Conductance from Reference 21 for Component Joints
2-III	Averaged Values of Joint Conductance from Reference 21 for Structural Joints
2-IV	Table of r_{σ} of Several Investigators
2-V	Test Results of Reference II, Separation of Bolted Plates
3-I	List of Equations used in Section 3 - Guidelines
3-II	Conversions
3-III	Nomenclature

LIST OF FIGURES

2-1	Nondimensional Conductance Correlation (Ref. 12)
2-1a	Copy of Ref. 12 Correlation Data Points
2-1b	Copy of Ref. 12 Correlation Data Points
2-2	Nondimensional Conductance Correlation (Ref. 30)
2-2a	Copy of Ref. 30 Correlation Data Points
2-3	Variation of Thermal Conductance Number with Dimensionless pressure and Temperature (Ref. 27)
2-4a	\bar{n}_a vs. Contact Pressure (Ref. 3)
2-4b	Average Surface Irregularity/rms Surface Roughness vs. rms Surface Roughness
2-5	Configuration and Dimensions for Component Joints (Ref. 21)
2-6	Configuration and Dimensions for Structural Joints (Ref. 21)
2-7	Pressure Distribution under a Bolt Head
2-8	Thermocouple Locations and Typical Test Configuration of Lap Joint Used in Ref. 20
2-9	Axial Force-Torque Variation (Ref. 20)
2-10	Bolted Lap Joint Conductance vs. Geometry (Ref. 20)
2-11	Sample Joint Geometry (Ref. 20)
2-12	Nondimensional "Zero Interface" Stress (Ref. 3)
2-13	Thermal Conductance vs. Torque (Ref. 38)
2-14	Configurations and Test Data from Ref. 46 Bolted Joints
3-1	Contact Conductance vs. Contact Pressure - Representative Data
3-2	Contact Conductance vs. Contact Pressure for AZ-31 Magnesium, 6061 T6 Aluminum
3-3	Contact Conductance vs. Contact Pressure, 2024 T4 Aluminum Assembled in Air, Vacuum
3-4	Contact Conductance vs. Contact Pressure, 2024 T4 Aluminum Assembled in Air, Vacuum
3-5	Contact Conductance vs. Contact Pressure, Beryllium CR, Assembled in Air, Vacuum

FIGURES - Continued

- 3-6 Contact Conductance vs. Contact Pressure, OFH Copper, Assembled in Air
- 3-7 Contact Conductance vs. Contact Pressure - 304 Stainless Steel Plated with Magnesium
- 3-8 Contact Conductance vs. Contact Pressure - 304 Stainless Steel Plated with Aluminum
- 3-9 Contact Conductance vs. Contact Pressure for OFH Copper, 304 Stainless Steel
- 3-10 Contact Conductance vs. Contact Pressure Pure Titanium
- 3-11 Contact Conductance vs. Contact Pressure - 6AL4V Titanium Alloy
- 3-12 Nondimensional Conductance Correlation (Ref. 30)
- 3-13 Nondimensional Conductance Correlation (Ref. 12)
- 3-14 \bar{m} vs. Contact Pressure (Ref. 3)
- 3-15 Average Surface Irregularity/rms Surface Roughness vs. rms Surface Roughness
- 3-16 Axial Force-Torque Variation (Ref. 20)
- 3-17 Bolted Lap Joint Conductance vs. Geometry (Ref. 20)
- 3-18 Nondimensional "Zero Interface" Stress (Ref. 3)
- 3-19 Thermal Conductance vs. Torque (Ref. 38)

ACKNOWLEDGEMENT

The author wishes to thank Mr. Jack Loose, Contract Technical Monitor, for his support throughout this program and in particular for his contributions to the format of the guidelines section. The work of Mr. Thomas Scollon in editing and publishing this final report is also gratefully acknowledged.

SECTION 1.0

INTRODUCTION

This report presents the results of a study which had the objectives of (a) a critical review of the existing information on the prediction of bolted joint heat transfer and (b) the selection and recommendation of guidelines and procedures to enable the thermal design engineer to predict, within reasonable limits, such joint heat transfer for spacecraft application. Included in this work are tables and graphs showing experimental data on bolted joints and related data. For convenience, item (b) is complete in itself and can be included in a "handbook" type document. A glossary of terms used is also included. Empirical approaches are used exclusively because analytical methods are not sufficiently developed to allow for reliable predictions of the load distribution in the joint or the area of apparent and real contact.

Contact conductance is defined as h , where

$$h = \frac{Q}{A_c \Delta T} \quad (1-1)$$

The potential users dilemma begins at this point, because there is no uniformity in the definition of either A_c or ΔT . For purposes of this report A_c will be set equal to A , the common area of the mating surfaces unless otherwise defined. The ΔT term will be defined as the difference between the average temperatures of contact surfaces. This is usually obtained by extrapolation from an interior point in the solid to the mating surfaces.

While there exist approximately 250 reports on research and experimental work on contact heat transfer, only 5% of these are concerned with bolted joints, and even fewer are pertinent to spacecraft application. This report and guideline is

based primarily on this small group, however, with due consideration of the vast body of background information available and the author's extensive experience in the field. For general background information on contact heat transfer, the reader is referred to the material in References 1, 2 and 3. Reference 3 is the most comprehensive review of bolted joint data. References 4 and 5 provide extensive bibliographies.

1.1 SUMMARY OF STATE-OF-THE-ART

At the outset of this report, it should be noted that there exist no satisfactory, experimentally verified, analytical methods to predict the thermal conductance for bolted joints. There do exist, however, some very limited applications of empirical results and, more importantly, some potential approaches leading to approximate methods. The latter involves the separation of the mechanical and load distribution effects from the purely heat transfer effect.

The mechanical or structural effects for a joint made up of two metallic plates include:

- plate deformation under load
- plate separation under load
- elastic or plastic deformation of asperities
- combined effects of the above as well as long-term yielding
- surface characteristics and finish

The thermal and heat transfer effects for such a joint include:

- thermal deformation effects
- thermomechanical or thermostructural effect
- heat transfer by solid conduction
- heat transfer by fluid conduction
- heat transfer by radiation

The mechanical contact (or joint*) parameters define which contiguous areas at the interface are in actual contact and which are not. A number of investigators have developed mostly analytical techniques to estimate or predict the load (stress) distribution at the interface of a bolted joint, or a pair of plates under load. In some instances, experimental work using highly idealized conditions was carried out to support such analysis, although not always successfully. The principal sources for such work are Lardner (8)**; Fernlund (9), Aron and Colombo (10), and Gould and Mikic (11). While not all existing work is cited, these cover most of the important information sources. However, no reliable experimental verification of interfacial load or stress distribution exists today.

Once the regions of contact and the appropriate regional stress distribution have been established, the surface characteristics must be known to estimate the actual microscopic areas in contact through which solid conduction can take place. One must distinguish between regional (macroscopic) and very localized (microscopic) contacts. The latter are particularly important for contacts in vacuum, since there is no heat conducting continuum surrounding the asperities of the surface.

The thermal and heat transfer effect must be considered at this point, because thermal expansion effects can influence the actual areas in contact or can change them as non-uniform heating takes place. This is discussed by Clausing (40) with respect to dissimilar metals.

* Reference 3 uses the term joint for a bolted plate contact and contact for rigid block contact.

** Reference Number

The spacing between the mating surfaces also affects the fluid conduction contribution, when a gas, liquid or grease is present in the interface. The effect of this spacing and its dimensional determination has been covered by Cetinkale (13), Fenech (14), and Laming (16) among others. Radiation heat transfer also may be influenced by the spacing and surface conditions. It is, however, generally neglected for most moderate temperature joints, since the other heat transfer modes make radiation negligible, except for high temperature or high temperature difference conditions.

As a result of the general interest in the subject of heat transfer between mating surfaces, there have been developed a number of highly analytical correlations. The greatest complexity of expressions cover the solid-solid conduction contribution, and are exemplified by references such as Cetinkale (13), Clausing (15), Fenech (14), Laming (16). Experimental and empirical approaches were reported by Fried (17, 18), Barzelay (19), Rolsma (20), Bevans (21), Aron (10), Fontenot (3), and Whitehurst (36). Several of these items included data on bolted joints, however, with limited correlation success.

Generalized correlation of contact heat transfer data has been attempted by a number of investigators. Among these were Graff (6), Fletcher (27) and Hsieh (12). However, none of these attempts were very successful over a wide range of data. Bevans (21) and Rolsma (20) attempted to correlate bolted joint data, but these efforts did not succeed, due to the nonreproducibility of tests.

In order to obtain the most up-to-date joint heat transfer data, a thorough review of the existing contact conductance literature was made, including the use of a NASA Literature Search. No new information was gathered. The work by Fontenot (3, 7)

provides one of the best summaries and reviews of bolted joint thermal performance information and Rolsma (20) provides the largest body of experimental data. It should be noted that many good sources of contact or bolted joint data were not mentioned in this brief summary. This is due to the fact that their analyses and data are included, utilized or reviewed in the cited work. Thus, the number of references cited could be kept within manageable limits.

The next section will provide capsule reviews and discussion of the important bolted joint data as well as pertinent other contact parameters.

SECTION 2.0

DATA REVIEW

In the course of this study a large number of contact heat transfer references were reviewed, with particular emphasis on the bolted joint problem. The References section of this report lists all cited references as well as the significant bolted joint references. References 4 and 5 show nearly all existing contact heat transfer references and are the most recent published bibliographies on the subject. While not all existing bolted joint references were obtained for review, their citation in recent work, personal communications, experience and knowledge of the general subject lead us to believe that we have covered all important material.

This section begins with a brief discussion of surface characterization and contact heat transfer, followed by a data correlation discussion and capsule reviews and summaries of pertinent bolted joint heat transfer work. Consideration is given to surface properties, material, loads and distribution and heat transfer. A listing of highlights of bolted joint work is given in Table 2-I.

The ratings shown in Table 2-I are based on the compiler's estimate of the adequacy of experimental procedures and techniques for providing useful data for reference purposes. The ratings are for thermal test only.

- A. Highest quality of measurements
- B. High quality
- C. Average quality

AUTHOR	Ref. No.	Type of Joint	Air	Vacuum	Test	Joint Materials	Rating	REMARKS
Barzelay, et al	19	Riveted Aircraft Stringer	X		X	Al - Alloy	B	High temperature transient tests to detect sample-to-sample variation, fastening type. Tests in air.
Bevans, et al	21	Component & Struct. Mnts.		X	X	Al - Alloy	B	Steady-state tests, using bare joints and filled joints, no surface control. Able to correlate unfilled joints data only.
Gould & Mikic	11	Bolted Plates			X	304 Stainless		Tested effect of load and dimensions on contact area only.
Rolsma	20	Bolted lap Joints		X	X	Al - Alloy	A	532 Data points were obtained for several configurations, bolt spacing, loads, and temperature levels. No correlation could be obtained.
Fontenot	3	Bolted Plates			X	Al - Alloy 304-55	A	Contact area and pressure measurement as well as analysis.
Feldmanis	38	Bolted Plates	X		X	Al - Alloy	C	Used 1/4"-20 machine screws. Was able to correlate some data and prediction. Primary application interest electronic chassis cold plates.
Aron & Colombo	10	Bolted Plates		X	X	Al - Alloy	B	Significant contribution is pressure profile based on photo-elastic model, showing pressure drops off rapidly with bolt distance.
Elliott	39	Bolted Plate		X	X	Al - Alloy	C	Performed extensive tests on thin Al sheet. Noted separation of plates at distance from bolt. Use of washers decreased separation.
Whitehurst	36	Bolted Plates		X	X	Al - Alloy	A	Proposed an equivalent fin method, requiring experimental determination of temperature gradients. No correlation with others.

TABLE 2-1 BOLTED JOINT INVESTIGATIONS

2.1 SURFACES

It is evident that existing standards for surface characterization are inadequate to describe a surface for contact heat transfer purposes. The standard (ASA B 46.1-1962, Ref. 22) issued by the American Standard Association states "... This standard is concerned with the geometric irregularities of surfaces of solid materials, physical specimens for gaging roughness and the characteristics of instrumentation for measuring roughness. It establishes definite classifications for roughness, waviness, lay and a set of symbols..." While the definition of terms used in this report is based on the ASA standards definition, other concepts will be introduced.

The most comprehensive survey of "contact area" is a translation from the Russian (Ref. 24); however, it does not do very much for the design engineer, besides telling him what he already knows, that there is no universal surface definition. The major reason for the existing difficulty is due to the two-dimensional characterization of a three-dimensional surface topography.

The use of special apparatus was considered by several investigators. Henry (34) used a "trolley" with a stylus, which fed a signal into an analog computer. By tracing a pattern for each surface, a three-dimensional pattern could be established and the surfaces matched. Cassidy (35) at NASA-Lewis Research Center, has developed a scanning device which is coupled to a digital computer to establish the surface characterization as part of the conductance prediction.

From a practical viewpoint, it would be desirable to have a device to scan and provide a surface mating output suitable for contact conductance calculation. Such a device, if practical or portable, would be too costly for normal use. For this reason statistical methods have been considered, because surface characteristics may be quite

amenable to random and averaging procedures. Thus, while the exact profiles are indeterminate, the average of the profile protuberances is statistically predictable, provided the method of fastening (bolted, riveted) does not distort the surface, resulting in waviness. The surface characterization must consider: (a) microscopic protuberances, (roughness, asperities, short wavelength, etc.), (b) waviness (longer wavelength), (c) mating surface separation due to load. Engineering practice in defining surfaces varies due to differences in instrumentation, techniques, calibration and texture. Surprisingly, as stated in a survey article (Ref. 23), sight and touch surface standards provide more reliable surface matching than do instruments. Because of the absence of instruments which are comparative, current practice is limited to "topographic instruments", which result in nonreproducibility of surfaces by conventional means. One technique to achieve a random surface is by use of glass shot blasting. This method is described in reference (34).

Attempts were also made to circumvent the surface definition problem by introducing a predictable surface by several means, such as interstitial materials: wire-cloth (25) silicone rubber (21, 26), metallic deformable foils (25, 26), silicone grease (21, 25). While extensive theses could be written on the subject of contact surface examination and definition, this is not the place. The reader is referred to References 23 and 24 for a concise treatment of the general subject.

2.2 CONTACTS

The theory for contact heat transfer as based on contacts for rigid surfaces such as cylinders has been covered extensively in the literature. The most prominent of these reviews are Fenech (14), Clausen (15), Cetinkale (13) and Laming (16). All of these theories are based on Holms' (31) constriction resistance concept. Although this report is not concerned with theory of contact heat transfer, the subject of data correlation based on theory is of interest. For this reason, data correlations were

reviewed extensively with the objective of design applications in mind. The most pertinent of these are discussed. For development of the contact theory, the reader is referred to References 13, 14, 15 and 16.

2.3 CORRELATIONS

While there exist many correlations for contact heat transfer data, most of these are not directly suitable for an engineering approach, because they require knowledge of certain parameters which are not known or are difficult to measure. The most desirable expression would be one of the form

$$h = Cp^n \quad (2-1a)$$

$$\text{or} \quad h = B + Cp^n \quad (2-1b)$$

where h = contact conductance as defined in equation 1-1

B, C = constants for the material, fastening method and interstitial fluid (if any)

p = contact pressure over entire area unless otherwise defined

n = an exponent less than 1

There exist several correlations which approach this expression for contacts between rigid blocks in a vacuum. Hsieh (12) has taken the data of many investigators and, by use of dimensionless groups, correlated much of this data. He considers two cases, (a) rigid flat surfaces where the contact spots are distributed uniformly over the total area, (b) wavy surfaces where the contact spots are concentrated in groups. Bolted joints fall into the latter category. Hsieh provided an expression

$$\frac{h\bar{a}}{k_s} = C \left(\frac{P}{Y} \right)^m \quad (2-2)$$

where \bar{a} is the radius of the contact spots, k_s is the solid thermal conductivity, P is the contact pressure and Y is the yield strength of the material. C is a constant taken as $\frac{2}{3\pi}$ by Hsieh. If the mating surfaces are made of dissimilar material, then

the harmonic mean conductivity $k_m = \frac{2k_1k_2}{k_1+k_2}$ must be used for k_s and the lower of the two yield strengths (Y) must be used. For a contact where there is a fluid conductance as well, the above equation 2-2 becomes

$$\frac{\frac{h}{k_g} \delta_g - 1}{\frac{k_s \delta_g}{\bar{a}k_g}} = \left(\frac{2}{3\pi} \right) \left(\frac{P}{Y} \right)^m \quad (2-3)$$

where subscript g is for interface gap, s is for solid, δ is equivalent gap thickness, and all other terms as defined for equation 2-2. When k_g goes to zero, as in a vacuum, equation 2-3 reverts to the form of equation 2-2. The value of m is approximately 1.

Figure 2-1 shows a correlation of a variety of data for tests in air and in vacuum as presented in Reference 12. Figures 2-1a and 2-1b show the Ref. 12 data points for reference only. A constant value of $30 \times 10^{-6}m$ was assumed for \bar{a} and is a customarily assumed value based on References 28 and 31. The curve shown is for metallic materials including aluminum alloys, copper, titanium, magnesium alloy, stainless steel for roughness values ranging from $0.13 \times 10^{-6}m$ to $50 \times 10^{-6}m$. This figure represents both rigid flat as well as wavy surfaces with the spread of data greater at low P/Y values for the latter. It should be noted that this relation is relatively independent of temperature, other than the temperature dependent properties of the material and fluids. This also implies that radiation is negligible.

An expression of the form of equation 2-2 has also been proposed and recently used for contacts in a vacuum by Malkov (30), a Russian investigator. Malkov's expression is:

$$\frac{\bar{h}a}{k_s} = 0.118 \left(\frac{P}{3Y} S \right)^{0.66} \quad (2-4a)$$

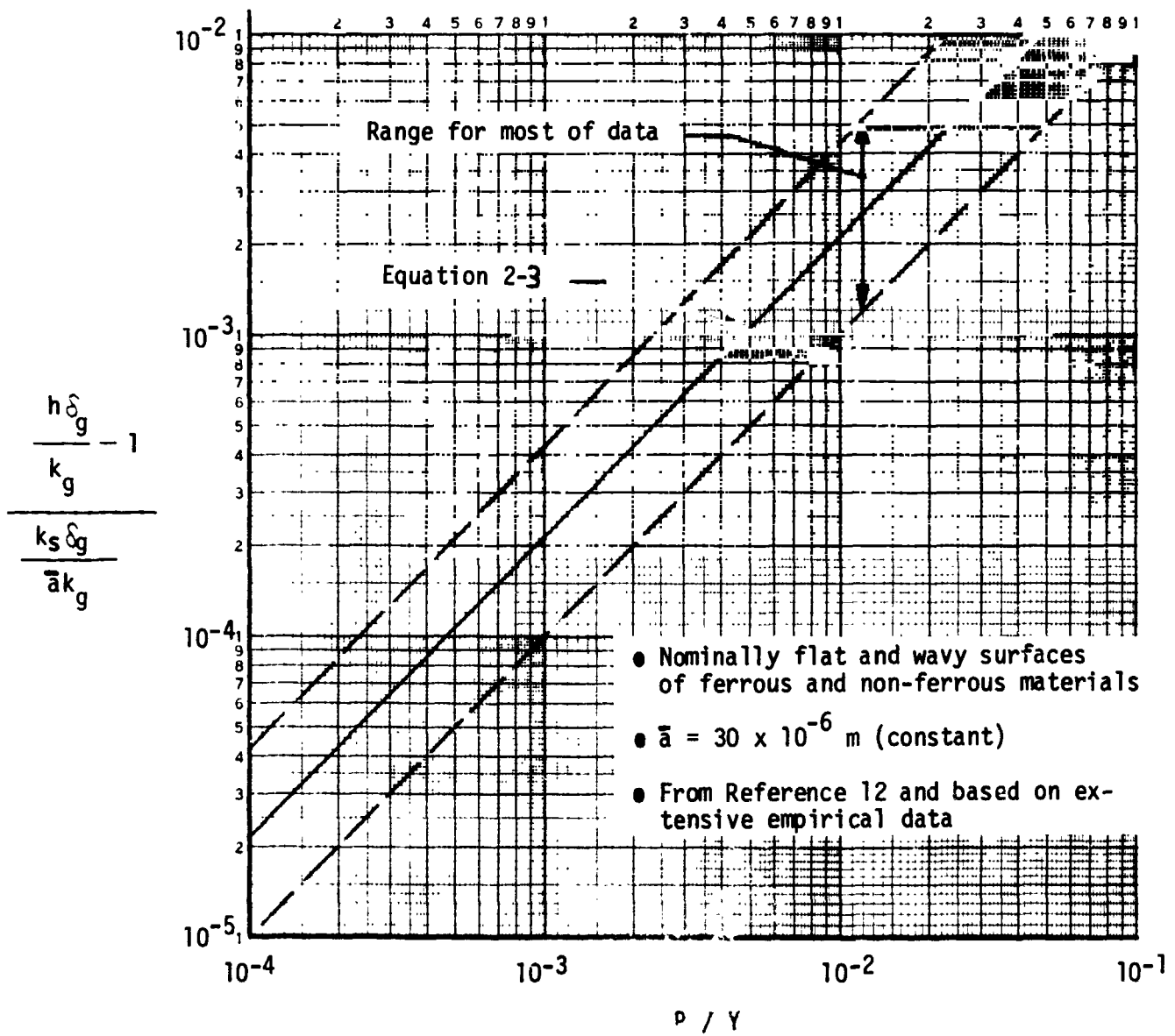
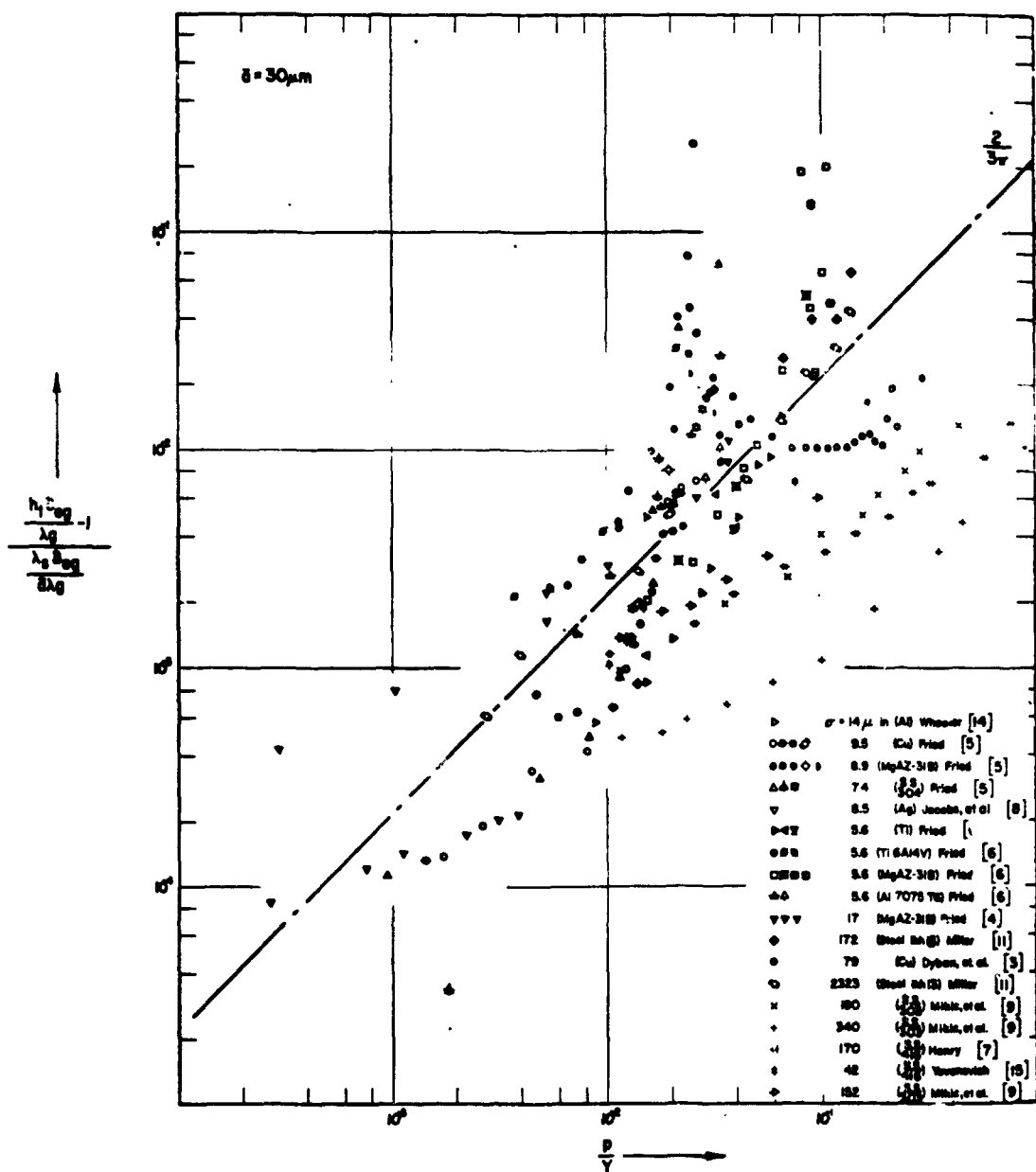
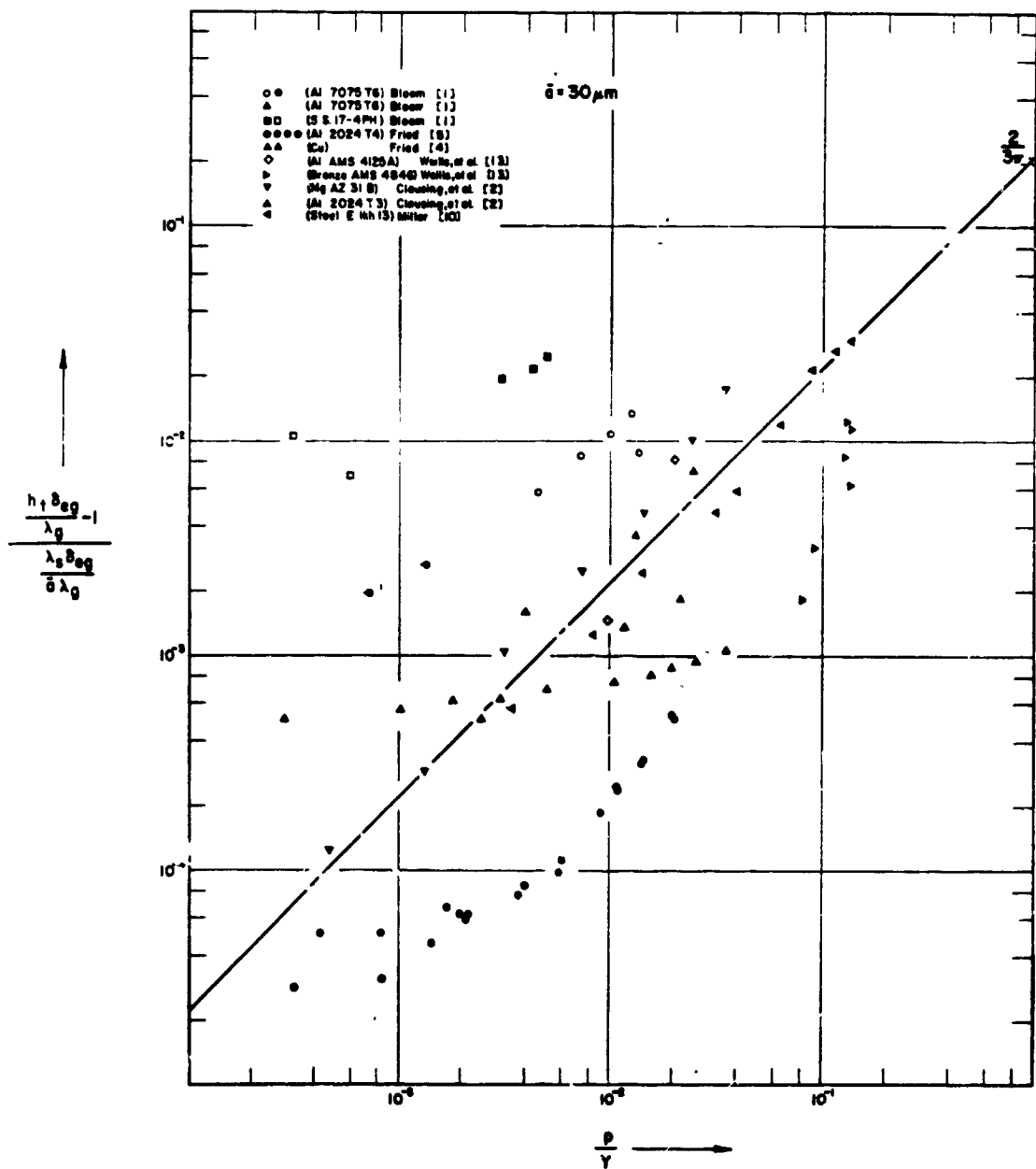


FIGURE 2-1
NON-DIMENSIONAL CONDUCTANCE CORRELATION (REF. 12)



Dimensionless Plot of $[(h_c \delta_{eg} / \lambda_g) - 1] / [\lambda_s \delta_{eg} / a \lambda_g]$ versus p/Y for Nominally Flat Surfaces of Ferrous and Non-Ferrous Materials with \bar{a} Taken as Constant.

FIGURE 2-1a COPY OF CORRELATION DATA POINTS IN REF. 12 (NOMINALLY FLAT SURFACES)



Dimensionless Plot of $[(h_t \delta_{eg} / \lambda_g) - 1] / [(\lambda_s \delta_{eg} / \bar{a} \lambda_g)]$ versus p/Y for Nominally Wavy Surfaces of Ferrous and Non-Ferrous Materials with \bar{a} Taken as Constant.

FIGURE 2-1b COPY OF CORRELATION DATA POINTS IN REF. 12 (NOMINALLY WAVY SURFACES)

which differs from equation 2-2 in the inclusion of S, a roughness factor depending on the height of the surface protuberances. Malkov uses a value for \bar{a} of $40 \times 10^{-6} \text{ m}$ as opposed to Hsieh (12), who used $30 \times 10^{-6} \text{ m}$. S is defined as shown below, where i_1 and i_2 are the mean height of the surface micro-projections. For all practical purposes this is roughly equal to the sum of the rms roughness values plus the waviness.

Sum of Surface Irregularities $i_1 + i_2$	$0-10 \times 10^{-6} \text{ m}$	$10 \times 10^{-6} \text{ m} - 30 \times 10^{-6} \text{ m}$	$30 \times 10^{-6} \text{ m}$
Engineering Units	$0-400 \times 10^{-6} \text{ in}$	$400 - 1200 \times 10^{-6} \text{ in}$	$1.2 \times 10^{-3} \text{ in}$
Value of S =	$\frac{(15 \times 10^{-6})}{i_1 + i_2}$	$\frac{(30 \times 10^{-6})}{i_1 + i_2}$	1

Figure 2-2 shows Malkov's attempt at dimensionless correlation of his own data as well as data from References 28, 29, and 18 taken in vacuum. For values of $SP/3Y$ above 10^{-2} , Shlykov's (29) equation

$$\frac{h \bar{a}}{k_s} = 0.32 \left(\frac{P}{3Y} \right)^{0.86} \quad (2-4b)$$

applies, whereas, at lower values, Malkov's equation (2-4a) correlates the data much better. It should, however, be noted that figures 2-1 and 2-2 are quite similar in values, while not in slope, over the range of interest, if it is recognized that P/Y in figure 2-1 must be divided by $S/3$ for comparison. The curve of figure 2-1 (Eq. 2-3) is shown in figure 2-2 for comparison. It is interesting to note that the proposed relations are quite close at P/Y values of 10^{-2} to 10^{-1} .

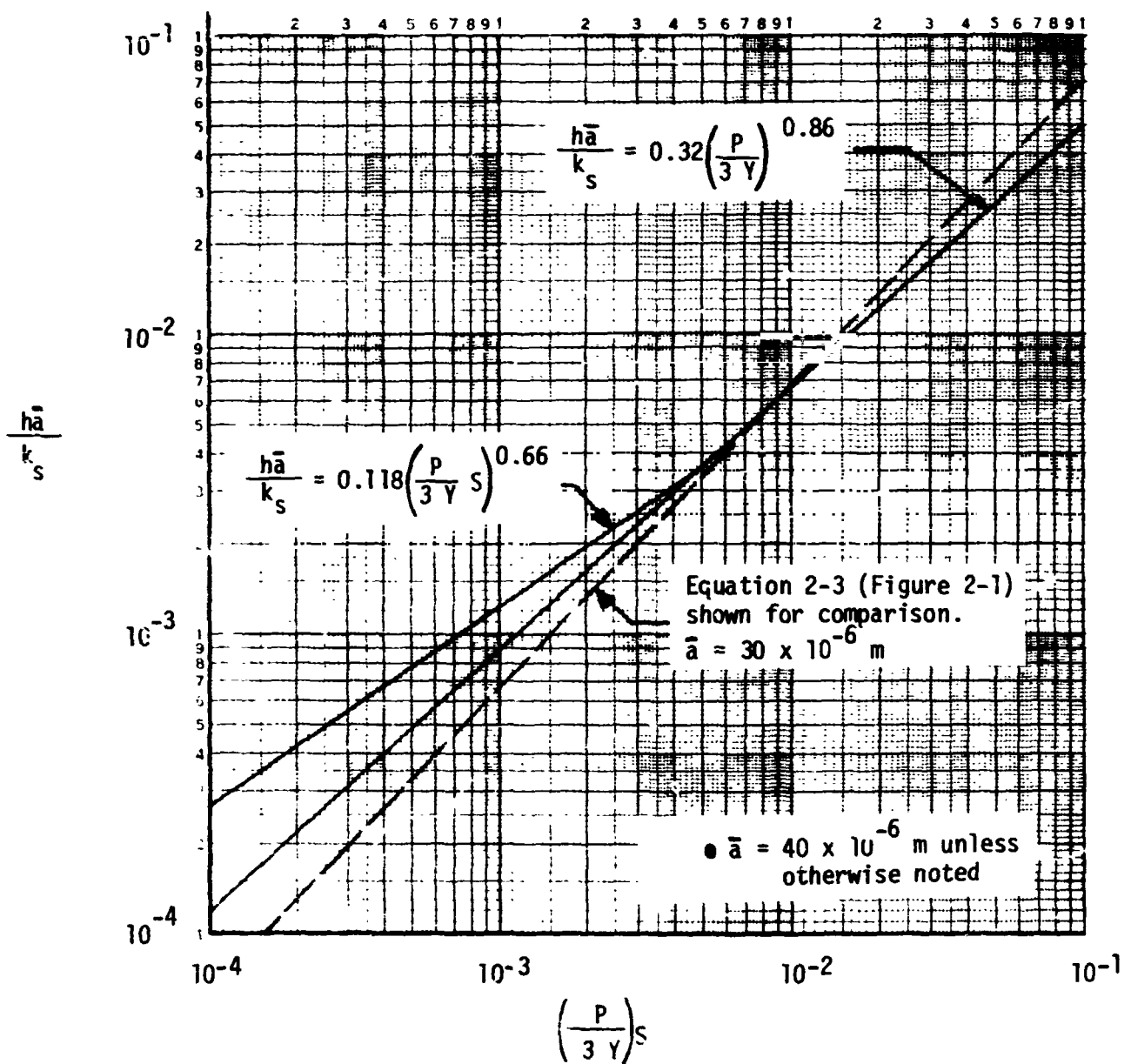
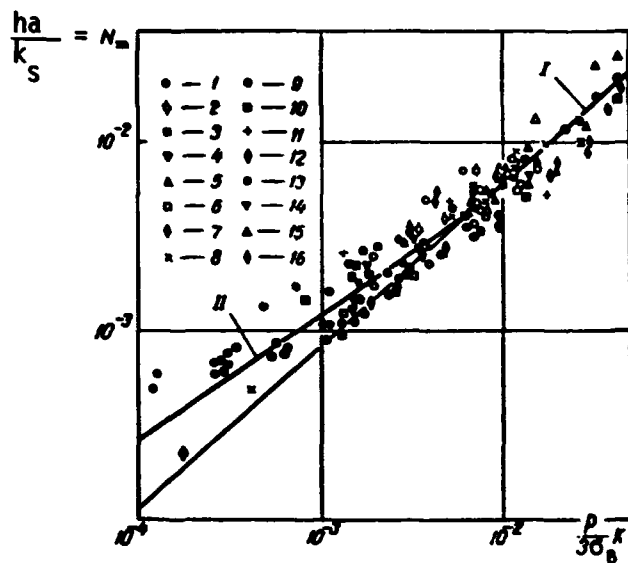


FIGURE 2-2

NON-DIMENSIONAL CONDUCTANCE CORRELATION (MALKOV IN REFERENCE 30)



Correlation of experimental data on heat transfer under vacuum in dimensionless coordinates.

- 1) Aluminum-uranium [5]; 2)-4) respectively aluminum-aluminum, aluminum-iron and aluminum-uranium [3]; 5) uranium-"magnox" alloy [4]; 6) stainless steel [2]; 7) DT 16 alloy [duraluminum?] [2]; 8) niobium [1], I) approximating equation (1) obtained from data described by points 1 through 8; 9) 45 steel, v_{10}/v_{10} [7] 10) 1 x 13 steel, v_{10}/v_{10} [7]; 11) 20 steel, v_{10}/v_{10} [8]; 12) magnesium v_{10}/v_{10} [6]; 13) molybdenum-stainless steel v_{10}/v_{10} , v_{10}/v_{10} , v_{10}/v_{10} ; 14) stainless steel turned to v_{10}/v_{10} ; 15) stainless steel ground to v_{10}/v_{10} ; 16) stainless steel turned and then lapped to v_{10}/v_{10} ; II) approximating equation (3).

FIGURE 2-2a COPY OF CORRELATION DATA POINTS IN REF. 30

Boeschoten (28) utilizes an expression of the form

$$\frac{h \bar{a}}{k_s} = 1.06 \left(\frac{P}{H} \right) \quad (2-5)$$

where H is the indentation hardness and is approximately equal to 3Y. Typical values given by reference 28 for H are $19 \times 10^4 \text{ N/cm}^2$ for steel, $14 \times 10^4 \text{ N/cm}^2$ for aluminum (the latter value is seven times that given in the literature). For example for an average value of \bar{a} of $30 \times 10^{-6} \text{ m}$ equation 2-5 becomes:

$$h = 0.33 \times 10^{-3} k_s \left(\frac{P}{H} \right) \quad (2-6)$$

with k_s in watts - $\text{cm}^{-1} \text{ } ^\circ\text{C}^{-1}$

h in watts - $\text{cm}^{-2} \text{ } ^\circ\text{C}^{-1}$

Fletcher (27) also developed a semi-empirical expression for the prediction of thermal contact conductance, based on experimental results in a vacuum of several investigators for materials such as aluminum, brass, stainless steel and magnesium, covering a wide range of test variables. Fletcher's correlation is:

$$\frac{h \delta_c}{k_s} = \sqrt{\pi} (3.8 \times 10^{-6} \delta_g^* + 0.026 P^* T^*)^{0.56} \quad (2-7)$$

where $T^* = T_{\text{mean}} \times \beta_s = \text{Dimensionless Temperature}$

$\beta_s = \text{Coefficient of thermal expansion}$

$P^* = P/E - \text{Dimensionless Pressure}$

$E = \text{Modulus of Elasticity}$

$P = \text{Apparent Pressure (as used previously)}$

$\delta_g^* = \text{Initial gap dimension/Apparent Contact Area Radius } (\delta_c/r)$

$r = \text{Sample Radius}$

Figure 2-3 shows the data points on which this equation is based and which is claimed to correlate this data within an average overall rms error of 24 percent or less for

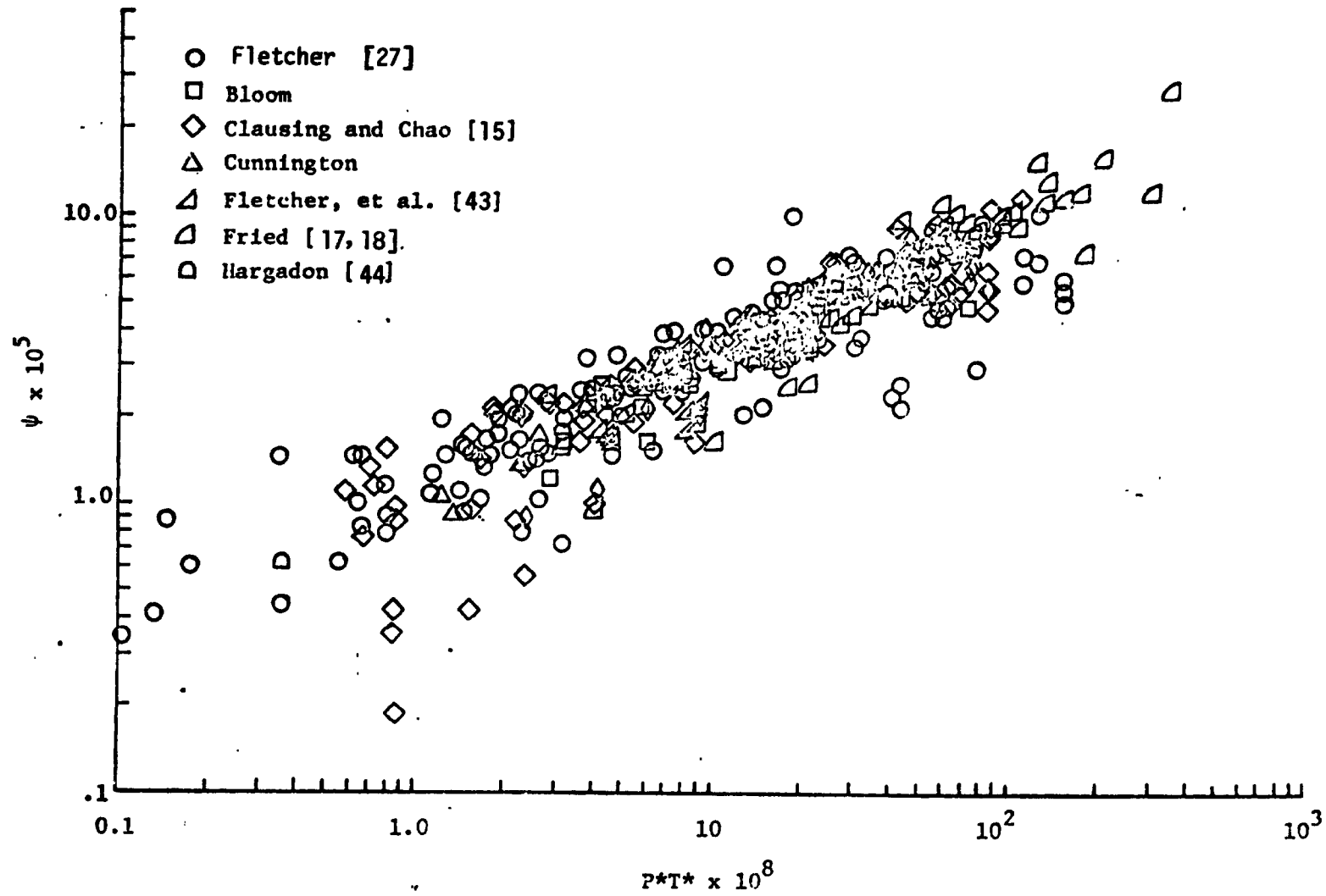


FIGURE 2-3
VARIATION OF THERMAL CONDUCTANCE NUMBER WITH
DIMENSIONLESS PRESSURE AND TEMPERATURE (REF. 27)

most of the data. This data covered a range of mean temperatures from -155°C (-250°F) to 260°C (500°F), apparent interface pressures of 0.69 N/cm² to 4930 N/cm² (10-7000 psi), flatness deviations of 38-11, 400 x 10⁻⁶ cm (15-4500 micro inches), and surface roughness ranging from 7.6 x 10⁻⁶ cm - 300 x 10⁻⁶ (3-120 micro inches). This data curve will not be used in the guidelines section because it requires extensive suboperation for input values. The equation is given for information only.

It is of interest to note that the conductance number $h \delta / k$ is always shown as a function of the applied load, an elastic deformation parameter and in some cases, the temperature. This implies that these correlations apply for the elastic region only, although it is reasonable to assume that some plastic deformation does take place.

Thus far, only equation 2-3 has considered the fluid conductance as an independent term. If one considers the total contact conductance h as being made up of the solid conduction term h_s and the gap conduction term h_g , then the latter term can be determined independently, as was done by Laming (16). Laming considered:

$$h_g = \frac{k_g}{\delta_g} \quad (2-8)$$

where, approximately,

$$\delta_g = 2/3 (i_1 + i_2)$$

This was determined experimentally by performing tests with several fluids in the gap. It is noteworthy to observe that a number of investigators found that the effective interface gap dimension δ_g is approximately equal to 2/3 of the sum of the peak-to-mean height (centerline average or rms values), $i_1 + i_2$ for the mating

surfaces. This does not take into account the waviness of the surfaces. Based upon the work of many contact conductance investigators, Fontenot (7) proposed an analytical approach to be used when no experimental data was available. The proposed expression is of the form $h = h_s + h_g$ and utilized previously discussed elements to provide:

$$h_c = \frac{k_g}{0.64 (i_1 + i_2)^{**}} + 2 (n \bar{a}) k_s \quad (2-9)$$

in consistent units. The first term is similar to Laming's (16) expression, equation 2-7, except that the coefficient for $(i_1 + i_2)^{**}$ is 0.64 instead of 0.67. The second term is the solid conductance term. Reference 3 replaces the $(i_1 + i_2)$ term, by using an empirically determined $(i_1 + i_2)^{**}$ term which apparently includes waviness effects. Fontenot (3) provides graphical means to relate i to surface roughness and load to the $n \bar{a}$ term, shown as figures 2-4a and 2-4b. Either of the above methods shown can be used, depending on the input data available. Application methods are shown in the Guidelines section. It should be noted that the cited experimental and analytical work assumes that all deformation are elastic and that all results are reproducible. This is not necessarily true. Cordier (32) and Popov (33) have observed experimentally that successive load applications result in increased conductance values. Cordier reports that not only did the repeated application of load result in higher conductances, but that the approach direction from higher and lower pressure made a difference. This was also observed by others. This is further complicated by the fact that long term contacts (months) result in increased conductance.

2.4 BOLTED JOINTS

This section provides capsule reviews of experimental and analytical work in the area of bolted joint heat transfer. For convenience, Table 2-1 provides an overview of the most important experimental work, however, each item is discussed in this section and where appropriate, used in the Guidelines.

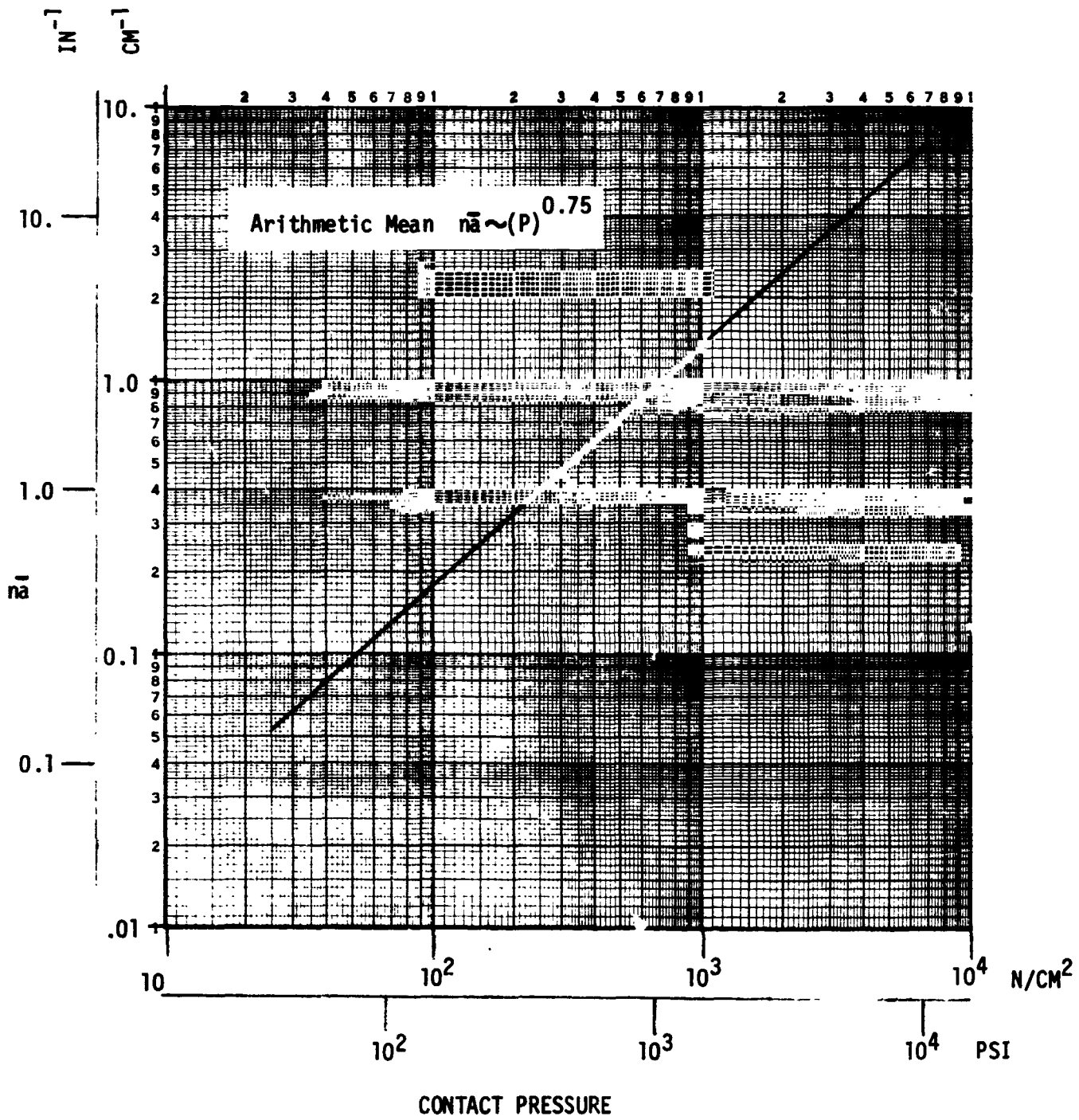


FIGURE 2-4a

CONTACT AREA PARAMETER VS. CONTACT PRESSURE (REF. 3)

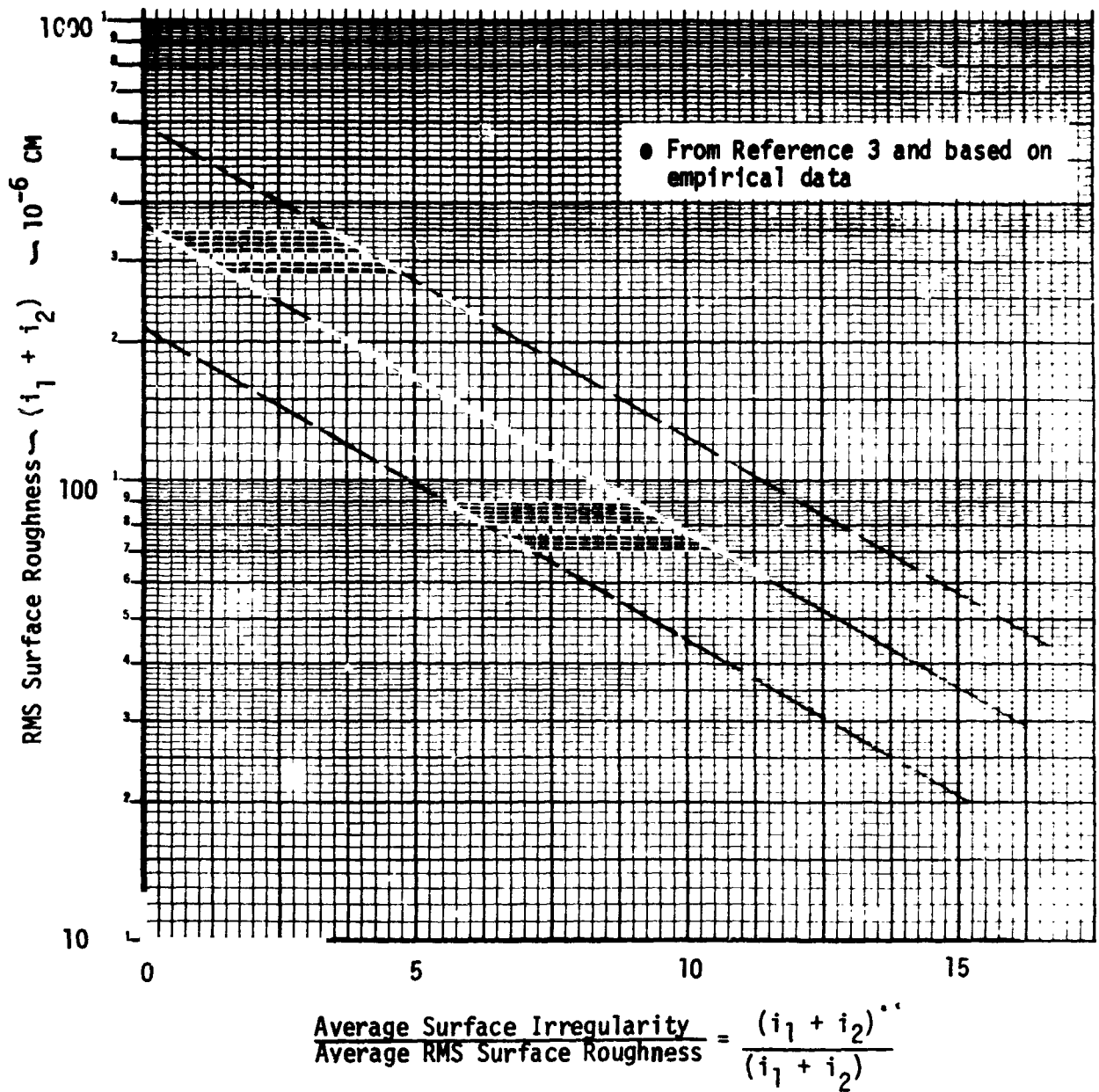


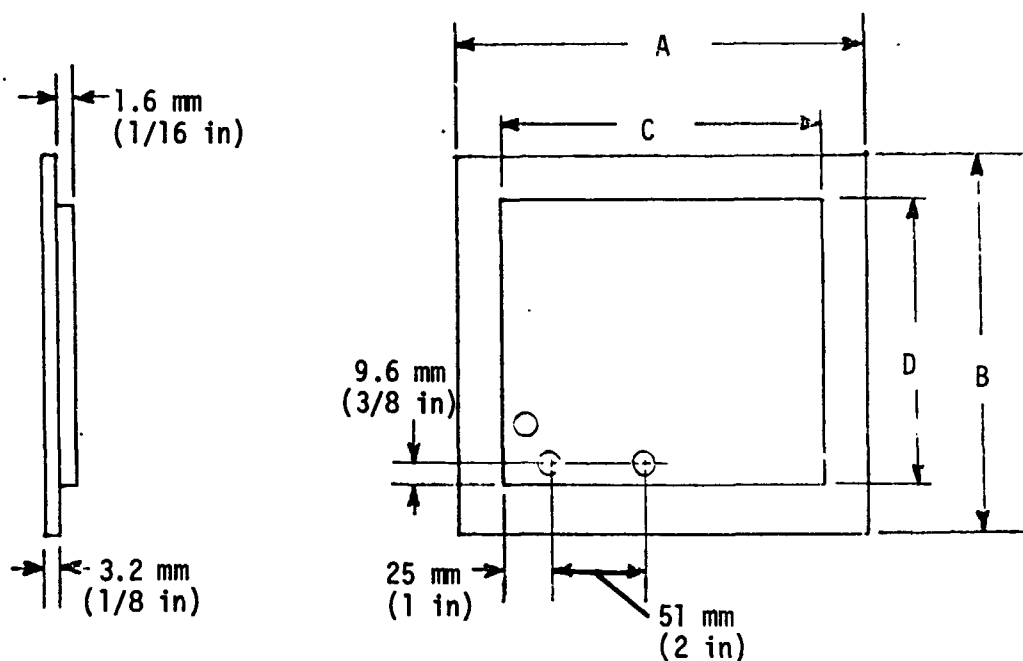
FIGURE 2-4b

RATIO OF AVERAGE SURFACE IRREGULARITY TO RMS SURFACE ROUGHNESS VS. RMS SURFACE ROUGHNESS (REF. 3)

Barzelay (19) performed a series of bolted and riveted aircraft stringer tests to determine the contact conductance of these joints under aerodynamic heating conditions. Other tests performed were on cylindrical column contact elements. The range of material tested included 2024T3 and T4,7075-T6 aluminum alloy and type 416 stainless steel. While the column tests were steady state, most of the others were transient tests in air, thus not suitable for our objectives. While observations and conclusions from Barzelay's work on roughness, contact pressure, use of interstitial filler material and temperature effects are used, none of the data will be shown in the Guidelines. Barzelay was the first investigator to report directional heat flow effects for dissimilar metal joints, however, the effects are not significant enough to be of concern in most design applications.

Bevans (21) performed an experimental program on component joints as well as structural joints, with the basic difference between the two being the greater rigidity of the latter. This work represents the first substantial attempt at evaluating "practical" spacecraft joints in a vacuum. Three types of structural and three sizes of component mounting joints were tested and a method for the correlation of bolted joints was proposed. The most obvious result reported was the inconsistency of data for presumably identical joints.

It should be noted that no special instructions were given to the technicians assembling the joint relative to the order of tightening the bolts, although the bolt torques were set with a calibrated torque wrench. This procedure was deliberate in order to achieve randomness of fabricated joints. Figures 2-5 and 2-6 taken from Reference 21 show the tested configurations. For each of these configurations, tests were performed on more than one sample and using a heat transfer promoting filler in some instances. Table 2-II shows the averaged results for the component joints.



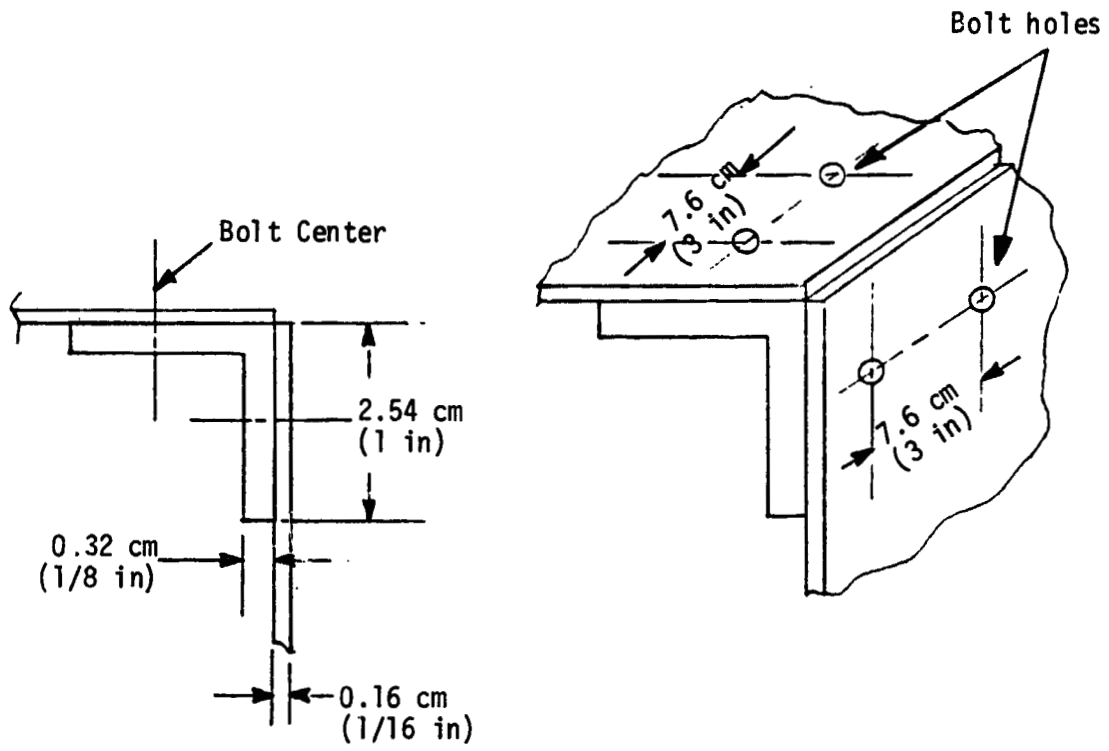
CONFIG.	A	B	C	D
1 12 Bolts	20.32 cm (8 in)	20.32 cm (8 in)	15.24 cm (6 in)	15.24 cm (6 in)
2 18 Bolts	35.56 cm (14 in)	20.32 cm (8 in)	30.48 cm (12 in)	15.24 cm (6 in)
3 24 Bolts	35.56 cm (14 in)	35.56 cm (14 in)	30.48 cm (12 in)	30.48 cm (12 in)

● Bolts were 4.75 mm (3/16 in) diameter

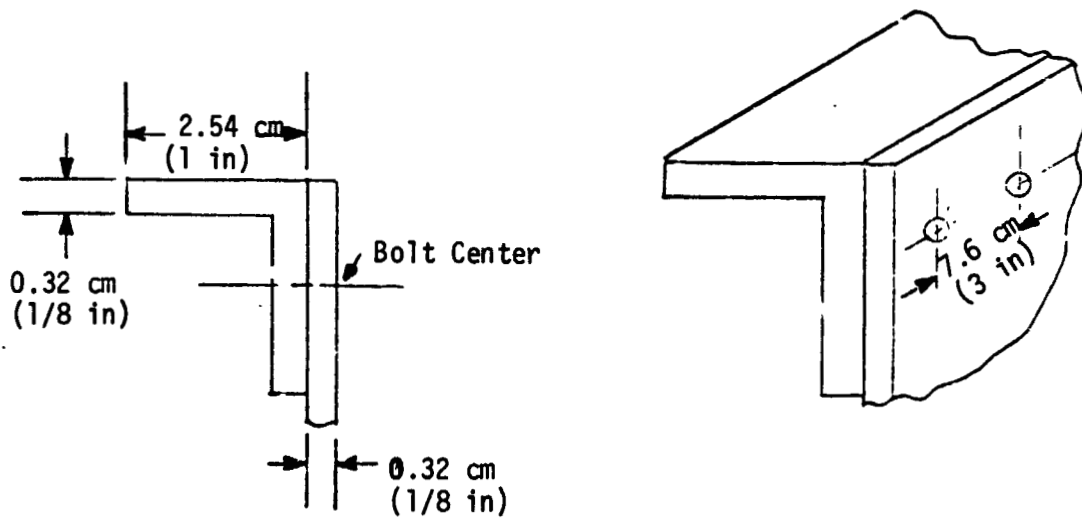
FIGURE 2-5
CONFIGURATION AND DIMENSIONS FOR COMPONENT JOINTS (REF. 21)

FIGURE 2-6

CONFIGURATION AND DIMENSIONS FOR STRUCTURAL JOINTS (REF. 21)



Configurations 4 and 5 (Material - Aluminum 6061-T6)



Configuration 6

TABLE 2-II

Test Config. (see fig. 2-)	BOLT TORQUE - mN (in-lbs)			Inter ce Filler
	1.35 (12)	2.71 (24)	3.39 (30)	
	Contact Conductance Watts-m ⁻² -°C ⁻¹ (BTU-hr ⁻¹ -ft ⁻² -°F ⁻¹)			
1	151.7 (26.7)	152.8 (26.9)	170.4 (30.0)	none
1	588.4 (103.6)	574.2 (101.1)	806.6 (142.0)	RTV II
1	291.4 (51.3)	277.2 (48.8)	323.8 (57.0)	G-683 silicone grease
2	--	102.2 (18.7)	--	none
2	--	553.8 (97.5)	--	RTV II
3	--	47.1 (8.3)	--	none
3	--	302.7 (53.5)	--	RTV II

AVERAGED VALUES OF JOINT CONDUCTANCE FROM REFERENCE 21
FOR COMPONENT JOINTS. (ENTIRE CONTACT AREA WAS USED IN
CALCULATION)

The reported surface finish was $28 \times 10^{-8} \text{ m}$ ($11 \times 10^{-6} \text{ in}$) rms across the roll marks and $10 \times 10^{-8} \text{ m}$ ($4 \times 10^{-6} \text{ in}$) rms with the roll marks. This is a fairly good finish for an "as received" surface. The component mounting plates also had a nonflatness of as much as $17.8 \times 10^{-5} \text{ m}$ (0.007 in.) for No. 2, and $7.6 \times 10^{-5} \text{ m}$ (0.003 in.) for the other joints. This nonflatness was reported to have had some beneficial effect on conductance when it improved the contact area, however, benefits cannot be clearly defined. Bevans (21) also reported that for thin plate joints, the principal thermal resistance was in the thin plate itself.

Results for joints using an interstitial filler of RTV-11 silicone rubber and G-683 silicone grease are shown for comparison purposes in addition to bare metal joint data. It should be noted that the area immediately under and adjacent to the bolt has a definite relation to the overall conductance, because most of the conduction heat transfer takes place in that region as opposed to the entire mounting area. This is due to the fact that while the number of bolts increases with the perimeter, the mounting area increases at a greater rate. Since the contact conductance was based on the total area, it decreased as the total interface area increased. Had the joint conductance been based on the area immediately adjacent to the bolts, i.e., a function of the number of bolts, then the conductances would have been less inconsistent. For example, dividing the total heat flux by the bolt area perimeter would make the conductances vary by 25%.

The data shown for interstitial fillers, shows a slightly better consistency for configurations 1 and 2, however, due to the potential variations in filler composition, thickness, etc., no real conclusion can be made other than that fillers do indeed help.

For the structural joints shown in figure 2-6, only the bare joint data will be considered. There were variations in contact conductance from joint to joint within each of the configurations, but for identical samples. Table 2-III shows the results for Reference 21, but averaged values only. It was observed that the heat flux through the joint was not a significant variable. The data for the rigid structural joint, configuration 6, is within the range used for bare joints on the NIMBUS spacecraft ($850 \text{ W-m}^{-2}\text{-}^\circ\text{C}^{-1}$).

Reference 21 describes a proposed method for predicting the conductance in a bolted joint. It postulates that the points of contact which contribute to the conductance are in the small region under the adjacent to the bolts. This is an agreement with the approaches of other investigators. The item of interest is the method of a) determining the apparent contact area and pressure and b) the corresponding conductance for the contact regions, where an averaged pressure is used over this contact region.

An expression providing a load distribution of the form shown in figure 2-7 was used and was based on work by Lindh (37). Similar load distributions were postulated by Aron (10) and others. Since the localized load values depend on the applied load, the uniform load within the bolt was determined by use of the following approximate relation,

$$\frac{\text{Bolt Torque}}{(\text{Tensile Force}) (\text{Major Thread Dia})} = 0.20 \quad (2-10)$$

using consistent units. This relation assumes a standard 60° thread and a friction coefficient of 0.15.

TABLE 2-III

Configuration	CONTACT CONDUCTANCE		Interface Filler
	Watts-m ⁻² -°C ⁻¹	(BTU-hr ⁻¹ -ft ⁻² -°F ⁻¹)	
4	480.0	(84.5)	none
5	531.7	(93.6)	none
6	825.9	(145.4)	none

Bolt Torque 2.71 m-N (24 in-lbs)

AVERAGED VALUES OF JOINT CONDUCTANCE
FROM REFERENCE 21 FOR STRUCTURAL JOINTS

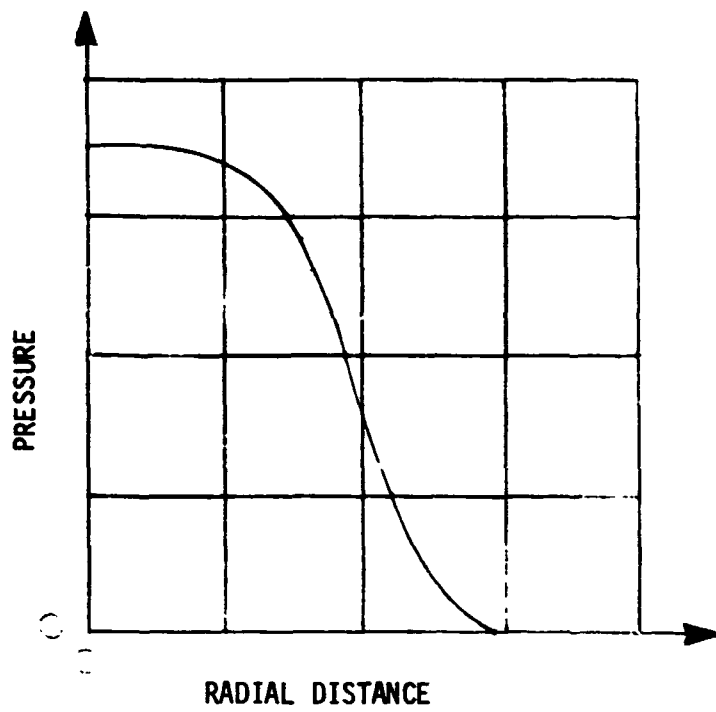


FIGURE 2-7
PRESSURE DISTRIBUTION UNDER BOLT HEAD IN BOLTED PLATE

An acceptable expression relating the localized load and radial distance from the bolt is needed. Once the localized or averaged load is determined, the corresponding contact conductance can be found from known experimental data or by use of an analytical expression.

Aron and Colombo (10) performed photoelastic experiments to evaluate the actual contact region as well as thermal experiments with a bolted joint. While their prediction of thermal tests was inconclusive, their estimation of contact region is useful. For a bolted joint of equal thickness plates, they assume the interface pressure to drop to zero at a radius equal to the loading radius plus 1.5 to 2 times the thickness of the plates.

Rolsma (20) performed one of the most extensive test programs for the evaluation of bolted joints in a vacuum. Three different lap joint configurations, with variations in thickness, bolt spacing torque, surface finish and temperatures were evaluated for a total of over 500 test points. Figure 2-8 shows a typical joint with thermocouple locations. The major conclusion for this work was that the experimental data was not suitable for deriving an analytical or empirical procedure. However, a number of very useful conclusions were made. These are:

- Joint samples with a bolt spacing/thickness ratio less than approximately six are thermally thick and the interface resistance is controlling. These samples exhibit a change in contact conductance with torque.
- Joint samples with a bolt spacing/thickness ratio greater than approximately six are thermally thin and controlling resistance lies in the material itself. These samples exhibit no consistent change in contact conductance with torque.
- The values of contact conductance which have been obtained are associated with the temperature difference as defined by the location of the sensing thermocouples. Any attempt to associate these coefficients with another temperature difference in an analytic procedure will lead to errors.

- Addition of a 1/16[•] inch phenolic laminate insulating spacer between the mating surfaces effectively blocks heat transfer across the interface.
- Addition of a pliable foil (Indium) between the mating surfaces increased the contact conductance even with samples which were thermally thin.

Of particular interest is an experiment Rolsma (20) performed to relate applied torque to axial bolt load and perhaps even pressure. A number of bolts were successively torqued to increasing values (0.11, 0.057, 0.085 meter-Newtons, /50, 75, 100 in-lbs) and this cycle was repeated 14 times. For each torque application, the axial load was recorded, based on the output of a strain gage load washer under the bolt head. As shown in Figure 2-9, the axial load did not stabilize for a given torque wrench application until the approximately seventh cycle. This would imply that the load for most bolted joint experiments is not stabilized unless at least seven applications have been made.

Observations made during the tests of Reference 20, indicated that there was virtually no heat flow across the joint near the edges (see Figure 2-8). Thus, the choice of what represents the actual joint area determines the average joint conductance. Furthermore, the locations, number and adequacy of thermocouples in a test joint strongly affects the quality of conductance data. The length of the undisturbed joint "length" also affects the temperature measurement adequacy to avoid performing measurements in the "disturbed" region.

Figure 2-10 shows joint conductance data from Reference 20 for a lap joint of the type shown in Figure 2-8 as type III. Figure 2-11 gives the actual joint geometry of the configurations tested in the work of Reference 20. This data (Figure 2-10) shows that, for a given torque loading on the bolts, the joint conductance decreases

• 0.16 cm

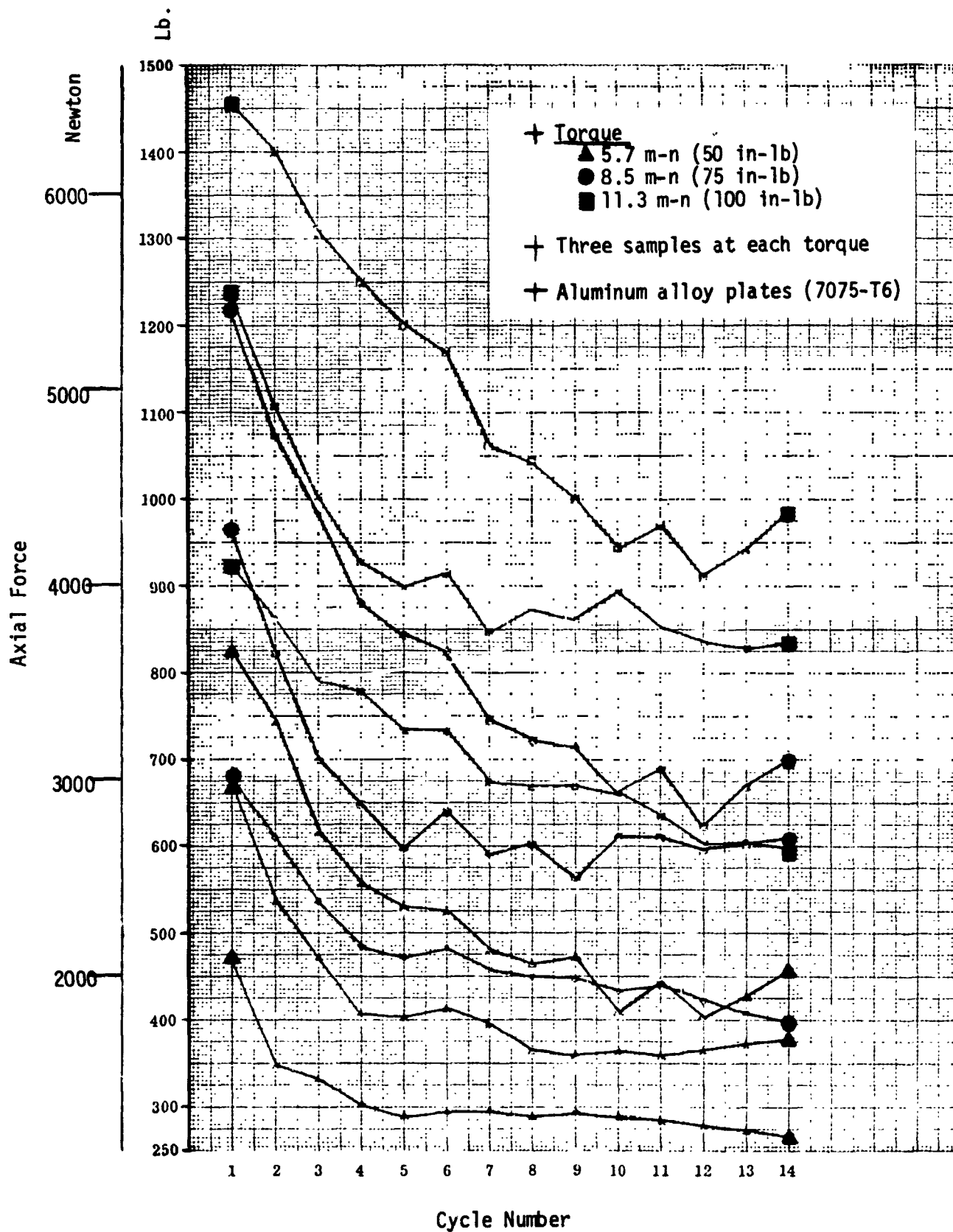


FIGURE 2-9

AXIAL FORCE VS. TORQUE VARIATION (REF. 20)

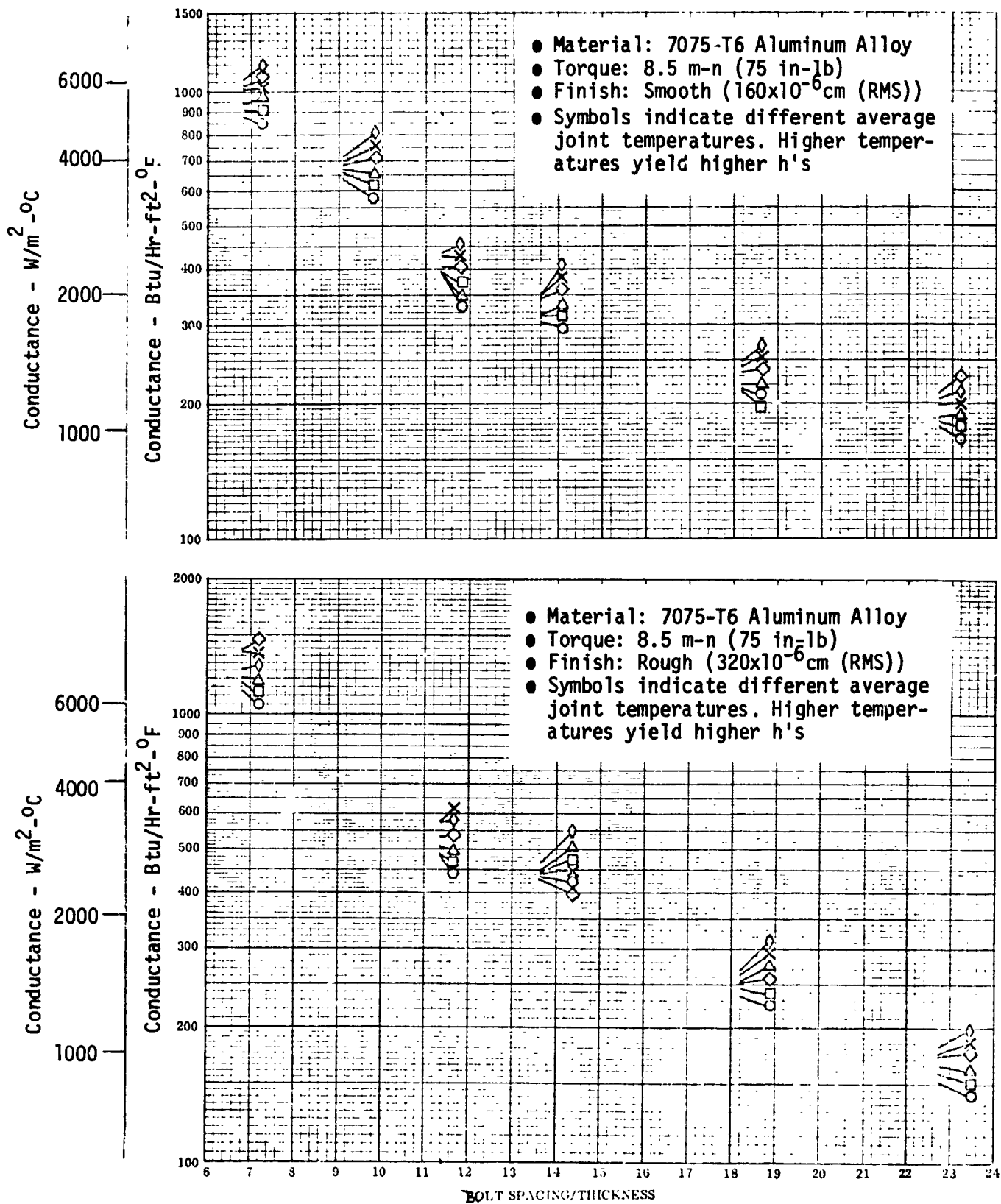
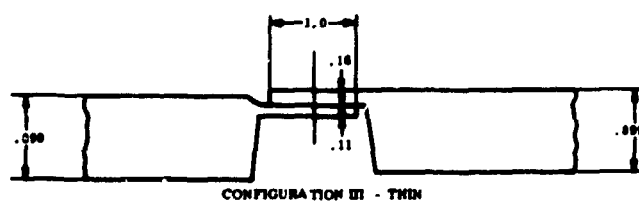
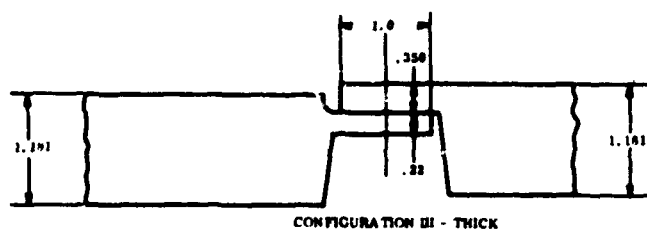
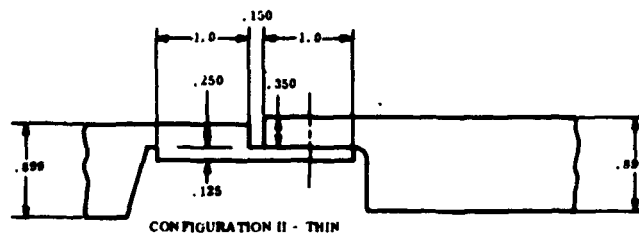
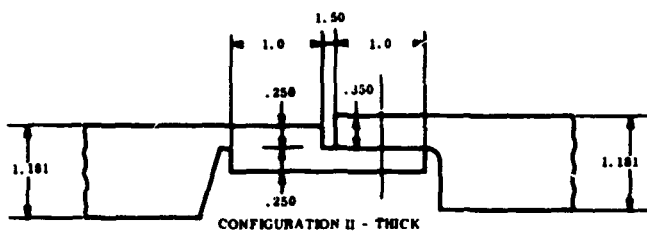
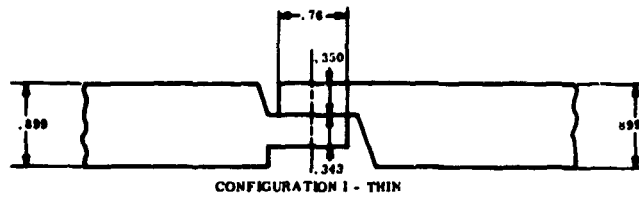
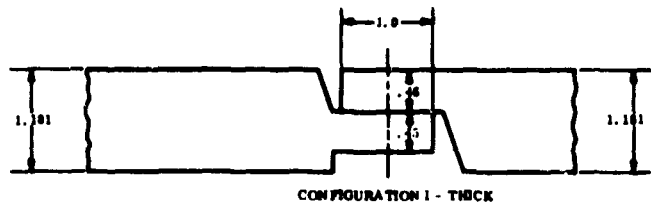


FIGURE 2-10

BOLTED LAP JOINT CONDUCTANCE VS. GEOMETRY (REF. 20)



All dimensions in inches
(1 inch = 2.54 cm)

FIGURE 2-11
SAMPLE JOINT GEOMETRY (REF. 20)

as the bolt spacing to thickness ratio increases. The temperature effect also is noticeable, with higher temperatures giving higher conductances. The effect of surface finish is within expectations, showing slightly higher conductances for rough finish surfaces. Other geometries follow similar relations.

It should be noted that the samples for the above work were made of 7075-T6 Aluminum alloy and were joined using captive 1/4-28 screws (Calfax Inc., Series CA 1137) and a floating nut (Kaynar Mfg. Company, MF-10-31-4). Smooth surfaces were 160×10^{-6} cm rms (63×10^{-6} in.) and rough surfaces were 320×10^{-6} cm rms (125×10^{-6} in.) machined finishes at the mating interfaces. This information is provided for reference because the extensive amount of test data provided by Ref. 20 may be directly suitable for some applications.

Fontenot (3) performed tests on a pair of relatively simple lap joints made of 6061-T6 aluminum and 301 stainless steel. The joint consisted of two plates, 17.8 cm (7 in.) long and 5.1 cm (2 inch) wide, with the aluminum plate 0.63 cm (1/4 inch) thick and the steel plate 0.32 cm (1/8 inch) thick. Two holes, approximately 0.6 cm in diameter and about 1.27 cm from the side and edges, were used for fastening the joints. Bolt torques were 10.83 m-N (96 in-lbs) and 20.31 m-N (180 in-lbs.). Average joint conductances are not provided in this reference, but local temperature differences are given. For this reason, the experimental thermal data is not directly useable. Comparison of the test joint of a sample configuration and instrumentation of Ref. 3 with other experiments such as that of Ref. 20, indicates that errors in heat flux uniformity and temperature measurement may have occurred.

Fontenot (3) did, however, investigate the problem of interface stress distribution and bolted plate deflection, drawing on the work by Fernlund (9), Lindh (37), Sneddon (45), Aron (10) and others. Of interest is the original work on the value of

r_0 , the radius of zero interface stress, where mating plates would separate. Figure 2-12 shows Fontenot's (3) data as well as that of others and can be used to determine the extent of the contact area under a bolt. Table 2-IV, also from Ref. 3, shows the actual values. It should be noted that for small values of b , i.e. thin plates, separation occurs near the bolt head. This data is of value in the guidelines section. Feldmanis (38) performed a number of bolted joint experiments, however, the test conditions were "too practical" to be of general use. Tests were performed including power input variation and bolt torque variations. Conductances ranged from $500-9000 \text{ W-m}^{-2}\text{-}^\circ\text{C}^{-1}$ ($100-1600 \text{ BTU-hr}^{-1}\text{ft}^{-2}\text{-F}^{-1}$) for bolt torques up to 5.6 m-N (50 in-lbs) with power input of up to 100 watts in a simulated "black box" mounted on a cold plate. For applications of this type, this data may be directly useable. Bolt spacing was 3.87 cm (1.5 inches) for $1/4\text{-}20$ machine screws. Feldmanis also investigated the use of steel bolts with aluminum plates to take advantage of differential thermal expansion. This resulted in thermal conductance increase of 100% when the heat input increased from 25 to 100 watts. Figure 2-13 shows this effect of heater power and bolt torque on conductance.

Whitehurst (36) investigated a simplified experimental method of lap joint conductance prediction. The test item was fairly simple and it is very probable that edge loss errors were present. An equivalent fin method (EFM) is proposed, which requires that temperature gradients be obtained on both sides of the joint of interest. Since this method requires construction of a prototype or a model, it does not really add to the body of prediction techniques, unless scale modeling is considered. Whitehurst states, that an analytical method of joint conductance prediction requires many assumptions and approximations, which may eventually render the method inaccurate. While experimental methods are more reliable, they also are subject to gross errors, as was reported in Ref. 20. The data reported does not add to the body of knowledge, although the EFM technique may be of interest in structural applications.

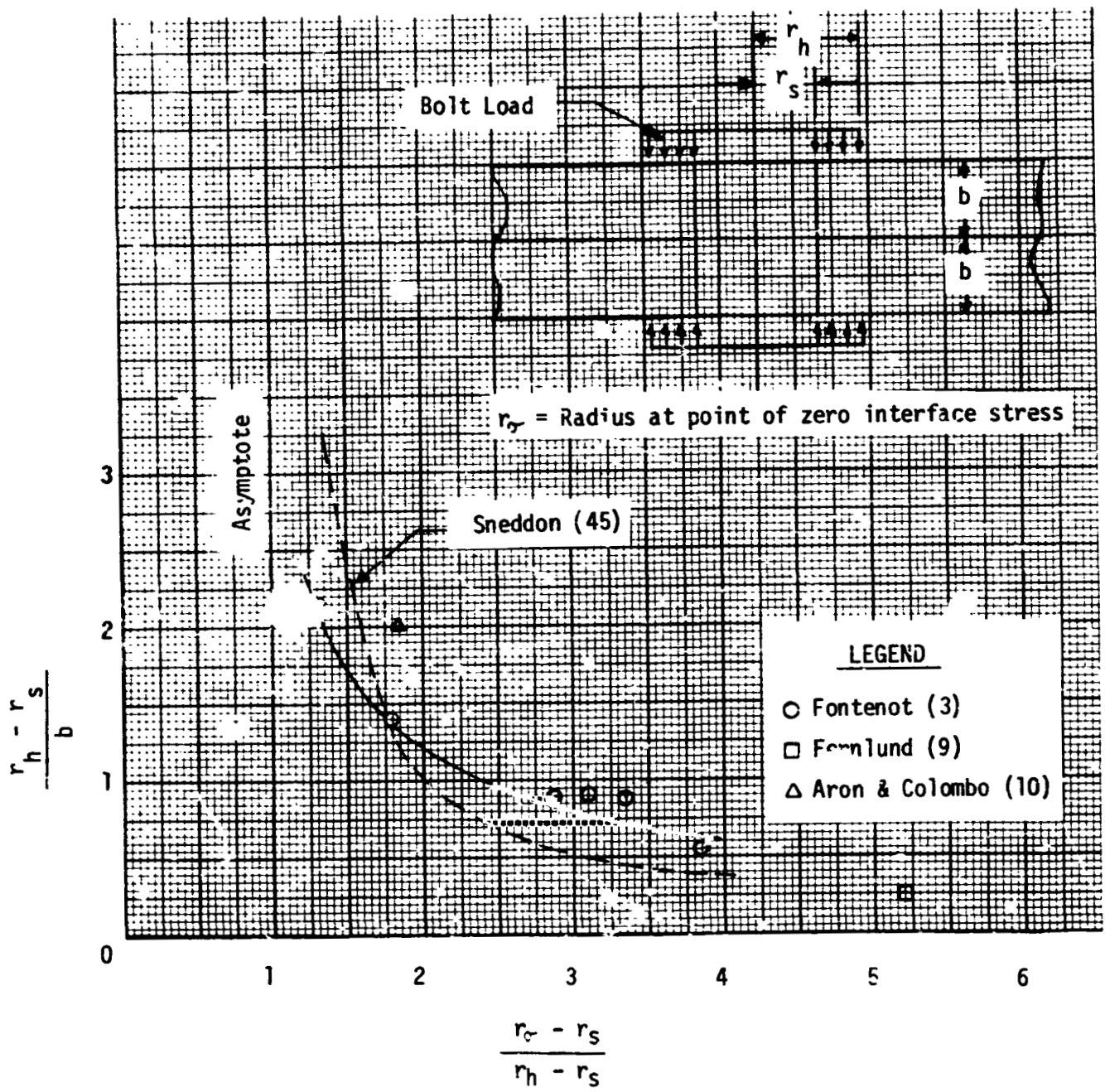


FIGURE 2-12

NON-DIMENSIONAL "ZERO INTERFACE STRESS" (REF. 3)

TABLE 2 - IV

VALUES OF r_{σ} AS DETERMINED BY VARIOUS INVESTIGATORS (Ref. 3)

$\frac{r_h - r_s}{b}$	$\frac{r_{\sigma} - r_s}{r_h - r_s}$	Type of Data	Source
0.5	3.0	Theoretical	Sneddon (45)
1.	2.0	Theoretical	Sneddon (45)
2.	1.6	Theoretical	Sneddon (45)
3.	1.4	Theoretical	Sneddon (45)
∞	1.0	Theoretical	Sneddon (45)
0.25	5.6	Theor. & Oil Press.	Fernlund (9)
2.00	1.83	Photoelastic	Aron&Colombo (10)
0.53	3.88	Oil Pressure	Fontenot (3)
0.89	3.32	Oil Pressure	Fontenot (3)
0.89	3.10	Oil Pressure	Fontenot (3)
0.89	2.88	Oil Penetration	Fontenot (3)
1.38	1.78	Oil Penetration	Fontenot (3)
2.62	1.27	Oil Penetration	Fontenot (3)

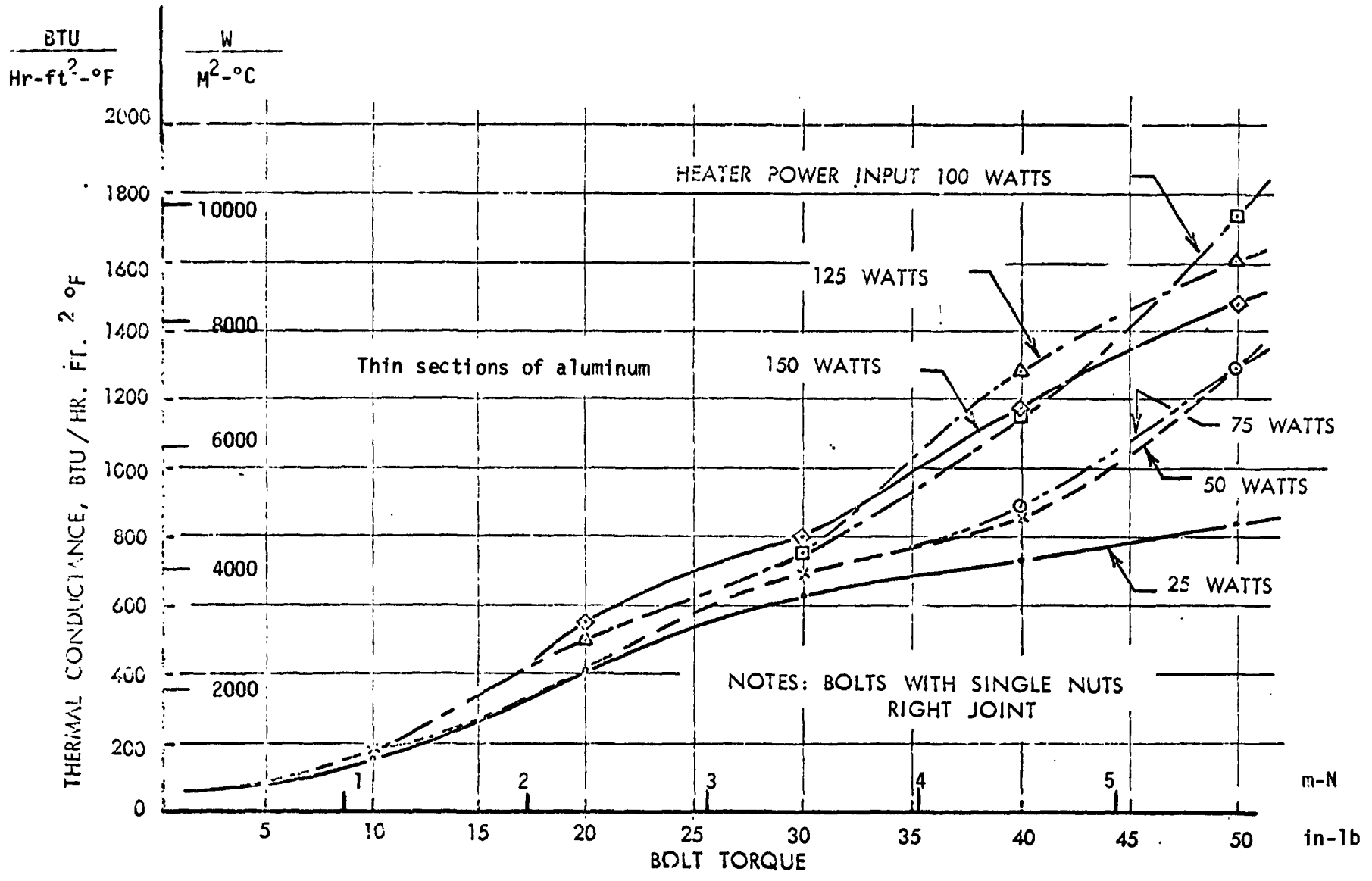
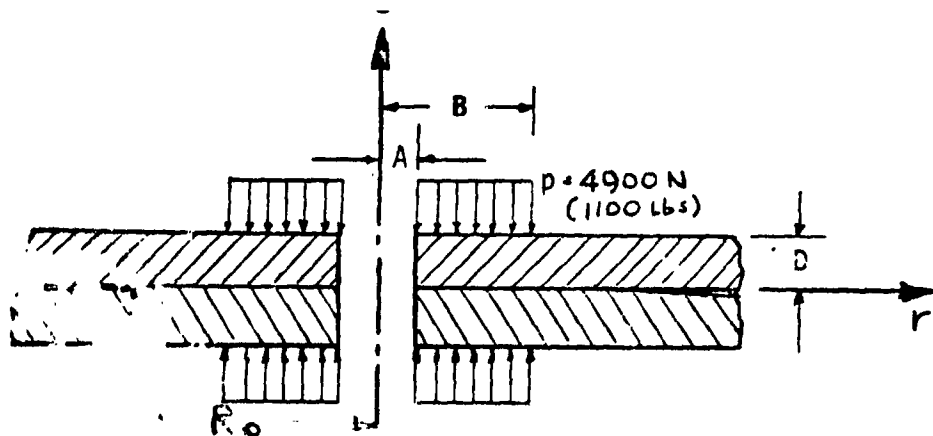


FIGURE 2-13
THERMAL CONDUCTANCE VS. TORQUE (REF. 38)

Gould and Mikic (11) performed an experimental and analytical study of the actual contact area in a bolted joint. The experimental program was performed to measure the actual contact area between bolted circular discs. One method utilized the polishing action at the interface when mating plates under load are rotated with respect to each other. The polished area represents the true contact area. Plates were made of 304 stainless steel. The second method employed an autoradiographic technique, where one plate of a mated pair was covered with radioactive silver and assembled with an untreated plate. All but one set of these plates were rotated once, followed by disassembly and measurement of the radioactive contamination on the previously untreated plate. Photographic x-ray techniques were also used in this test. These tests were performed with loads of 4900 N (1100 lbs.) with an applied torque of 7.9 m-N (70 in-lbs.). The computational approach, employing a finite element technique is in substantial agreement with these experiments and yielded smaller zones of actual contact than the data in the existing literature indicates. This appears primarily due to the previous assumptions based on single plate models, rather than a two plate model as used by Gould. Test results are shown in Table 2-V which also shows the joint geometry designation. It should be noted that this data applies to stainless steel plates and that a computer program is necessary for predictions. It would be of interest to see whether this technique will work for aluminum alloys as used in spacecraft systems.

Shih (46) attempted to apply thermal scale modeling techniques to bolted joints. Experimental work was performed on 2024-T4 aluminum, ZH62A magnesium and 304 stainless steel joints. While the modeling work was claimed to be successful, the experimental work is of greater interest because of the large number of test points and test sample approach. Figure 2-14 shows the configuration and test results for ungreased joints. The conductance values are within expected ranges for this type of joint.

TABLE 2-V
 TEST AND ANALYTICAL RESULTS FOR RADII
 OF SEPARATION OF BOLTED PLATES (REF. 11)



Case	Plate Thickness D in.	2B in.	Separation Diameters, $2 R_o$ - in.				% Discrepancy Between Computed Values and Tested Values		
			"Rubbing Test"		Autoradiographic Test		Computed	Rub. Test	Autorad. Test
			Range	Average	Range	Average			
1	.065	.422	.42-.48	.45	.41-.46	.44	.488	7.8	9.8
2	.124	.422	.50-.53	.51	.4 - .6	.55	.554	7.9	.7
3	.191	.422	.58-.64	.62	.76-.81	.78*	.620	0	25.8
4	.253	.422	.70-.76	.72	.68-.73	.7**	.700	2.9	0
5.	Unmatch- ed Pair .124/ .257	.422	.54-.58	.56	—	—	.588	4.8	—
6.	.124	1.0	1.06-1.10	1.09	—	—	1.104	1.3	—
7.	.191	1.0	1.11-1.17	1.16	—	—	1.210	4.1	—

Stainless Steel (304)

1 inch = 2.54 cm

* Original x-ray film shows hole in plate and 0.6 inch diameter zone more distinctly than remainder of area sensitized by the radioactive contamination. Loose radiographic contamination observed during test.

** Assembled and disassembled radioactive and non-radioactive plates without rotating plates relative to each other.

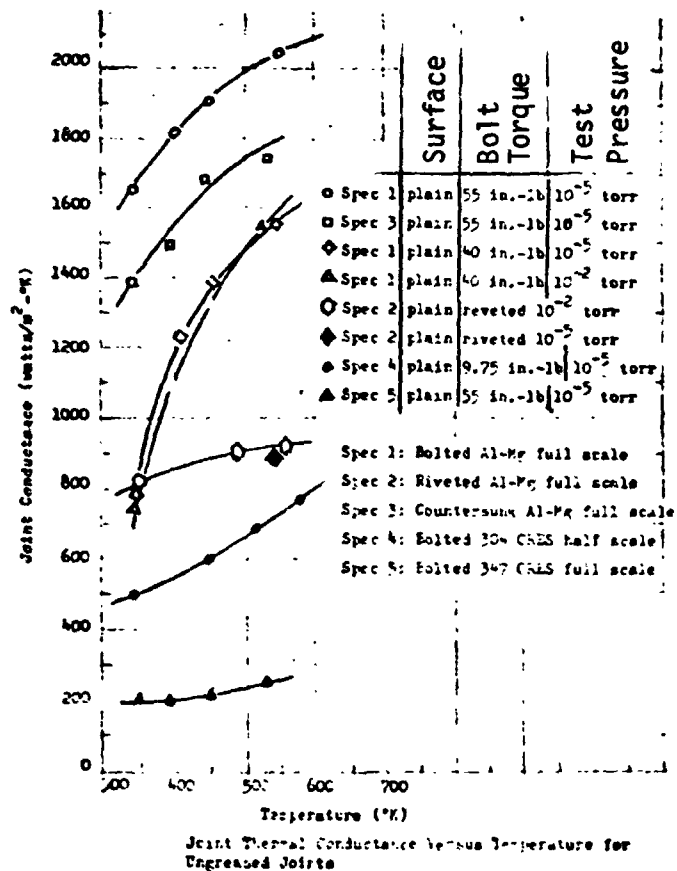
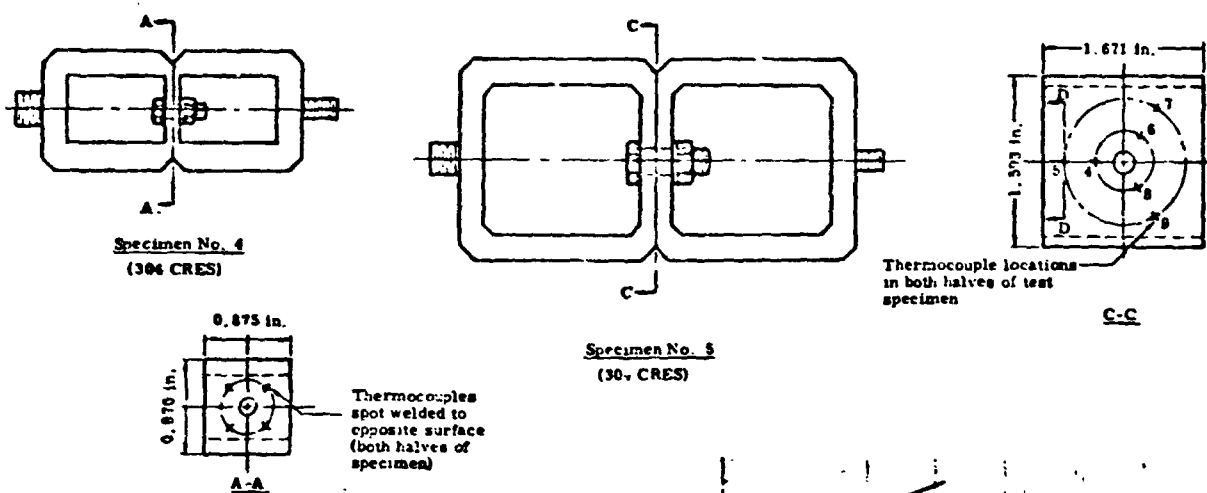
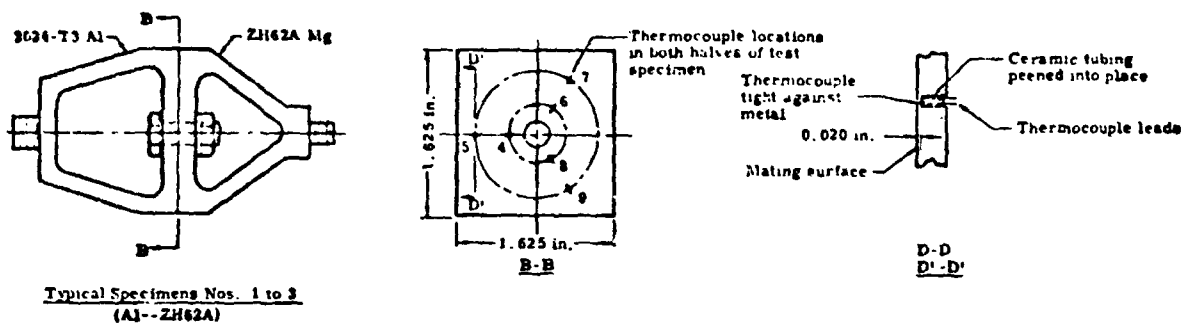


FIGURE 2-14
CONFIGURATION AND TEST RESULTS
TAKEN FROM REFERENCE 46

The strong temperature dependence of the magnesium and aluminum alloy joints is probably due to differential thermal expansion loading due to the use of steel bolts, which increases the contact pressure with increasing temperatures. This was reported by Feldmanis (38) and mentioned earlier.

While there exist other bolted joint reports, besides those mentioned herein, it is believed that all currently significant material has been covered.

SECTION 3.0

GUIDELINES

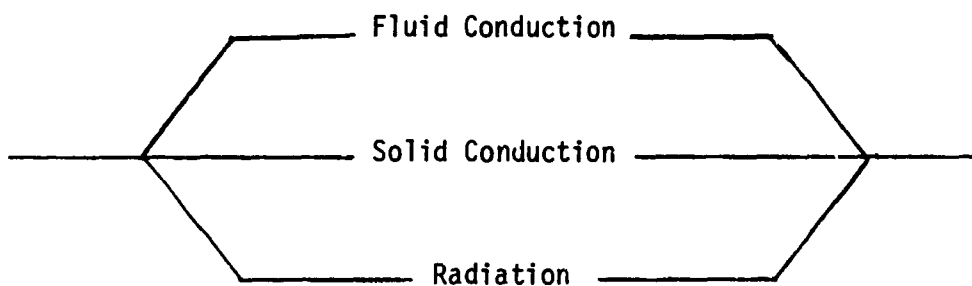
This section is intended to provide the design engineer with a procedure to determine the contact conductance (or resistance) of a joint, with particular emphasis on bolted joints as used in spacecraft applications. There are no valid analytical methods in existence, which can be used for this purpose, although there have been attempts to develop empirical techniques (Ref. 3, 21, 27 and 38), with varying degrees of success. The work of Ref. 3 and the several references cited in the preceding section, probably provide the most practical methods to date, however, they must be organized.

This section was originally intended to be self-sufficient, i.e. no additional material was required. For this reason some of the figures from Section 2 will be repeated as they are required. It will be noted that wherever possible, a non-dimensional approach has been taken, because experience and judgement have shown this to be the most practical way of data presentation. The choice of taking a conservative approach or the opposite is often difficult, because of the uncertainty of the data used in preparing equations and data graphs.

This section consists of recommended approaches, data graphs and a glossary. The data graphs taken from many sources provide values in the International System of Units (SI) and, in most cases, in common engineering units. For the cases where only SI units are given, the glossary provides the necessary conversions.

3.1 RECOMMENDED APPROACH

The determination of the contact conductance for a bolted or otherwise fastened joint requires an assessment of the modes of heat transfer in the joint. These can be solid conduction, fluid (gap) conduction and radiation, as shown in the simplified resistance sketch below. Fluid convection in the joint is not a probable mode for the gap dimensions considered here.



For spacecraft joints in a vacuum and at moderate temperatures, the fluid conduction and radiation contribution to the joint conductance can be considered negligible. If they need to be considered, existing techniques and equations are available, as is contact conductance data including such interstitial fluid effects. Following are some observations of the contact and joint effects on heat transfer which must be considered.

3.1.1 CONTACT RESISTANCE

If the surfaces of two dry metal blocks are placed in contact, there remains a considerable resistance to heat flow from one block to the other, unless the surfaces are bonded together by a solid metal bond as in welding, brazing, or soldering. This thermal resistance, known as "contact resistance," is a function of the actual contact area, the presence of a solid, fluid or vacuum in the gap between the surfaces and the presence of oxide layers on the contact surfaces. Significant changes in the mean interface temperature may also produce changes in any or all of the above conditions.

The actual contact area is a function of the physical properties of the contact material, the surface conditions and finish, the flatness of the material, and the contact pressure.

Contact resistance is present in addition to the usual resistances of the materials themselves. The resistance of the contact may be large compared with the other resistances, and should rarely be neglected for metals. The contact resistance in a vacuum or at very low interstitial gas pressures is considerably greater than in the presence of air or other fluids, or conversely, the conductances are much lower. Figure 3-1 shows representative data from a number of sources for stainless steel. Shown below are representative ranges of contact conductance in vacuum.

	$\text{@}10^5 \text{ N/m}^2 (20 \text{ psi})$	$\text{@}10^7 \text{ N/m}^2 (1000 \text{ psi})$
Stainless Steel	400-1500 $\text{W-m}^{-2}\text{-}^\circ\text{C}^{-1}$	2500-15,000 $\text{W-m}^{-2}\text{-}^\circ\text{C}^{-1}$
Copper	1000-10,000 " " "	20,000-100,000 " " "
Magnesium Alloy	3000-6000 " " "	25,000-50,000 " " "
Aluminum Alloy	2000-6000 " " "	25,000-50,000 " " "

CAUTION: The contact resistance of warped or wavy surfaces may be decreased by the use of sandwich materials. The reason for this is that with warped surfaces most of the thermal resistance is introduced by a relatively thick layer of gas (or liquid) between the blocks and replacement of a poor conducting medium such as air by a better conductor will effect a decrease in contact resistance.

3.1.2 WARPING OR NONFLATNESS

If the surfaces considered are warped, then this nonflatness may have more effect on contact resistance than the roughness of the surface. The expressions in Section 2 consider both.

3.1.3 ELASTIC RECOVERY

With lessening of contact pressure, at the temperatures and pressures considered herein, the results are repeatable provided the elastic limit of the asperities has not been exceeded on either of the mating surfaces. When plastic deformation occurs in the asperities in contact with each other, the contact resistance will decrease due to the increase in actual contact area caused by this deformation. If the contact pressure is increased enough to produce plastic deformation, then a subsequent reduction of pressure will increase the contact resistance, but the resistance will not become as high as it formerly was at the same reduced pressure. (Ref. 32).

3.1.4 EFFECT OF TEMPERATURE

For bolted joints where the mating surfaces are made of aluminum or magnesium and the bolt is made of steel, differential thermal expansion will increase the pressure and overall conductance of the joint when the temperature is increased. Otherwise, the temperature dependence of joint conductance is fairly moderate. Where no temperatures are given on curves, normal room temperature is to be assumed.

3.1.5 EFFECT OF SANDWICH MATERIALS

The effect of addition of thin metal shims on the overall contact resistance of a joint depends on the relative hardness of the blocks and the shim material. For example, blocks of material which are hard relative to the shim material (as for example, steel with aluminum or brass shims) will show a decrease in the overall contact resistance as compared to the same joints without shims, especially at high pressures. Conversely, blocks which are soft relative to the shim material exhibit contact resistances which are higher than for the same surfaces without shims (e.g., blocks of aluminum with and without brass shims). Aluminum blocks with aluminum shims seem to show no difference from the same aluminum joints without shims.

Nonmetallic sandwich material such as silicone rubber may increase the contact resistance by as much as 10 to 1, if applied so thick that it actually moves the blocks apart rather than merely replacing the air in the interstices.

3.1.6 DISSIMILAR METALS

It has been reported that the thermal conductance across joints of dissimilar metals depended on the direction of heat flow. The most generally accepted reason for this, as reported in Ref. 40 is due to thermal strain, rather than exotic effects mentioned by earlier investigators.

3.1.7 BOLT TORQUE

For reproducibility all bolted joints should be assembled and disassembled at least seven times, based on the data of Figure 3-4 (Ref. 20).

3.1.8 CONTAMINANTS

The presence of deliberate or accidental contaminants, such as oils, grease, on the mating surfaces tends to increase the conductance (reduce resistance). The presence of powders or excessive dust, particularly in a vacuum, tends to reduce conductance (increase resistance).

3.1.9 PLATING

Metallic or nonmetallic plating of contact surfaces, causes the surface to have a contact resistance much closer to that of the plating material, than to the substrate material. This is usually true for aluminum or magnesium plating of steel surfaces.

The use of a metallic, deformable foil, such as indium or lead foil, as an interstitial filler will achieve similar results.

3.1.10 BOLT SPACING

The effective heat transfer area in the vicinity of a bolt usually has an approximate two bolt head diameter radius. Thus a bolt spacing of more than four bolt head diameters will cause increased thermal resistance per total area.

TABLE 3-I
LIST OF EQUATIONS USED IN
SECTION 3 - GUIDELINES

$$\bullet \frac{\frac{h_c \delta_g - 1}{k_g}}{\frac{k_s \delta_g}{\bar{a} k_g}} = \left(\frac{2}{3\pi} \right) \left(\frac{P}{Y} \right) \quad (3-1)$$

For $k_g = 0$, i.e. in vacuum, Eq. 3-1 reduces to

$$\bullet \frac{\bar{h}\bar{a}}{k_s} = \left(\frac{2}{3\pi} \right) \left(\frac{P}{Y} \right) \quad (3-2)$$

\bar{a} is assumed to be 30×10^{-6} m

$$\bullet \frac{\bar{h}\bar{a}}{k_s} = 0.118 \left(\frac{P}{3Y} S \right)^{0.66} \quad (3-3)$$

\bar{a} is assumed to be 40×10^{-6} m

$S = 1$ for very rough and wavy surfaces.

$S =$ approximately 3 for fairly smooth surfaces.

When in doubt, use $S=1.5$ for moderately rough surfaces.

$$\bullet \frac{\bar{h}\bar{a}}{k_s} = 0.32 \left(\frac{P}{3Y} \right)^{0.86} \quad (3-4)$$

$$\bullet h_c = h_s + h_g \quad (3-5)$$

$$\bullet h_g = \frac{k_g}{\delta_g} \quad (3-6)$$

TABLE 3-I Cont'd

- $\delta_g = 2/3 (i_1 + i_2)$ (3-7)

where i_1 , i_2 , are the individual mean or rms values of surface irregularity.
For wavy surface increase value to include flatness deviation.

Using Fig. 3-15 an empirically modified value of $(i_1 + i_2)$ can be obtained -
 $(i_1 + i_2)^{**}$ which can be used in (3-7).

- $$h_s = \frac{k_g}{0.64 (i_1 + i_2)^{**}} + Z \bar{n} k_s$$
 (3-8)

Use Figures 3-14, 3-15 for $(i_1 + i_2)^{**}$, and \bar{n} determination.

- Tensile Force = $\frac{5 \text{ (Bolt Torque)}}{\text{Major Thread Diameter}}$ (3-9)

TABLE 3 -II

CONVERSIONS

1 watt-cm ⁻² -°C ⁻¹	=	1761-hr ⁻¹ -ft ⁻² -°F ⁻¹ -BTU
1 BTU-hr ⁻¹ -ft ⁻² -°F ⁻¹	=	0.568 x 10 ⁻³ watt-cm ⁻² -°C ⁻¹
	=	5.68 watt-m ⁻² -°C ⁻¹
1 inch-lb	=	0.113 meter-Newton
1 m-N	=	8.85 inch-lbs.
1000 Newton	=	224.82 lbs. (f)
1 micro-inch	=	2.54 x 10 ⁻⁶ cm
1 lb-inch ⁻²	=	6.89 x 10 ³ Newton
1 micro-inch	=	2.54 x 10 ⁻⁸ m
1 micron	=	10 ⁻⁶ m

3.2 PROCEDURES

The prediction or determination of the joint conductance of contact or bolted joints requires a knowledge of physical, environmental and structural (mechanical) properties. Armed with this complete or partially complete information, the existing data and data correlations can be surveyed to determine or at least estimate the heat transfer properties of the joint of interest.

It is assumed that the following information is known or can be obtained readily.

- a. Material and physical properties for each of the mating surfaces.
- b. Surface roughness and flatness deviation (These can be taken from drawings, specifications or obtained by comparison with known surfaces).
- c. Interfacial average pressure or load, or applied bolt torque.
- d. Geometrical relations and dimensions.
- e. Thermal properties of mating material and interstitial gap.

Using the above information, the existing experimental and analytical data can be evaluated for the best approach.

Table 3-I lists the equations required in the guidelines suggested below.

Table 3-II lists conversion factors.

Since there exists several valid correlations for evaluating an interface conductance (as evident in Section 2), the procedure, as followed through, will identify alternate methods for evaluating the conductance for the same joint. The alternate value(s) may differ significantly from the initial value, due to the variation of data and correlations obtained by the cited researchers. In such cases, it must become the burden of the user of this guideline to select the value he will actually use. He must consider his own application and determine whether conservatism (selection of highest or lowest value) or an average of values is appropriate. All symbols used in

this procedure are defined in table of symbols. Section 2 and cited references should be consulted for background details of the data and correlations used in this procedure. The interface conductance, h , is defined as:

$$h = q/A\Delta T$$

where A = apparent area in contact

ΔT = temperature drop across the interface

q = total heat flow rate across the interface resulting from ΔT and h

For case of nonbolted plate as block contact - use Procedure I

For case of bolted joint - use Procedure II

3.2.1 PROCEDURE I - BLOCK CONTACTS OR THICK NON-BOLTED PLATES

3.2.1.1 Minimum Information Required

- Contact geometry
- Materials of mating surfaces
- Surface finish & flatness
- Environmental Factors (vacuum, etc.)
- Average Interface pressure - P (= Load/Apparent Contact Area)
- Approximate interface temperature

3.2.1.2 Experimental Data in Figures 3-1 to 3-11 provide h as a function of contact pressure and finish at temperatures from -30°F (-30°C) to 250°F (120°C). For the following materials:

- AZ 31B magnesium
- 303, 304, 416 stainless steel
- 6061-T6, 2024T4
- Beryllium CR
- Oxygen free high cond. copper

- 304 S.S. Plated with aluminum
- 304 S.S. Plated with magnesium
- Titanium
- Titanium Alloy 6Al 4V

3.2.1.3 For the above, surfaces 1 and 2 are of the same material.

3.2.1.4 Procedure: Survey Figures 3-1 to 3-11, determine which of the information categories is appropriate, and use corresponding subprocedure.

- Note: Temperature effects are usually considered in the property values, for moderate temperature joints. For higher temperatures add a "radiation between flat plates" term.

Procedure I Categories

Subprocedure

- Graphical experimental data exists for
 - Material
 - Surface finish
 - Pressure
 - Temperature

in Figures 3-1 to 3-11 or in other available sources
(see references) (most data is for contacts in vacuum)

I-1
- Graphical Experimental data exists for
 - Material
 - Temperature Range
 - Pressure or Surface Finish are slightly out of range.

I-2
- Graphical Experimental data does not exist for
 - Material
 - Or surface finish } significantly differs
 - Or pressure } from given experimental
 - Or temperature } data
 - Contacts in vacuum I-3
 - Contacts in air or gas or fluid I-4
 - Dissimilar materials I-5
- Contacts with thin layer of interstitial material I-6

Subprocedure I-1

1. Use graphical data directly, linearly interpolate surface finish (Vacuum data only). Graphical data is given in Figures 3-1 to 3-11. If other data is available, use it judiciously if it is more representative.
2. If air or other fluid is in gap, use Subprocedure I-4.
3. If contact is in vacuum use subprocedure I-3 for alternate value of h.

Subprocedure I-2

1. Obtain contact conductance h by extrapolating graphical data curve trend for pressure or surface finish.
2. If fluid in gap, use subprocedure I-4 for value of h.
3. If vacuum in gap, use subprocedure I-3 for alternate value of h.

Subprocedure I-3

1. Obtain additional information;
$$Y, k_s, \bar{a} = 40 \times 10^{-6} \text{m}$$
2. Use Eq. 3-3 and/or Figure 3-12 (Let $S = 1.5$).
3. Alternately use Eq. 3-4 also shown on Fig. 3-12. (Let $S = 1.5$).
4. For alternate value of h use Eq. 3-2.
5. Alternately use Eq. 3-8 but do not use fluid conductance term.

Subprocedure I-4

1. Obtain additional information:
$$Y, k_g, \bar{a} = 30 \times 10^{-6} \text{m}, \delta_g \text{ (from Eq. 3-7)}$$
2. Use Eq. 3-1 and check with Figure 3-13.
3. Alternately determine h_s in vacuum using Step 1 of subprocedure I-2 or subprocedure I-3 (omit Step 4). Then determine total h_c by adding the gaseous conduction contribution following Eq. 3-5 and 3-6.

Subprocedure I-5

1. Obtain indentation hardness of the mating materials to determine which one is softer. This one controls. Find Y for the softer material, calculate $k_s = k_m = 2k_1k_2/(k_1 + k_2)$, and follow subprocedures I-3 for vacuum and I-4 for fluid in gap.

Subprocedure I-6

This is perhaps the most approximate procedure for contacts.

1. Obtain additional information:
 - Filler thickness
 - k_g for interstitial material
 - Determine whether interstitial material is metallic or capable of deformation and flow (plastic, film, fluid, etc.). If metallic, obtain Y_g .
 - δ_g using Eq. 3-7, then add filler thickness to obtain $\bar{\delta}_g$, the modified gap thickness
2. First compute the value of h_s in vacuum as if no filler were present using Eq. 3-2, 3-3, or 3-4. If filler is metallic, use Y_g in these equations. The h_s obtained is the base value.
3. Determine h_g term (Eq. 3-6) using $\bar{\delta}_g$, k_g obtained above for fluids which completely fill gap. Determine total h_c using Eq. 3-5. For plastic films, ceramic fibers, and other semi-deformable fillers, use same approach but take a median value for overall conductance between the base value (h_s) and the modified h_c .
4. CAUTION: For thick fillers, treat as two distinct interfaces and include conduction through the filler as a third element in heat flow path.

3.2.2 PROCEDURE II - BOLTED JOINTS

3.2.2.1 Minimum Information Required

- Same as for Procedure I
- Plus additional information:
 - Area used is apparent actual contact area, as defined in procedures which follow.
Average contact pressure for above area or load or bolt torque
 - Effect of differential temperatures on load.
 - Deformation data on joint members at and near joint, to determine contact area.

- Figure 3-16 shows effect of repeated torque application on same bolt.
Rule: Less than 7 successive load/unload cycles are not reproducible.
- Figure 3-17 shows typical "thick" bolted joint, conductances for 7075-T6 aluminum alloy.
- Figure 3-18 shows zero-interface stress point for bolted plates.
- Figure 3-19 shows thin plate conductances.

3.2.2.2 Procedure: Determine which of the following subprocedures is appropriate.

Procedure II Categories	Subprocedure
<ul style="list-style-type: none"> ● Contact Area - (Actual) known <ul style="list-style-type: none"> ● Average Contact Pressure known (or bolt torque and geometry known) ● Principal heat flow path at and near bolts. 	II-1
<ul style="list-style-type: none"> ● Contact Area at bolt <u>not</u> known <ul style="list-style-type: none"> ● Principal heat flow paths known ● Contact Load (or torque) known 	II-2
<ul style="list-style-type: none"> ● Contact Areas (regions) <u>not</u> known, (such as edge clamped boxes). <ul style="list-style-type: none"> ● Heat flow paths unclear ● Contact load unknown 	II-3
<ul style="list-style-type: none"> ● Any of the above with filler or interstitial material. 	II-4

Note: If there are facings, but not contacting areas of significance, calculate radiation between parallel plates and added to h.

Subprocedure II-1

1. If contact pressure is known, skip next step.
2. If bolt torque is known, use Eq. 3-9 to find force, W , and calculate contact pressure as W/A_c .
3. Use appropriate subprocedure I-1 to I-5 to find h knowing contact pressure.

Subprocedure II-2

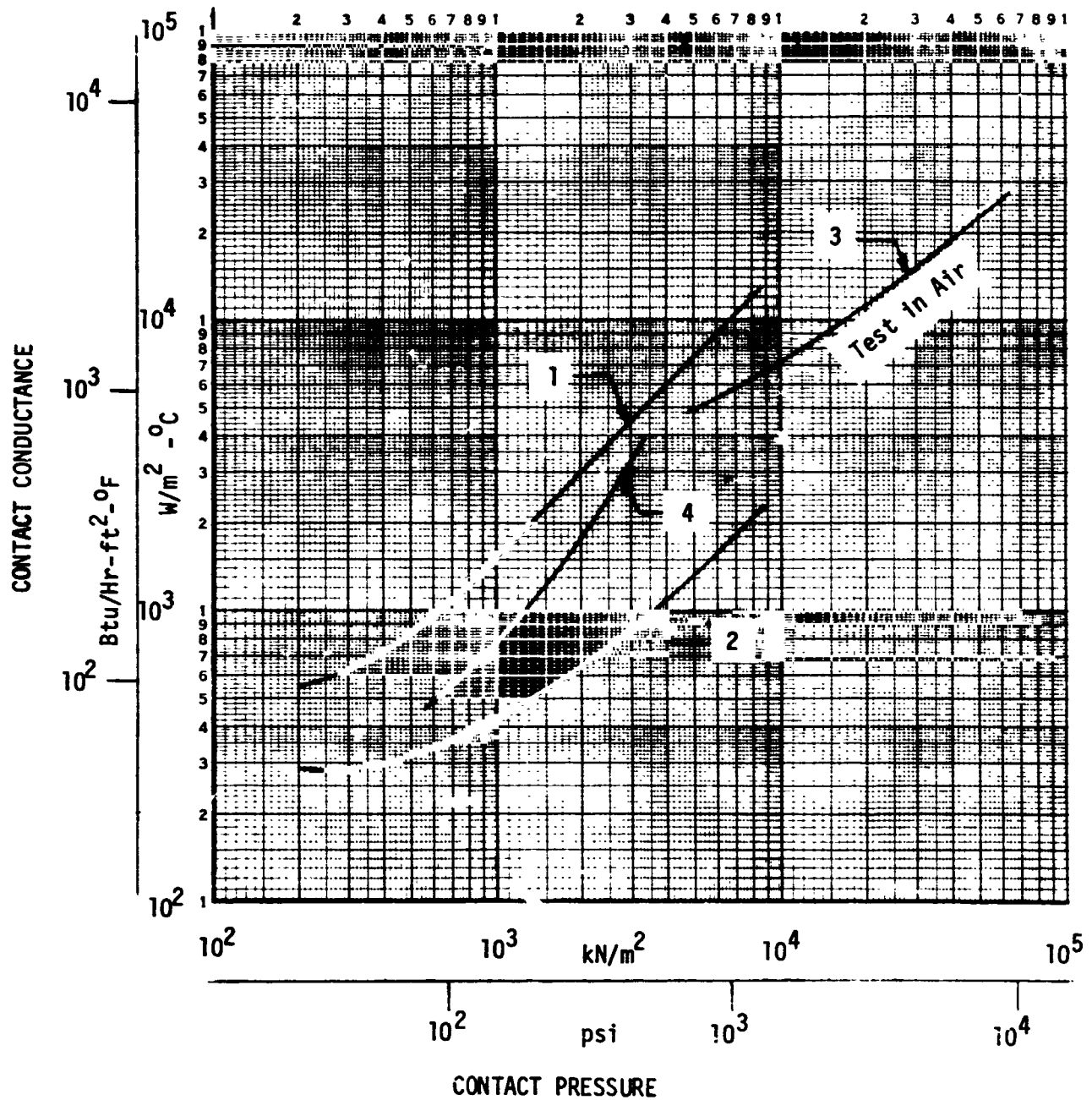
1. Obtain additional information:
 - Bolt head or nut radius (r_h), hole radius (r_s), plate thicknesses (b_1, b_2)
2. Using Fig. 3-18, determine radius at which zero interface stress exists. For plates of different thickness, use smaller value of b . The apparent actual contact area is determined as $\pi(r_h^2 - r_s^2)$.
3. Proceed as in subprocedure II-1.

Subprocedure II-3

1. From drawing data and using Steps 1 and 2 of subprocedure II-2 above, determine apparent actual contact area.
2. If bolt spacing is known, obtain approximate value of h from Fig. 3-17 and apply over apparent actual contact area.
3. If bolt spacing is unknown, assume an h of $3000 \text{ Watt-m}^{-2}\text{-}^\circ\text{C}^{-1}$ and apply over apparent actual contact area.
4. If further investigation is warranted, bolt torque must be assumed based on knowledge of the function of the particular bolted joint. Assume torque and proceed as in subprocedure II-1 (Steps 2 and 3), using apparent actual contact area calculated in Step 1 of this subprocedure (II-3).

Subprocedure II-4

1. Determine contact area and load using subprocedures II-1, 2, or 3 as appropriate.
2. Applying over apparent actual contact area, use subprocedure I-6.



No.	Material	RMS Surface	Investigator
1	304 S.S.	0.3 μm	Fried & Atkins (18)
2	304 S.S.	1.2 μm	Fried & Atkins (18)
3	415 S.S.	1.4 μm	Henry & Fenech (34)
4	303 S.S.	0.08 μm	Clausing & Chao (15)

FIGURE 3-1
CONTACT CONDUCTANCE VS. CONTACT PRESSURE - REPRESENTATIVE DATA

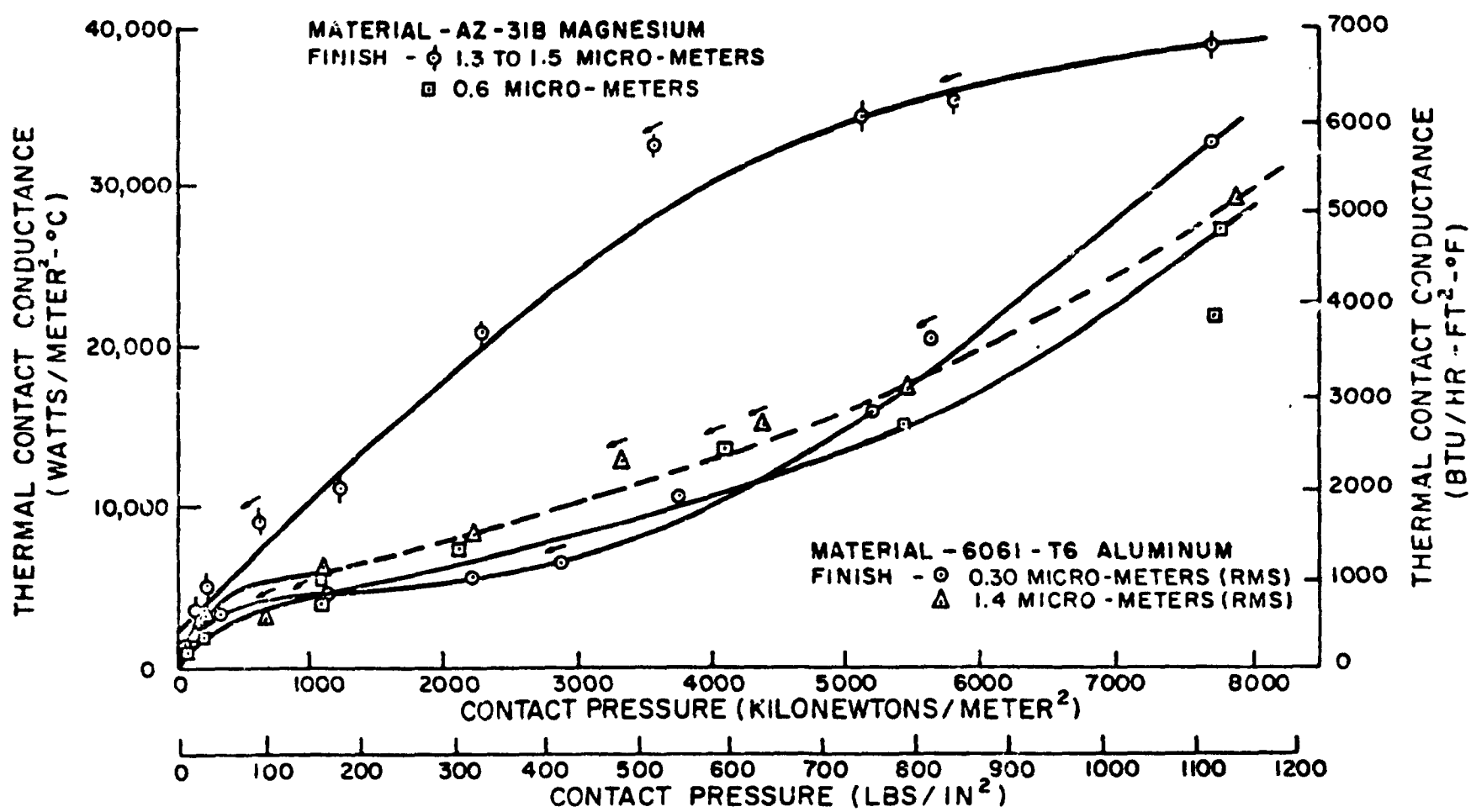


FIGURE 3-2

CONTACT CONDUCTANCE VS. CONTACT PRESSURE FOR AZ-31 MAGNESIUM, 6061-T6 ALUMINUM (REF. 18)

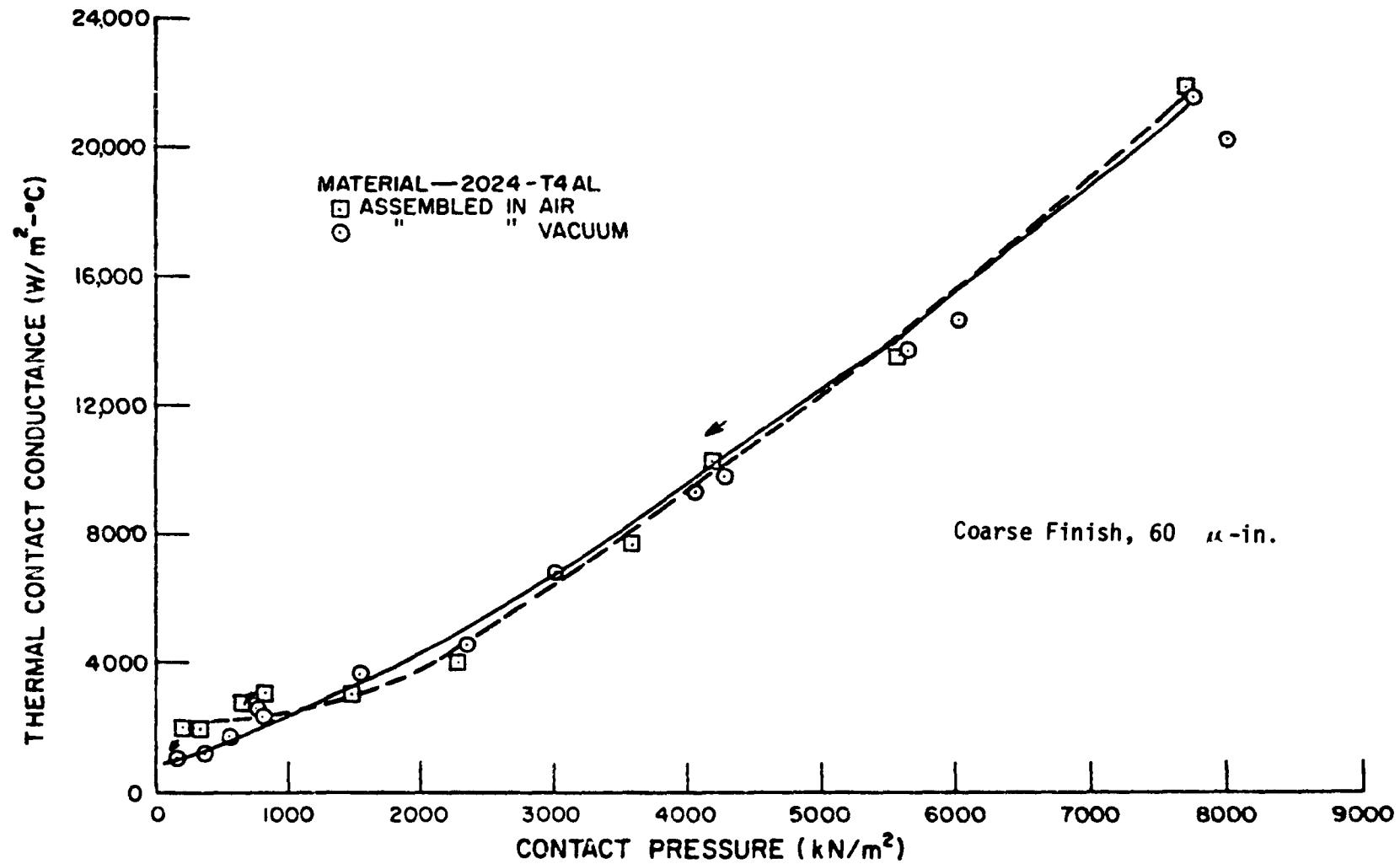


FIGURE 3-3

CONTACT CONDUCTANCE VS. CONTACT PRESSURE FOR 2024-T4 ALUMINUM
ASSEMBLED IN AIR, VACUUM (REF. 17)

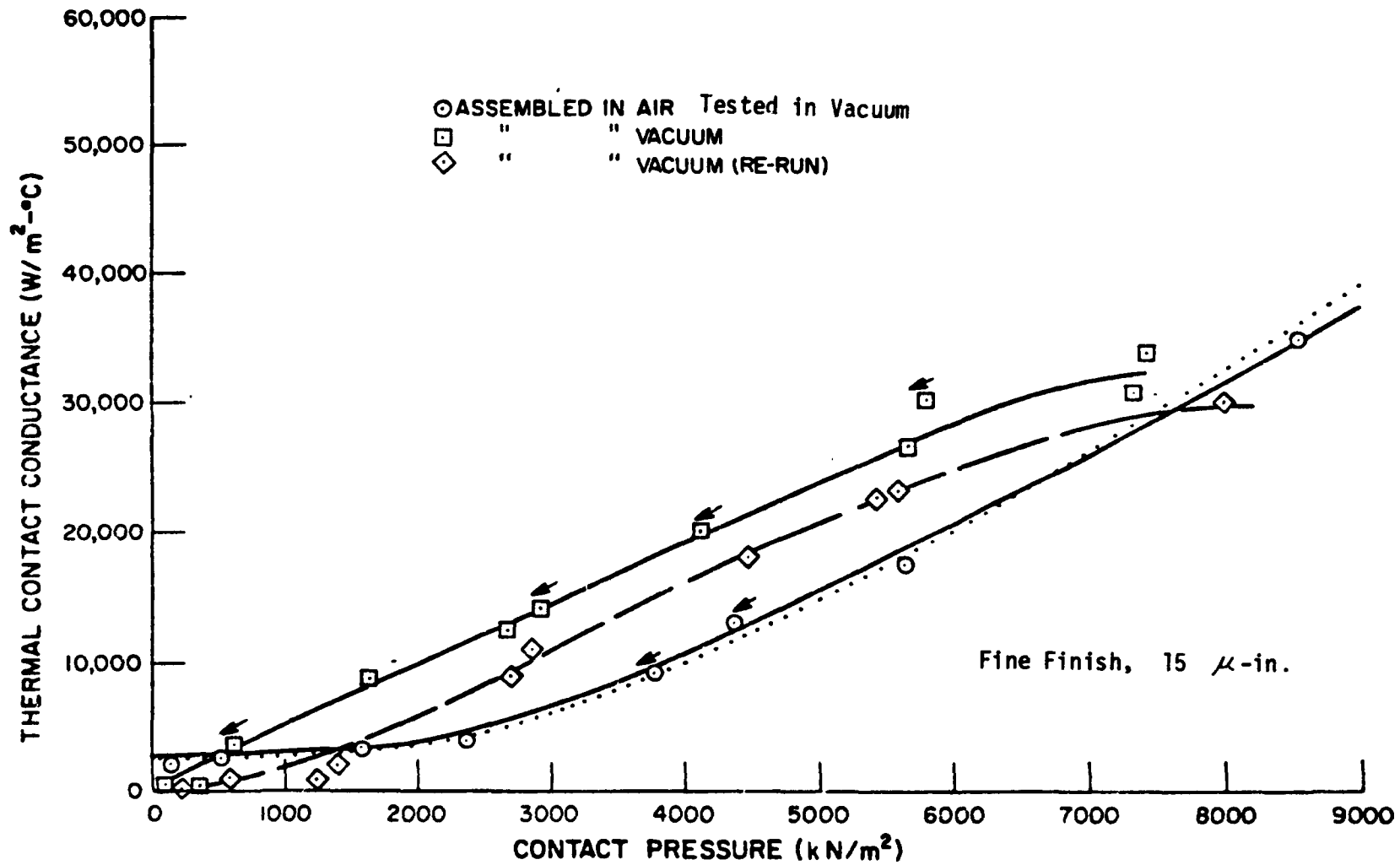


FIGURE 3-4
CONTACT CONDUCTANCE VS. CONTACT PRESSURE FOR 2024-T6 ALUMINUM
ASSEMBLED IN AIR, VACUUM (REF. 17)

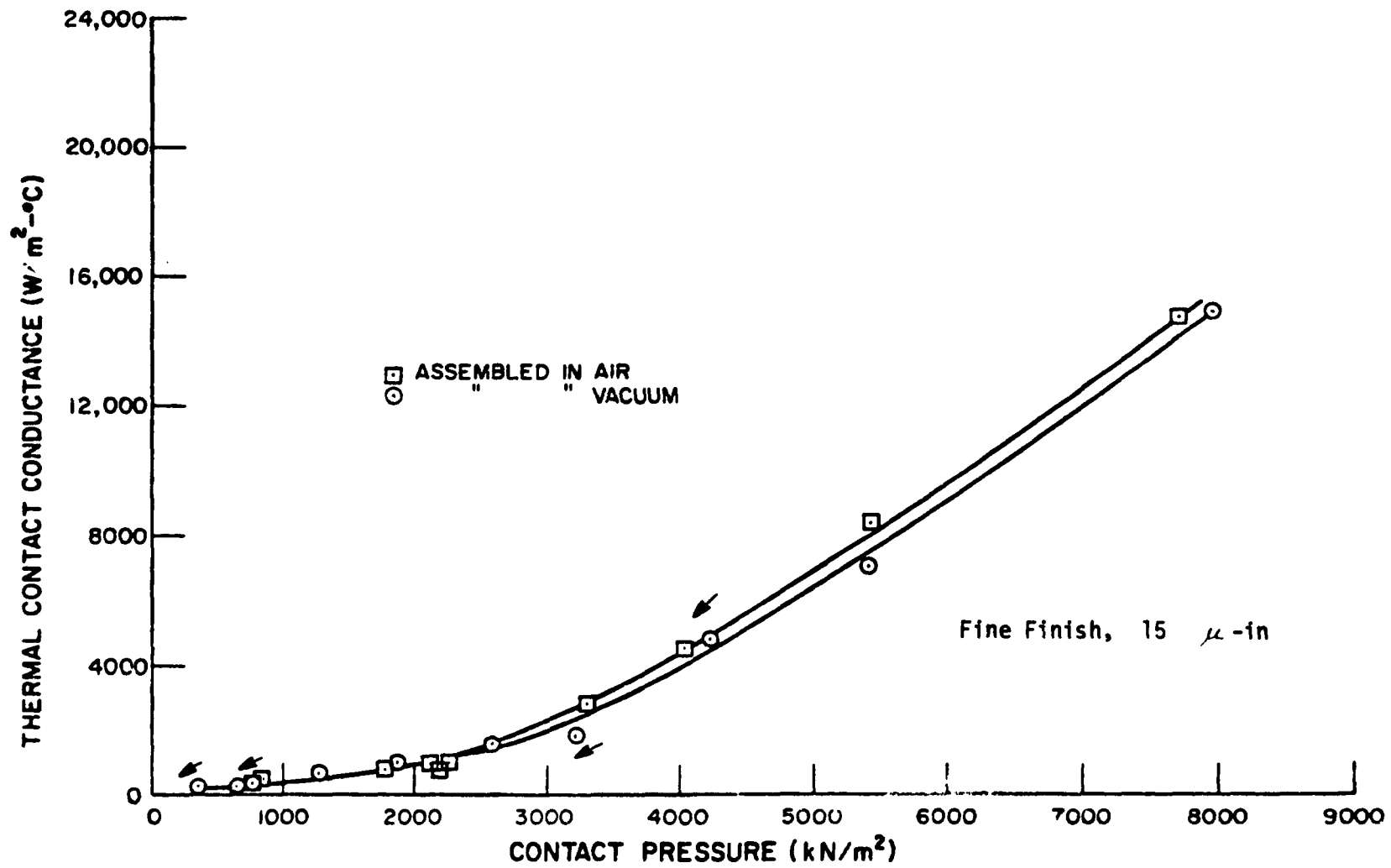


FIGURE 3-5
CONTACT CONDUCTANCE VS. CONTACT PRESSURE FOR BERYLLIUM CR
ASSEMBLED IN AIR, VACUUM (REF. 17)

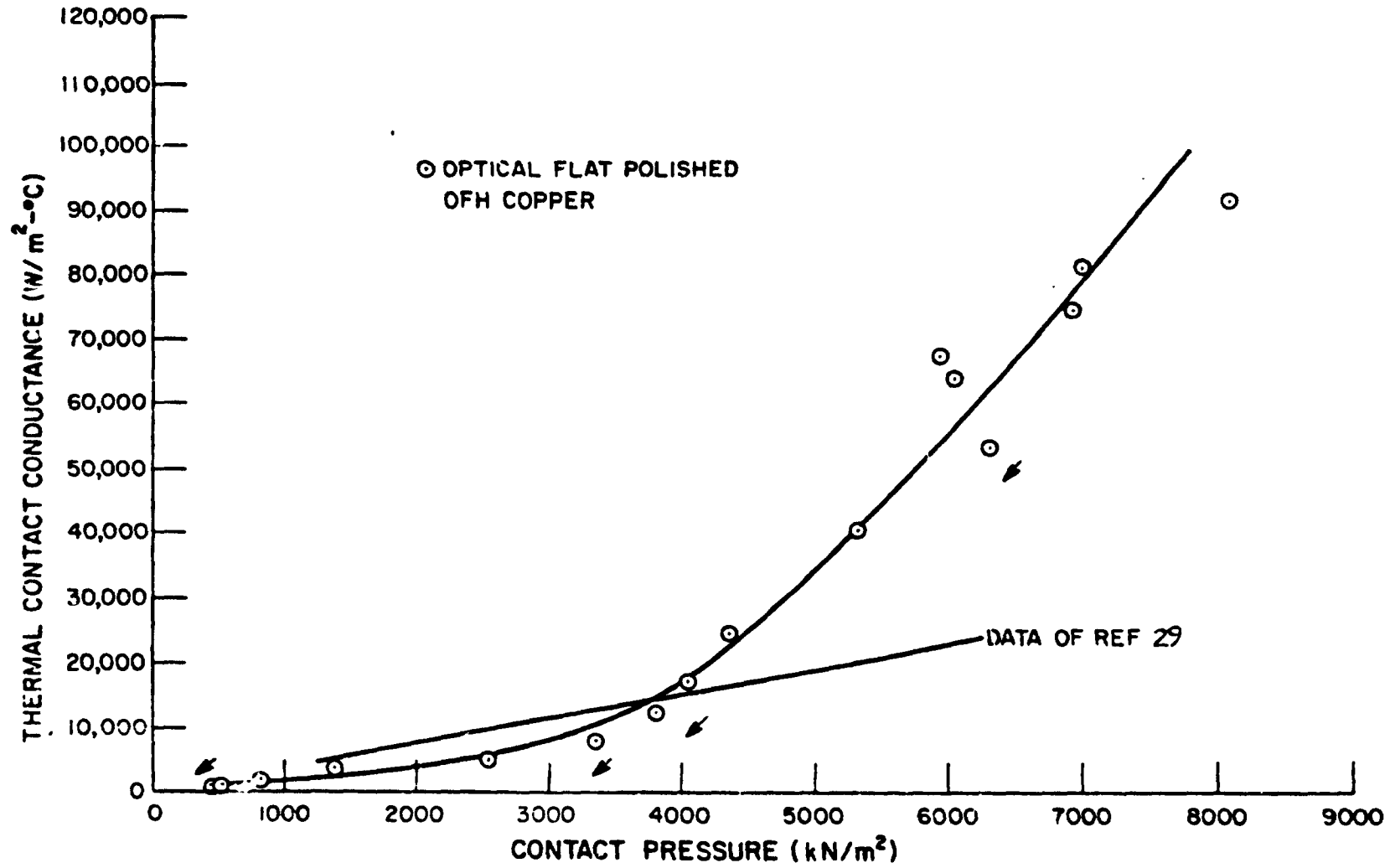


FIGURE 3-6

CONTACT CONDUCTANCE VS. CONTACT PRESSURE FOR OFH COPPER ASSEMBLED IN AIR (REF. 17)

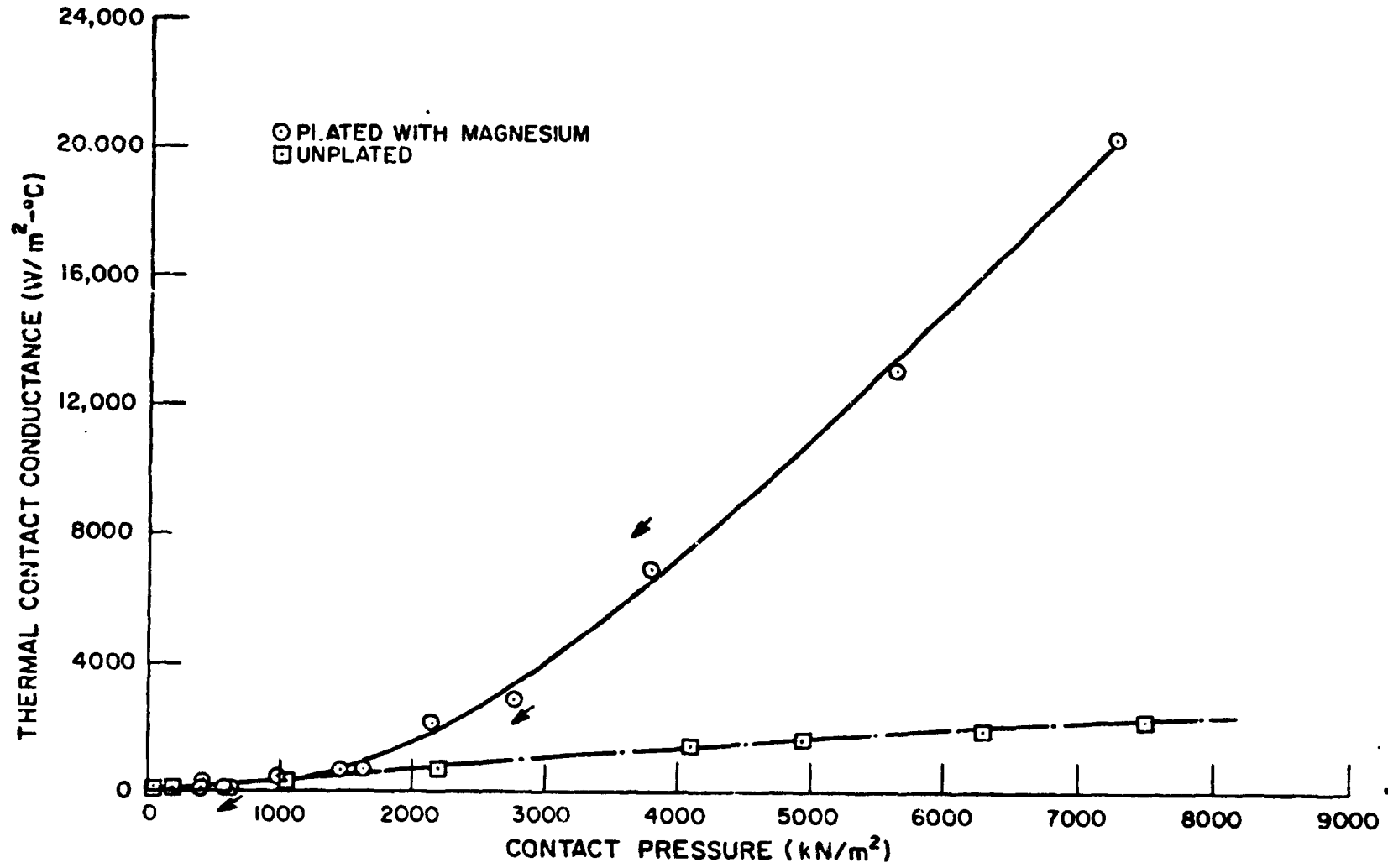


FIGURE 3-7
CONTACT CONDUCTANCE VS. CONTACT PRESSURE FOR 304 STAINLESS STEEL
PLATED WITH MAGNESIUM (REF.17)

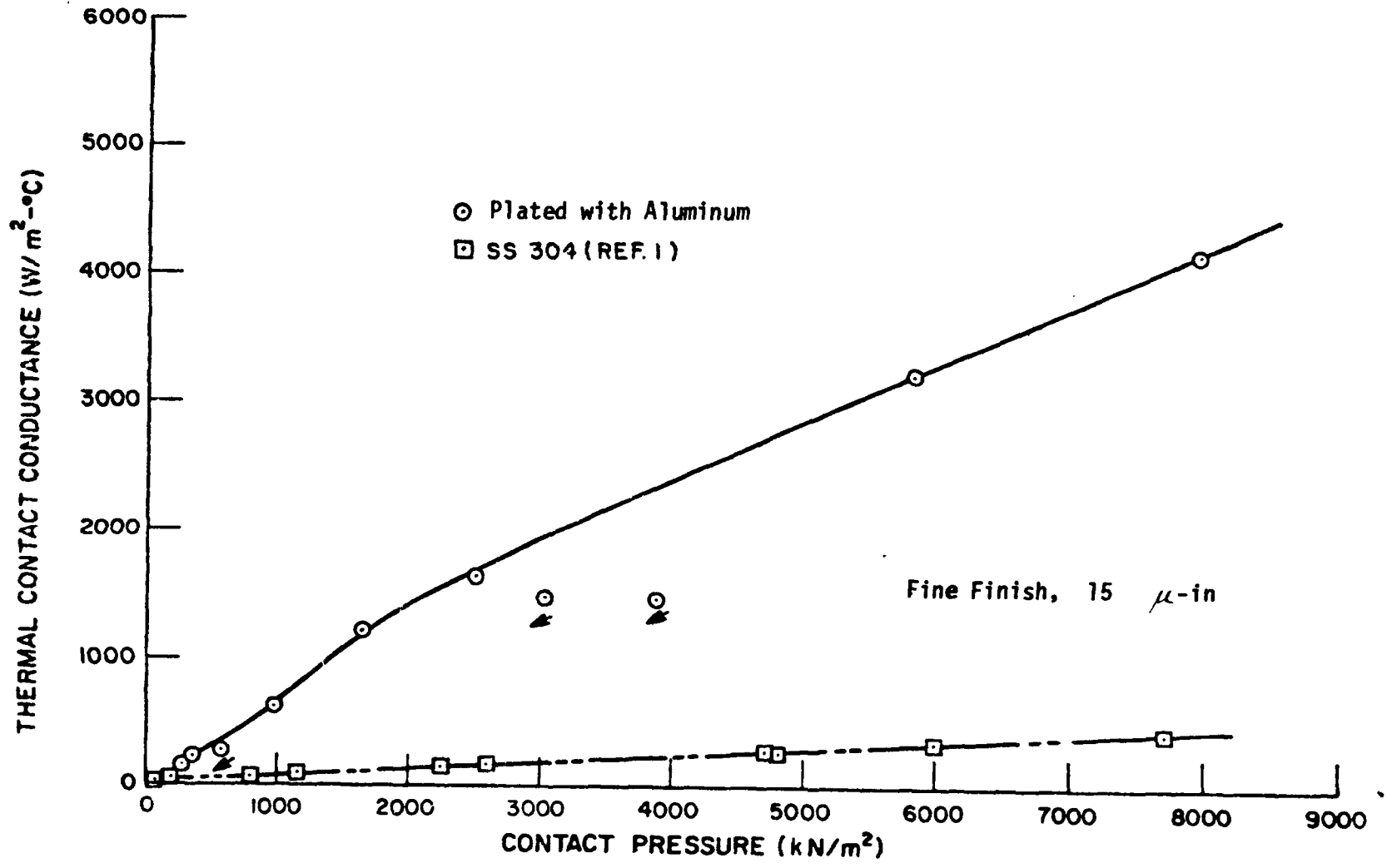


FIGURE 3-8
CONTACT CONDUCTANCE VS. CONTACT PRESSURE FOR 304 STAINLESS STEEL
PLATED WITH ALUMINUM (REF. 17)

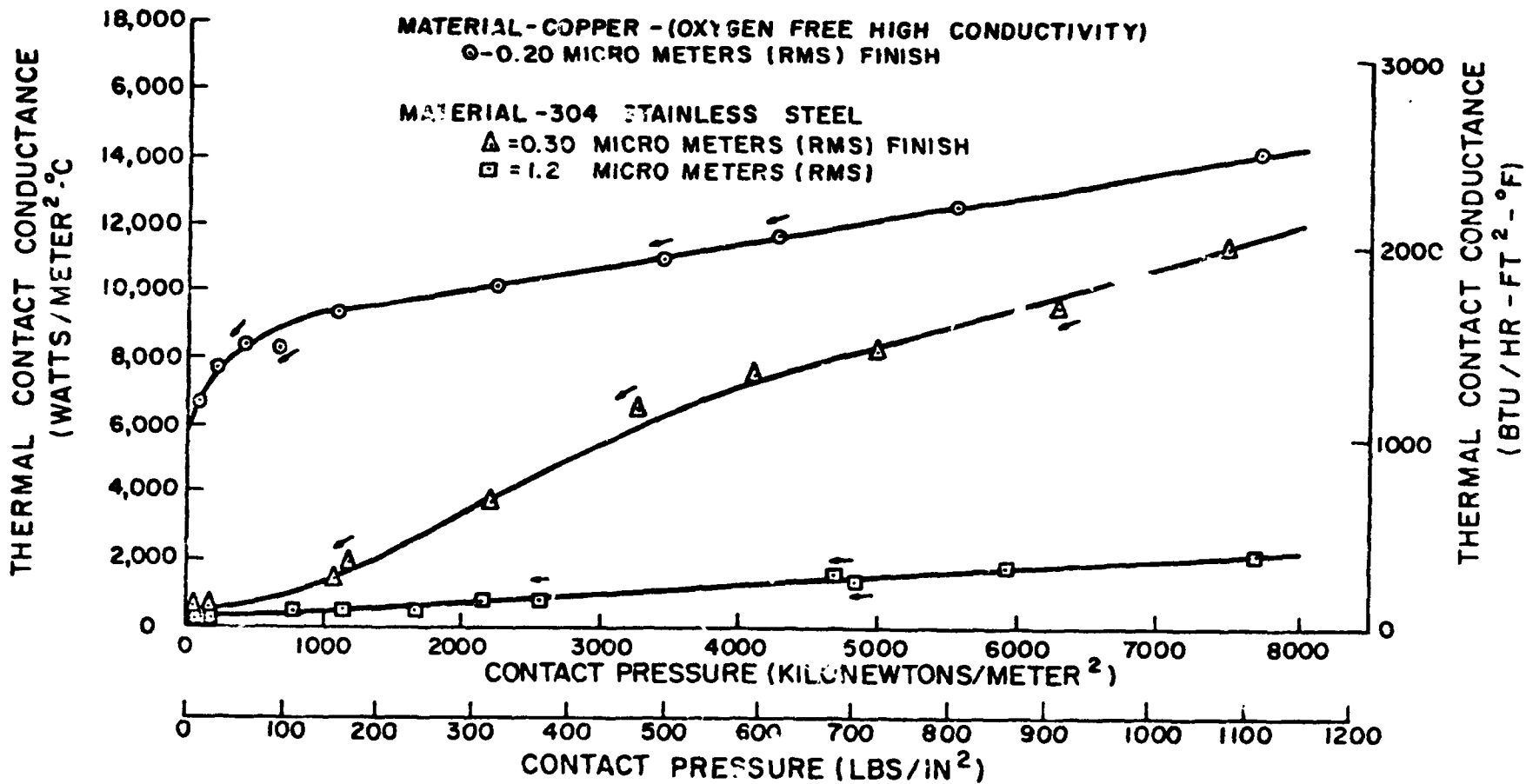
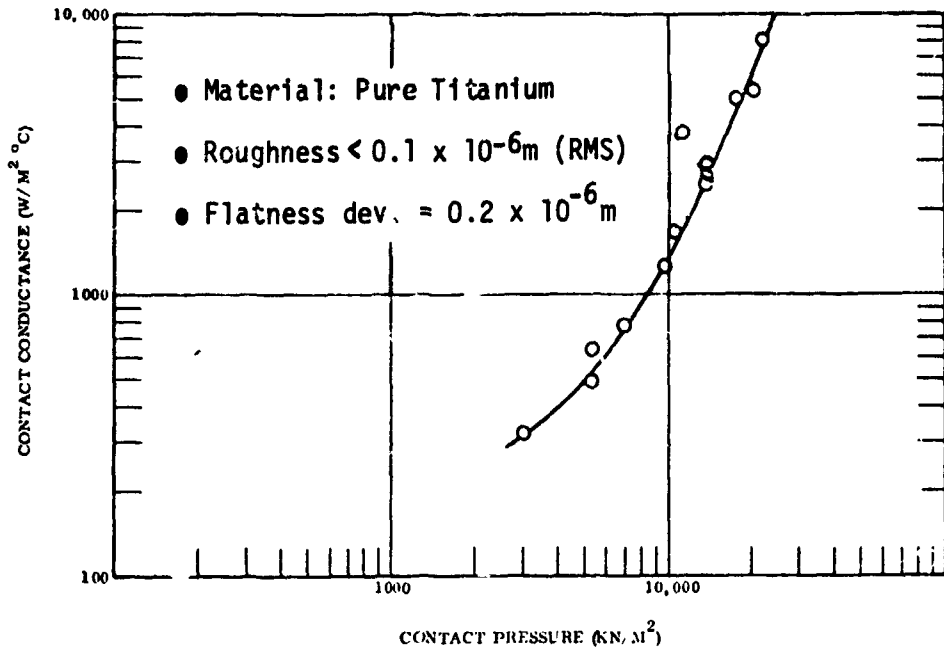
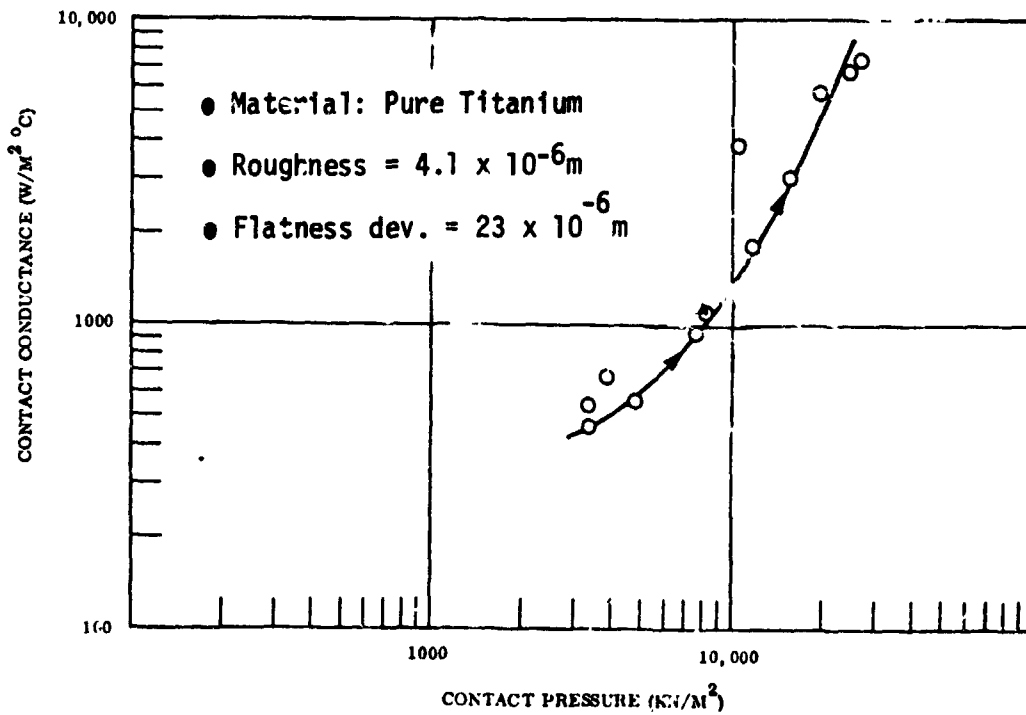


FIGURE 3-9

CONTACT CONDUCTANCE VS. CONTACT PRESSURE FOR OFH COPPER, 304 STAINLESS STEEL (REF. 18)



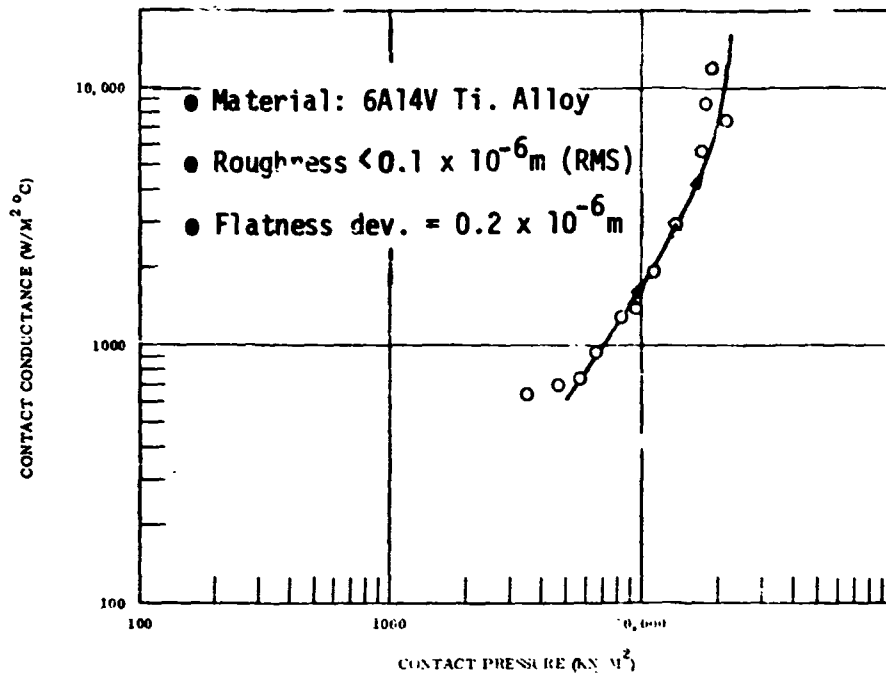
(a) Optical Finish



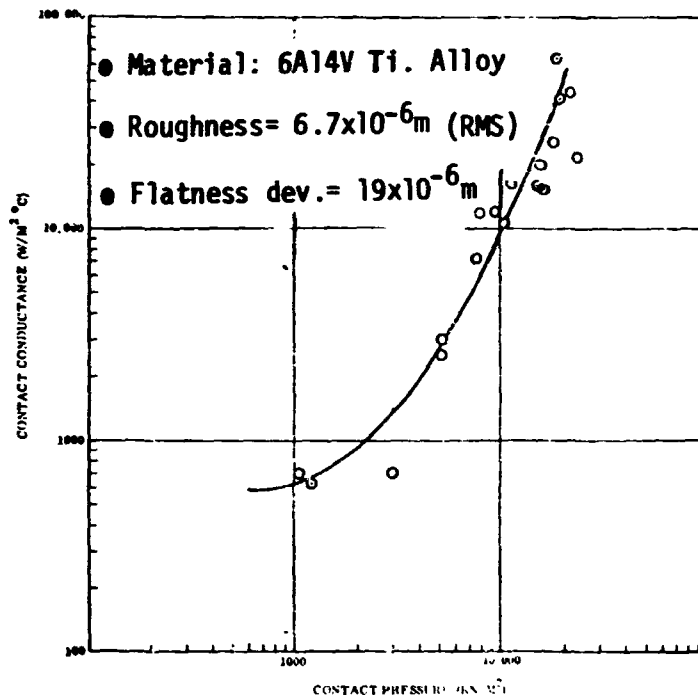
(b) Milled Finish

FIGURE 3-10

CONTACT CONDUCTANCE VERSUS CONTACT PRESSURE - TITANIUM (REF. 47)



(a) Optical Finish



(b) Milled Finish

FIGURE 3-11

CONTACT CONDUCTANCE VERSUS CONTACT PRESSURE - 6A14V TI ALLOY (REF. 47)

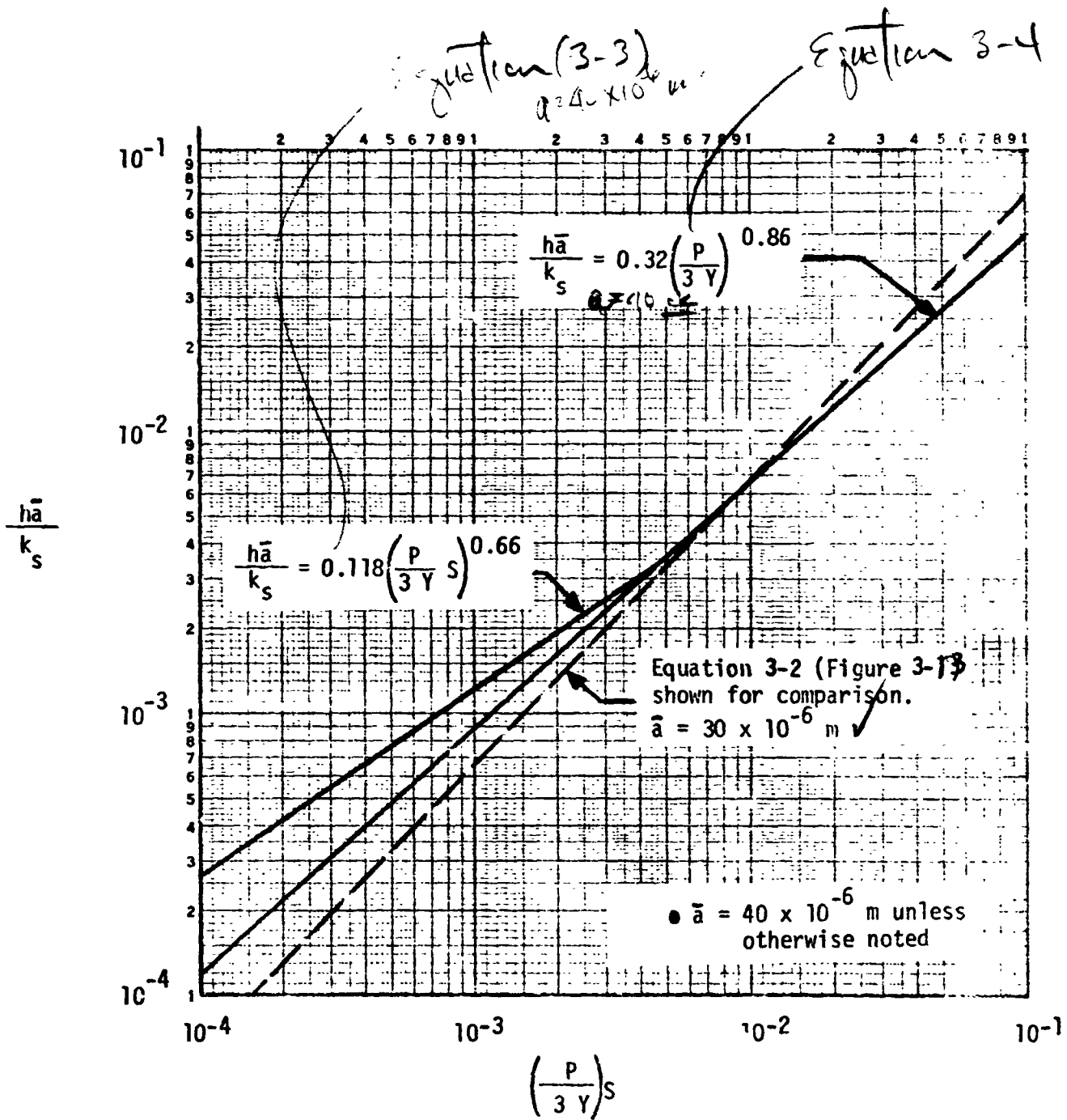


FIGURE 3-12

NON-DIMENSIONAL CONDUCTANCE CORRELATION (MALKOV IN REFERENCE 30)

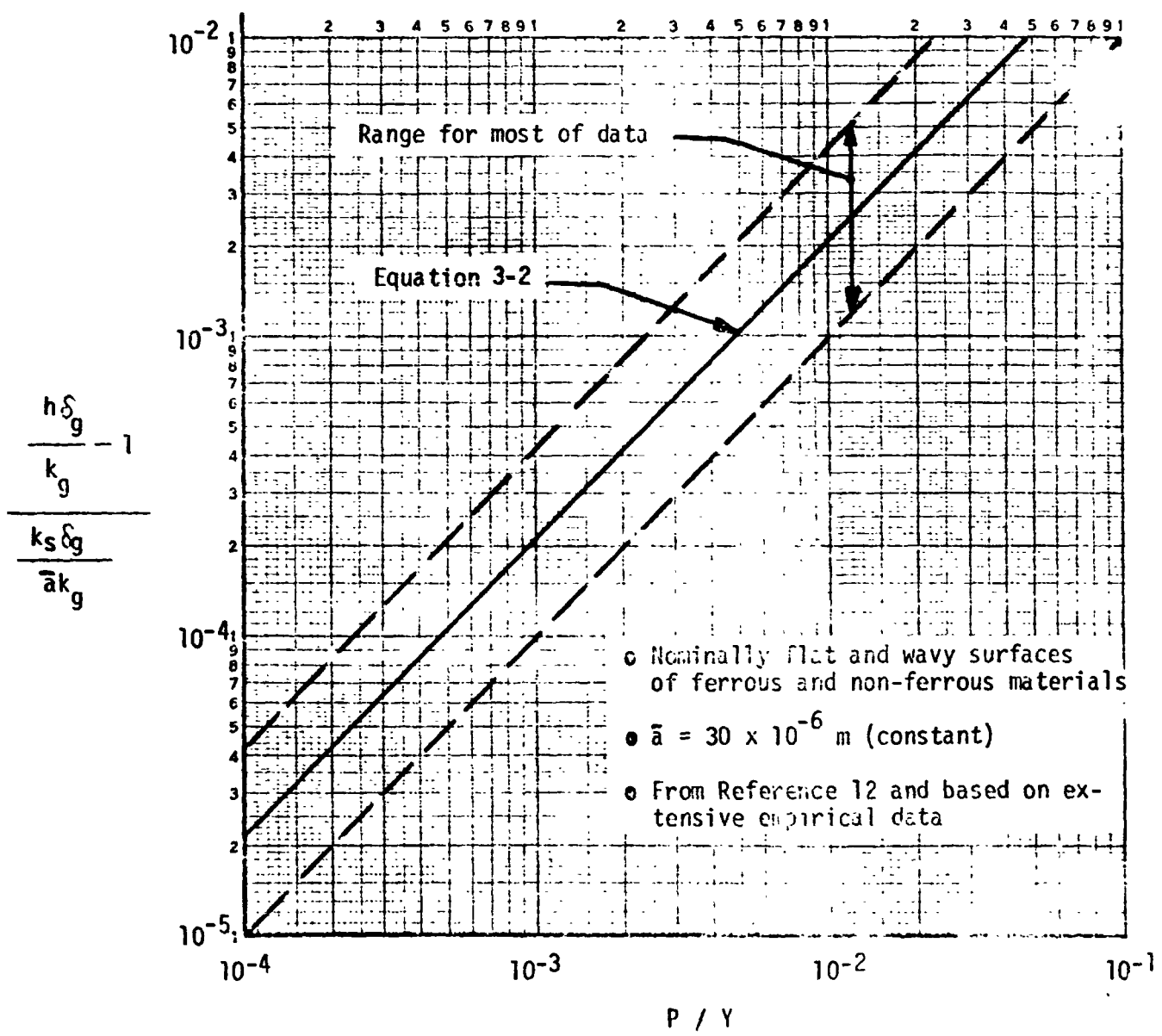


FIGURE 3-13
 NON-DIMENSIONAL CONDUCTANCE CORRELATION (REF. 12)

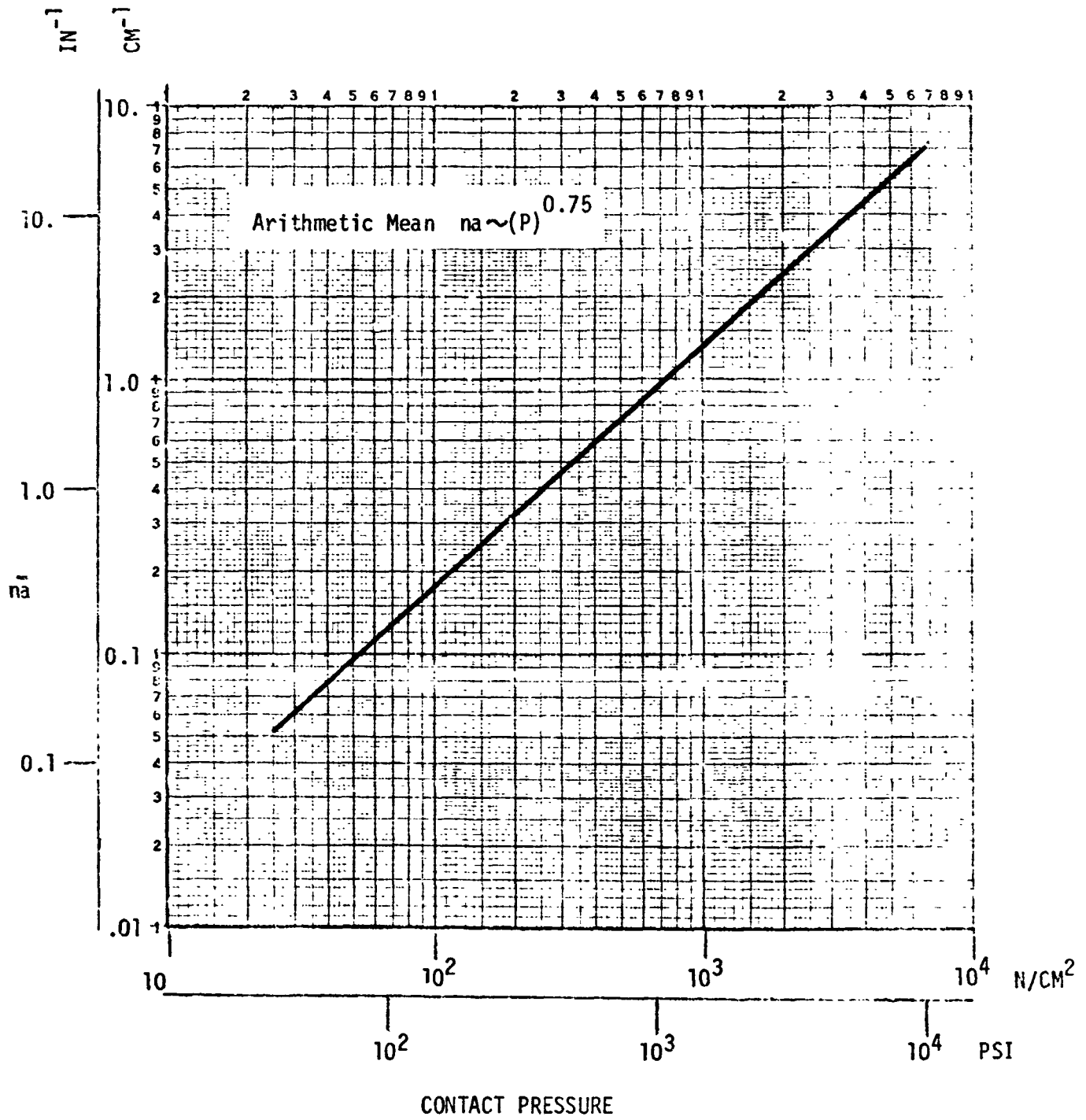


FIGURE 3-14

CONTACT AREA PARAMETER VS. CONTACT PRESSURE (REF. 3)

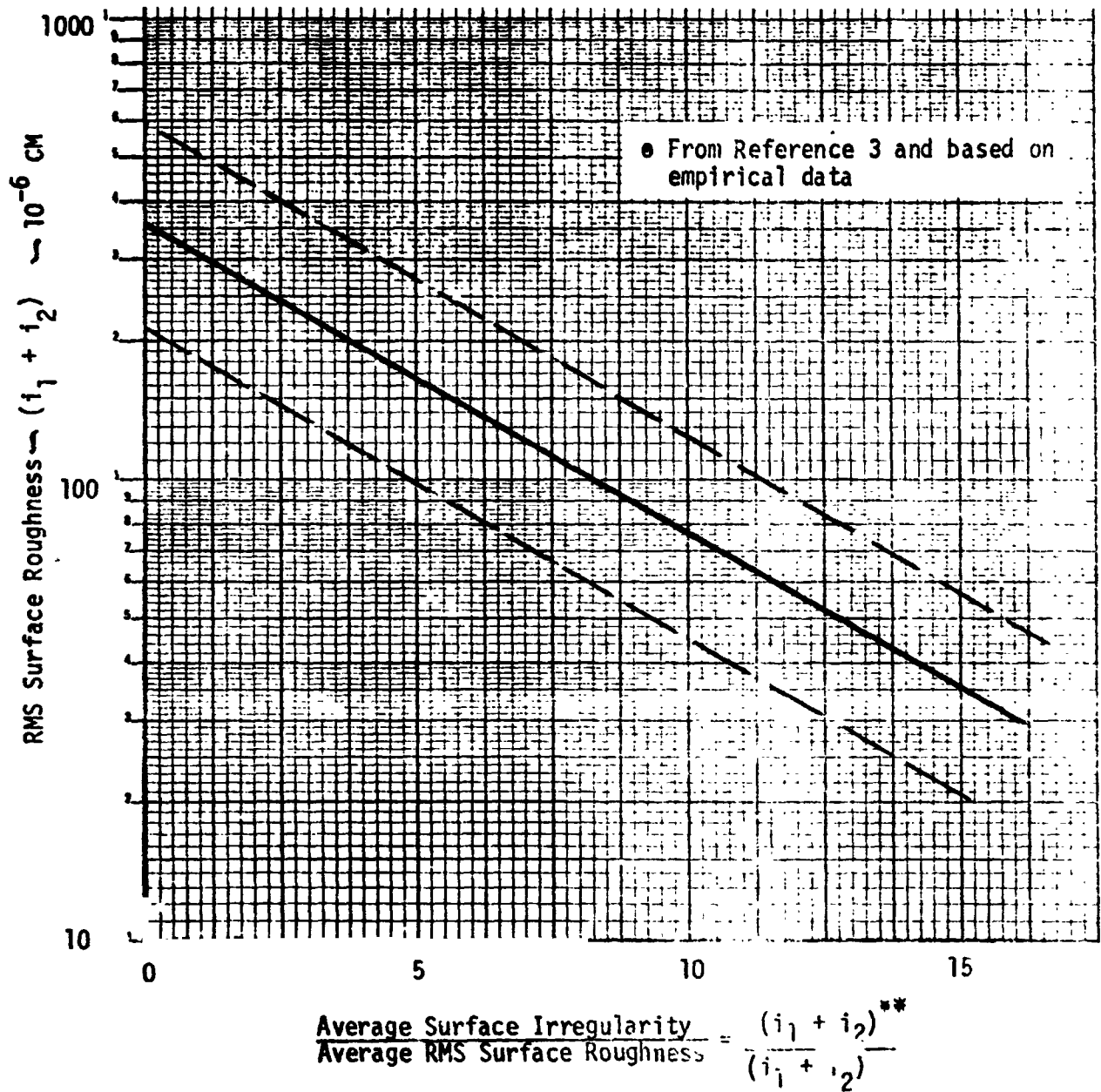


FIGURE 3-15

RATIO OF AVERAGE SURFACE IRREGULARITY TO RMS SURFACE ROUGHNESS VS. RMS SURFACE ROUGHNESS (REF. 3)

REPRODUCIBILITY OF THE ORIGINAL PAGE IS POOR.

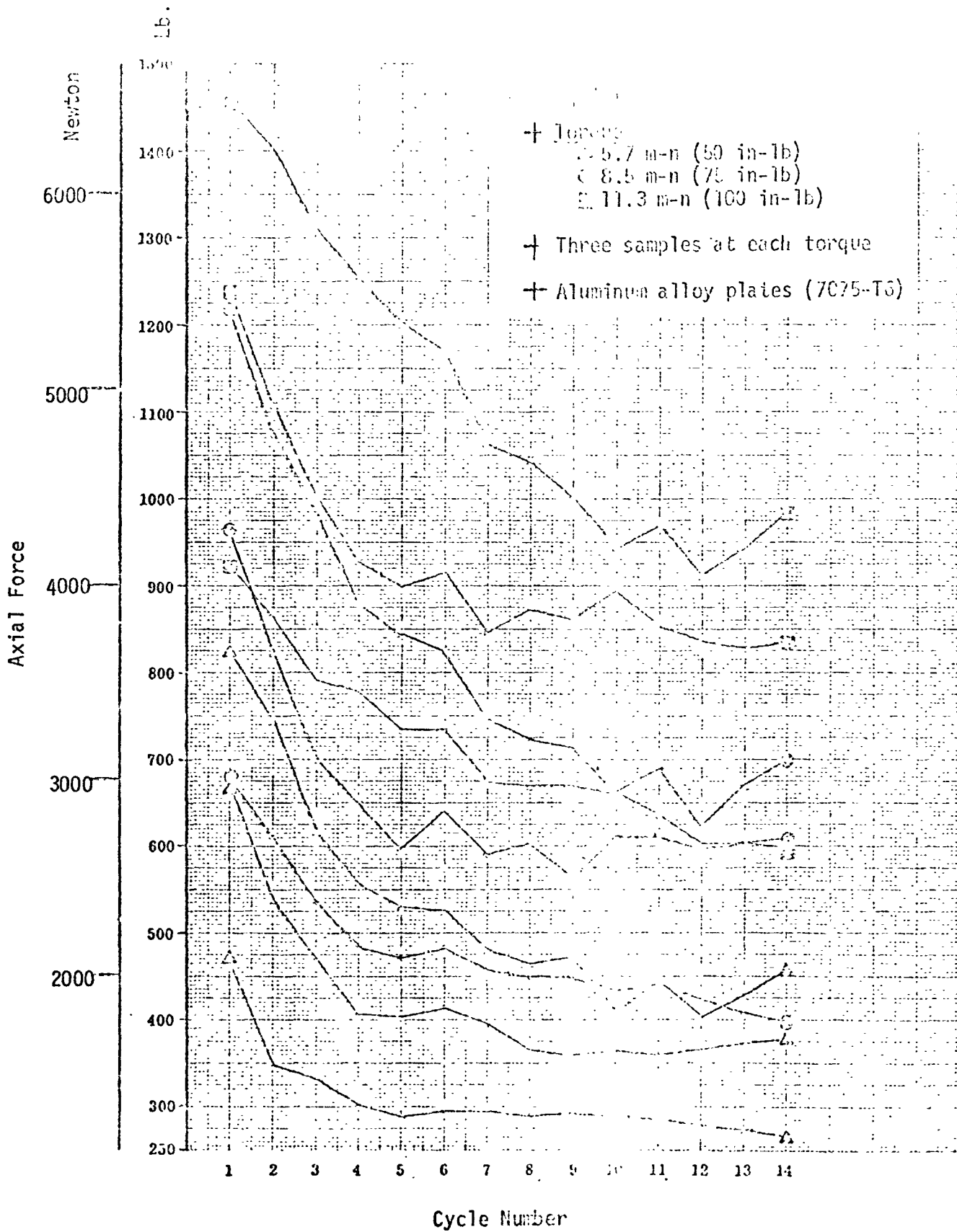


FIGURE 3-16

AXIAL FORCE VS. TORQUE VARIATION (REF. 20)

REPRODUCIBILITY OF THE ORIGINAL PAGE IS POOR.

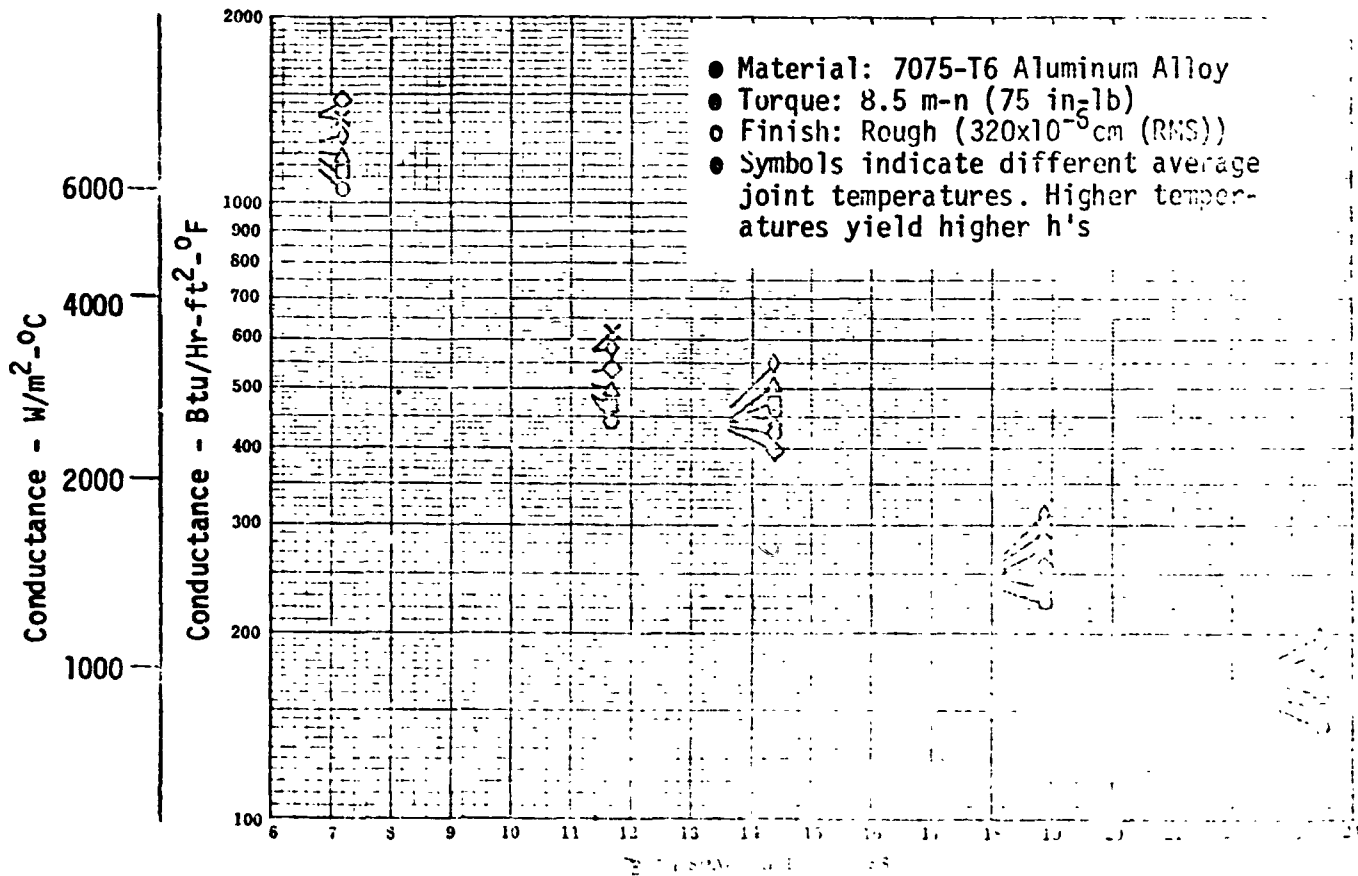
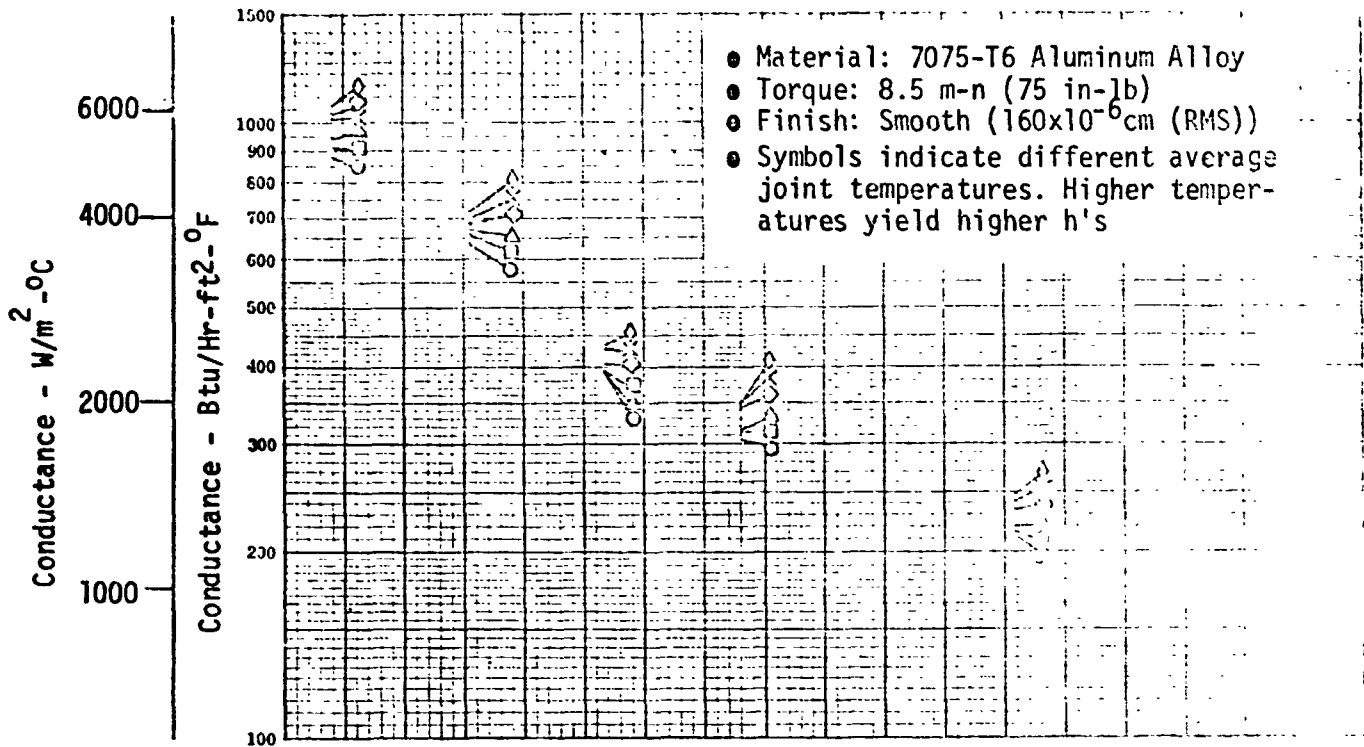


FIGURE 3-17

BOLTED LAP JOINT CONDUCTANCE VS. GEOMETRY (REF. 20)

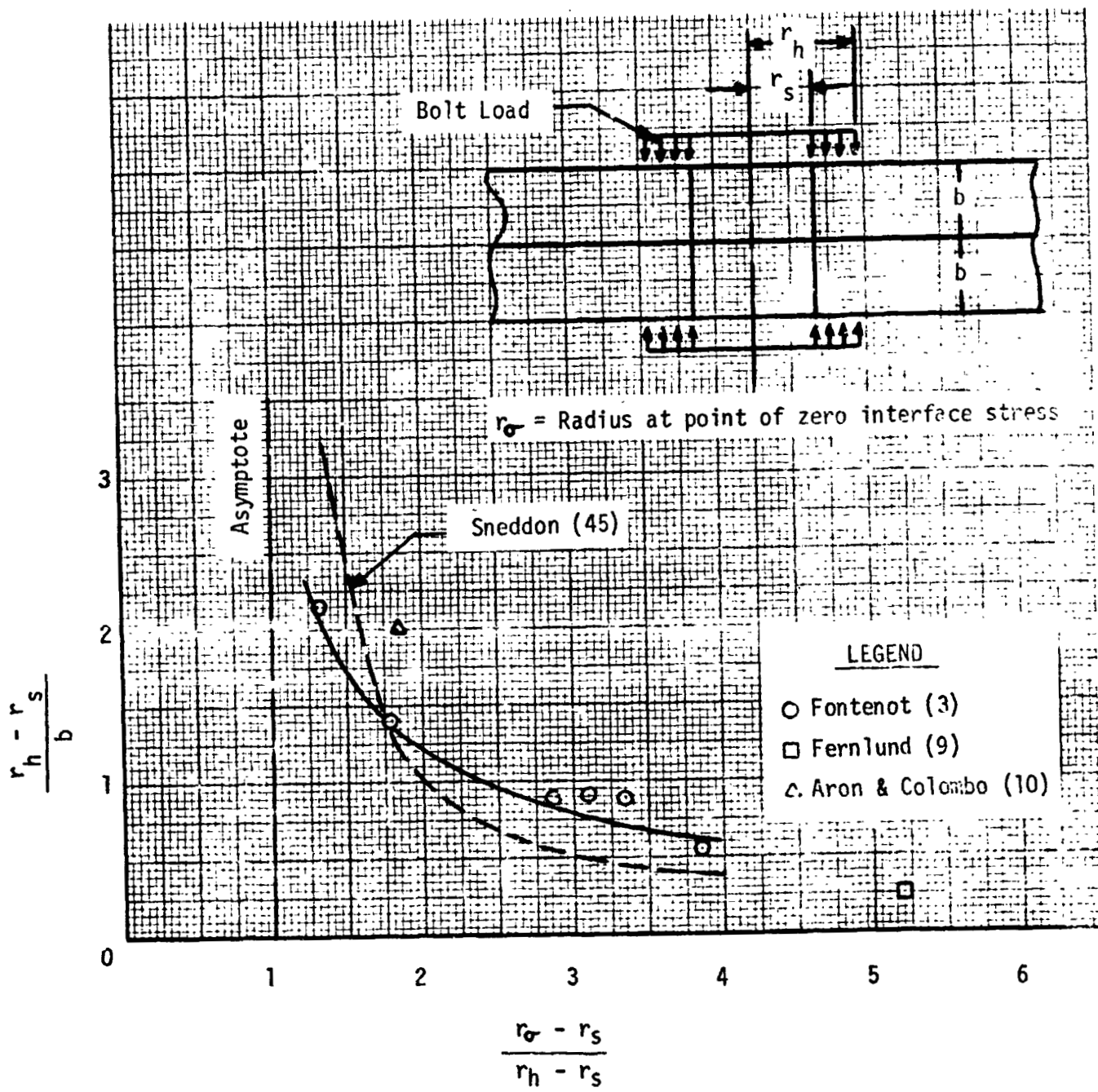


FIGURE 3-18

NON-DIMENSIONAL "ZERO INTERFACE STRESS" (REF. 3)

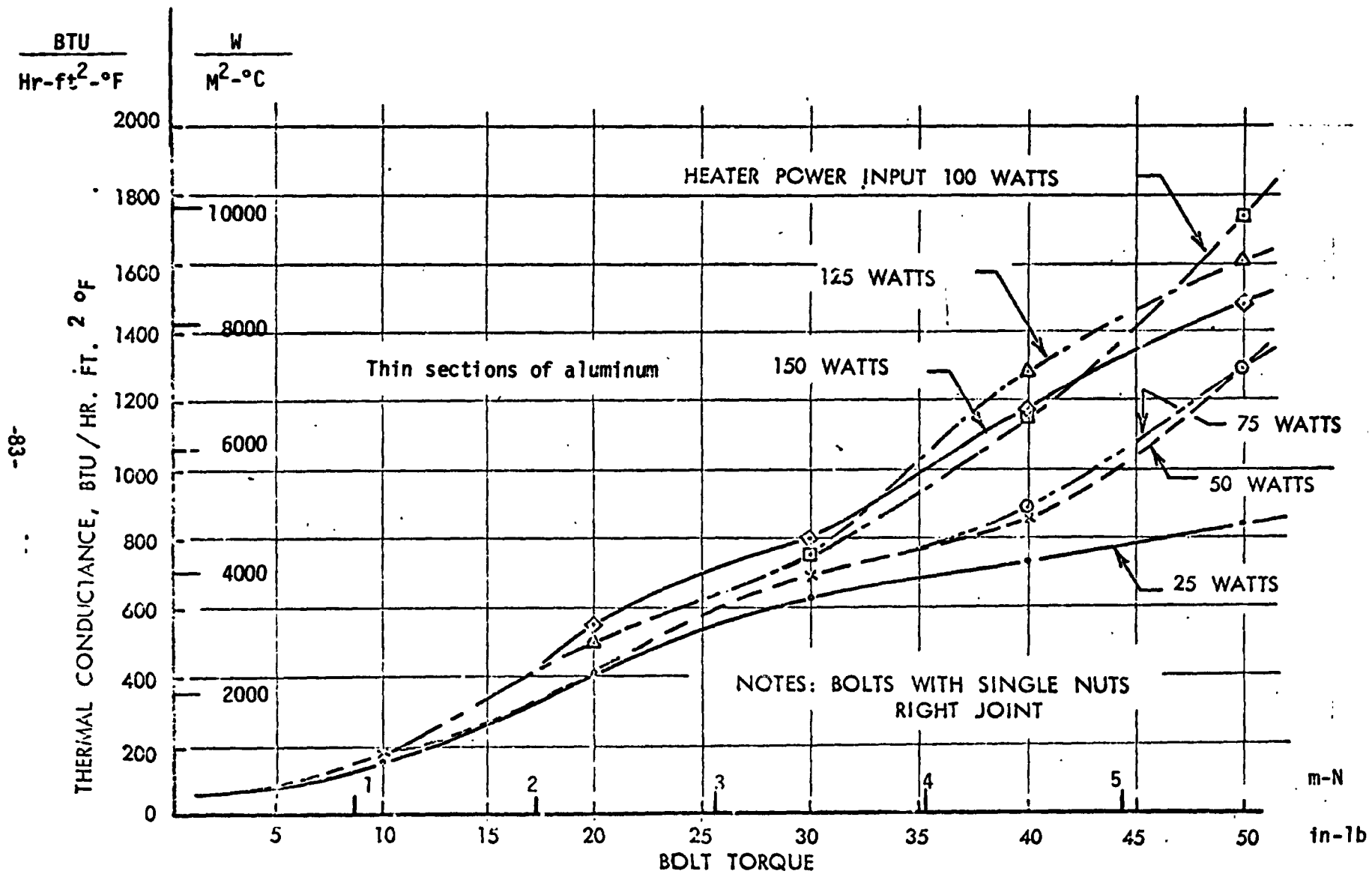


FIGURE 3-19

THERMAL CONDUCTANCE VS. TORQUE (REF. 38)

3.3 GLOSSARY AND NOMENCLATURE

ASPERITY	as used on contact heat transfer, a very small protuberance, many of which make up the roughness pattern. Sometimes called an a-spot.
A-SPOT	See asperity
LAY	the direction of the predominant surface pattern, usually determined by the production method used.
MACROSCOPIC	constriction resistance. The resistance due to small surface irregularities such as groups of asperities in contact.
MICROSCOPIC	constriction resistance. The resistance due to small surface irregularities such as asperities in contact.
PRIMARY WAVINESS	generally refers to roughness, surface finish, shortwavelength.
SECONDARY WAVINESS	flatness deviation, larger scale undulations than primary waviness, longer wavelengths.
WAVINESS	component of surface texture. In conventional practice, the widely spaced undulations, i.e. secondary waviness.
ROUGHNESS	the finer irregularities in the surface texture (primary waviness)
PROFILOMETER	device to measure two-dimensional topographical features of surface. (Talysurf, Micrometrical, Surfanalyzer, are some of the commercial devices).

TABLE 3-III

NOMENCLATURE

A	Area (m^2)
B	Constant
C	Constant
E	Modulus of Elasticity ($N-m^{-2}$)
H	Mating Material Indentation Hardness
P	Pressure (Apparent) ($N-m^{-2}$)
Q	Heat Flow (w)
S	Surface Parameter
T	Temperature ($^{\circ}C$)
W	Load Force (N)
Y	Yield Strength ($N-m^{-2}$)
\bar{a}	Radius of Contact Spot (m)
h	Conductance ($w-m^{-2}-^{\circ}C^{-1}$)
i	Peak-to-mean surface undulation of each mating surface (rms value) (m)
k	Conductivity ($w-m^{-1}-^{\circ}C^{-1}$)
m	Exponent
n	Number
p	Contact Pressure = Load/Apparent Contact Area ($N-m^{-2}$)
r	Radius (m)
β	Coefficient of Thermal Expansion ($m-m^{-1}-^{\circ}C^{-1}$)
δ	Equivalent (effective) Gap Thickness (m)
ρ	rms roughness (m)
ψ	Conductance Number $h\delta / k$
T*	Nondimensional Temperature $T\beta$
P*	Nondimensional Pressure P/E

Subscripts and Superscripts

c	Contact
g	Gap
s	Solid
m	Mean
1, 2	Surfaces or materials
*	Nondimensional
**	Modified Value (used with Eq. 2-9)

4.0 REFERENCES

1. Minges, M. L., "Thermal Contact Resistance," Vol. I, AFML TR 65-375 (April 1966).
2. Fried, E., "Thermal Conduction Contribution to Heat Transfer at Contacts," in Thermal Conductivity, Vol. 2, Chap. 5 (Ed. by R. Tye) Academic Press, 1969.
3. Fontenot, J. E., Jr., "Thermal Conductance of Bolted Joints," Louisiana State University, (N68-24656), May 1968.
4. Hsieh, H., Doris, F. E., "Bibliography on Thermal Contact Conductance," AFML-TR 69 24, March 1969.
5. Moore, C. J., Atkins, H. L., and H. A. Blum, "Subject Classification Bibliography for Thermal Contact Resistance Studies," ASME paper 68 WA/HT 18, 1968.
6. Graff, W. J., "Thermal Conductance Across Metal Joints," Machine Design, 32, 19, p. 166-72, 1960.
7. Fontenot, J. E., Jr., "Thermal Conductance of Contacts and Joints," Boeing Document D5-12206 (AD 479008).
8. Lardner, T. J., "Stresses in a Thick Plate with Axially Symmetric Loading," J of Applied Mechanics, Transactions ASME, Series E, Vol. 32, June 1965 (458-459).
9. Fernlund, I., "A Method to Calculate the Pressure Between Bolted or Riveted Plates," Transactions of Chalmers, University of Technology, Gothenburg, Sweden, No. 245, 1961.
10. Aron, W. and G. Colombo, "Controlling Factors of Thermal Conductance Across Bolted Joints in a Vacuum Environment," ASME paper No. 63-WA 206 (November 1963).
11. Gould, H. H., and B. B. Mikic, "Areas of Contact and Pressure Distribution in Bolted Joints," Report ESR 71821-68, MIT Heat Transfer Lab, June 1970.
12. Hsieh, C. K. and Y. S. Touloukian, "Correlation and Prediction of Thermal Contact Conductance for Nominally Flat Surfaces," in Thermal Conductivity, Plenum Press, 1969.

References, Continued

13. Cetinkale, T. N. and M. Fishender, "Thermal Conductance of Metal Surfaces in Contact," General Discussion on Heat Transfer, IME and ASME, 1951, pp. 271-294.
14. Fenech, H. and Rohsenow, W. H., "Prediction of Thermal Conductance of Metallic Surfaces in Contact," J. of Heat Transfer, 85:1, (February 1963), pp. 15-24.
15. Clausing, A. M., and Chao, B. T., "Thermal Contact Resistance in a Vacuum Environment," Journal of Heat Transfer, Vol. 87, No. 2, February 1965, p. 243.
16. Laming, L. C., "Thermal Conductance of Machined Contacts," International Developments in Heat Transfer, The American Society of Mechanical Engineers, New York (1963), pp. 65-76.
17. Fried, E. and Kelley, M. J., "Thermal Conductance of Metallic Contacts in a Vacuum," in Thermophysics and Temperature Control, (Ed. by G. Heller) Academic Press, New York (1966).
18. Fried, E. and Atkins, H. L., "Interface Thermal Conductance in a Vacuum," J. of Spacecraft and Rockets, No. 4, (July-August 1965), pp. 591-593.
19. Barzelay, M. E., "Range of Interface Thermal Conductance for Aircraft Joints," NASA TN D-426, May 1960.
20. Rolsma, B., "Evaluation of Contact Conductance at Critical Joints in the Apollo Spacecraft," GE Report 66SD4487, Contract NAS 9-4516, Final Report, Sept. 1966.
21. Bevans, I. T., T. Ishimoto, B. R. Loya, E. E. Luedke, "Prediction of Space Vehicle Thermal Characteristics," Report AFFDL TR 65-139, August 1965.
22. American Standard ASA B46.1-1962, Surface Texture. American Society of Mechanical Engineers, New York.
23. Bryan, J. B., G. I. Boyadjieff, E. R. McClure, "A State of the Art Report. Measuring Surface Finish," Mechanical Engineering, Dec. 1963, p. 40.
24. D'Yachenko, P. E. et al, "The Actual Contact Area Between Touching Surfaces," Consultants Bureau, New York (1964).

References, Continued

25. Fried, E., "Thermal Joint Conductance in a Vacuum," ASME Paper 63-AHGT-18, (1963).
26. Fried, E. and F. A. Costello, "Interface Thermal Contact Resistance Problems in Space Vehicles," ARS Journal, Vol. 32, pp. 237-243 (1962).
27. Fletcher, L. S., "Thermal Contact Resistance of Metallic Interfaces: An Analytical and Experimental Study," Ph. d. Thesis, Arizona State University, June 1969.
28. Boeschoten, F. and E. F. M. VanderHeld, "The Thermal Conductance of Contacts Between Aluminum and Other Metals," Physics, XXIII, (1957) pp. 37-44.
29. Shiykov, Yu. P., Ganin, E. A., "Thermal Resistance of Metallic Contacts," Int. Journal Heat Mass Transfer, Vol. 7, No. 8, 1964, pp.921-929.
30. Malkov, V. A., "Thermal Contact Resistance of Machined Metal Surfaces in a Vacuum Environment," Heat Transfer-Soviet Research, Vol. 2, No. 4, p. 24, July 1970.
31. Holm, R., Electrical Contacts, Almqvist and Wiksells Akademiska Hanbocker, Stockholm, Sweden, (1946).
32. Cordier, H., and R. Maimi, "Experimental Study of the Influence of Pressure on Thermal Contact Resistance," Acad. des Sciences, Comptes Rendus, 250/11/2853-55, Paris, France, April 1960.
33. Popov, V. M., "Determination of the Thermal Contact Resistance of Plane Rough Surfaces with the Roughness Deforming in Different Manners," Heat Transfer - Soviet Research, Vol. 2, No. 4, p. 24, July 1970.
34. Henry, J. J., and Fenech, H., "The Use of Analogue Computers for Determining Surface Parameters Required for Prediction of Thermal Contact Conductance," J. of Heat Transfer, Vol. 86, Series C, No. 4, November 1964, pp. 543-552.
35. Cassidy, J. F., and H. Mark, "Thermal Contact Resistance Measurements at Ambient Pressures of 1 Atm. to 3×10^{-12} mm Hg," NASA TMX-52566, NASA Lewis Research Center, June 1969.
36. Whitehurst, C. A., W. T. Durbin, "A Study of Thermal Conductance of Bolted Joints," NASA Grant 19-001-068. Louisiana State University, Baton Rouge, La. (1970).

References, Continued

37. Lindh, K. G., et al, "Studies in Heat Transfer in Aircraft Structure Joints," University of California, Los Angeles, Report 57-50, May 1957.
38. Feldmanis, C. J., "Investigation of Passive Electronic Equipment Temperature Control Devices," TM-69-13-FDFE AF Flight Dynamics Lab., Wright Patterson AF Base, August 1969.
39. Elliott, D. H., "A Study of Thermal Resistance Across Aluminum Joints in a High Vacuum," ASME Paper No. 65-HT-53, August 1965.
40. Clausing, A. M., "Heat Transfer at the Interface of Dissimilar Metals-- The Influence of Thermal Strain," International Journal Heat Mass Transfer, 9, pp. 791-801, 1966.
41. Bloom, M. F., "Thermal Contact Conductance in a Vacuum Environment," Douglas Aircraft Company Report SM-47700, December 1964.
42. Cunnington, G. R., Jr., "Thermal Conductance of Filled Aluminum and Magnesium Joints in a Vacuum Environment," ASME Paper No. 64-WA/HT-40, November 1964.
43. Fletcher, Leroy S., Paul A. Smuda, and Donald A. Gyrog, "Thermal Contact Resistance of Selected Low Conductance Interstitial Materials," AIAA Paper No. 68-31, January, 1968.
44. Hargadon, Joseph M., Jr., "Thermal Interface Conductance of Thermo-electric Generator Hardware," ASME Paper No. 66-WA/NE-2, November 1966.
45. Sneddon, I. N., "Fourier Transforms," McGraw-Hill Book Company, New York, (1962), pp. 479-480.
46. Shih, C., "Thermal Scaling of Bolted Joints," 1968 Space Simulation Conference Proceedings, Institute of Environmental Sciences, pp. 176-183.
47. Fried, E., "Study of Interface Thermal Contact Conductance," Final Report, Contract NAS8-11247, GE Report 66SD4471, 1966.